

The copyright of this thesis rests with the University of Cape Town. No quotation from it or information derived from it is to be published without full acknowledgement of the source. The thesis is to be used for private study or non-commercial research purposes only.

Optimisation of Complex Distillation Column Systems using Rigorous Models

Michael John Hughes
11th May 2010

Thesis presented for the degree of Doctor of Philosophy
In the Department of Chemical Engineering
University of Cape Town

University Of Cape Town

Abstract

Since distillation is still the most widely used separation technique used in the petrochemical industry, optimisation of these unit operations are important to minimise costs and maximise production. This thesis focuses on the development of a tool using rigorous non-equilibrium distillation models to optimise complex columns.

Non-equilibrium distillation models are usually avoided in optimisation studies due to the time required to solve them, but this has been overcome by using a technique called orthogonal collocation in which the profiles in the columns are represented by polynomials of a lower order than would be required normally. This significantly reduces the process times and makes the use of non-equilibrium models a possibility in optimisation studies.

The orthogonal collocation technique was applied to a packed distillation column model and shown to be effective in modelling the system. A system consisting of a distillation column with integrated external side reactors was chosen as a case study to investigate the use of the methods. These systems have been shown to be effective in certain circumstances in literature, when comparing them to other forms of process intensification, such as reactive distillation.

The toluene disproportionation reaction was considered as a potential use for the technology and the optimisation tool was used to find optimum system configurations for achieving maximum toluene conversions and minimum costs. Nonlinear programming techniques were used initially to optimise these systems, but due to the discontinuities associated with multiple side streams, they were replaced by a genetic algorithm.

Various system configurations were identified as achieving maximum conversions and minimum costs. These results were used in a comparison with results obtained from a literature study and the results showed significant promise. Unfortunately, the two studies did not have enough in common to truly produce a comprehensive result. This

lead to further comparisons with another system using the same information.

The results obtained in the toluene disproportionation case study showed that there was some possible benefits for using the side reactor systems, but the conventional system was still 30 and 60% cheaper in terms of capital and utility costs respectively.

Another case study was investigated that looked at the synthesis of methyl acetate from acetic acid and methanol. The packed collocation model was used as a comparison with another investigation performed in literature (using equilibrium distillation models). Both showed comparable results, but still had significant differences.

Costs were also compared between the side reactor system and a more conventional system for methyl acetate synthesis. The side reactor systems were found to be more cost effective than the conventional system. Additionally, an increase in the number of external reactors resulted in lower utility costs (mainly as a result of lower flow rates in the side streams).

Overall, the reaction and process conditions are important considerations when deciding whether or not to use a side reactor system. For the gas phase toluene disproportionation reaction, the side reactor systems were not cost effective, when compared to the conventional system. However, the liquid phase methyl acetate reaction proved to be more conducive to side reactor systems in terms of cost.

This thesis has shown the applicability of using rigorous disequilibrium distillation models in optimisation studies. The side reactor systems have been found to be complex systems that require a holistic approach to find optimum configurations instead of optimising individual process units.

Declaration

I hereby:

- grant the University free license to reproduce the above thesis in whole or in part, for the purpose of research;
- declare that:
 - the above thesis is my own unaided work, both in conception and execution, and that apart from the normal guidance of my supervisor, I have received no assistance;
 - neither the substance or any part of the thesis has been submitted in the past, or is being, or is to be submitted for a degree at this University or any other university.
 - I am now presenting the thesis for examination for the Degree of PhD.

Michael Hughes

University Of Cape Town

Acknowledgements

Of the many people who deserve thanks, some are particularly prominent:

Firstly, my supervisor Prof. Klaus Möller who was the initial catalyst, getting me started with the project and then letting me get on with it. I appreciate the informal update sessions to make sure that I was on track throughout and the enthusiasm shown towards the project itself.

Secondly, I'd like to thank UCT's Department of Chemical Engineering, in which I have felt at home for the last nine years (the last five in particular) and for all the staff and students who I have interacted with over the years. In particular I'd like to mention the help and guidance offered by Jako Nieuwoudt and Martina Welz who seemed to be working on similar problems along the way and we were able to reach a solution together.

I would also like to thank my parents for encouraging me along the way, even though they are on the other side of the country and finally, I'd especially like to thank Shelagh, my wife, for putting up with all the talk of "Genetic Algorithms" and other strange terms, particularly when things weren't going quite the way that I was expecting.

The financial assistance of the National Research Foundation (NRF) and Sasol towards this research is also acknowledged. Opinions expressed and conclusions arrived at, are those of the author and are not necessarily to be attributed to the NRF or Sasol.

University Of Cape Town

Contents

List of Figures	xv
List of Tables	xix
1 Introduction	1
1.1 Optimisation of Distillation Columns	1
1.2 Collocation	1
1.3 Catalytic Distillation and Side Reactor Systems	2
1.4 Objectives & Key Questions	2
2 Literature Review: Mass Transfer and Distillation	3
2.1 Fick's Law	4
2.2 Maxwell-Stefan Relations	5
2.3 Binary Distillation	6
2.3.1 McCabe-Thiele Diagram	6
2.3.2 Murphree Efficiency	6
2.4 Multicomponent Distillation	9
2.4.1 Pseudo McCabe-Thiele Diagrams	9
2.4.2 Equilibrium Models	9
2.4.3 Efficiency Models	11

2.4.4	Rigorous Rate-based Model	12
2.5	Packed Columns	15
2.5.1	Modelling	15
2.5.2	HETP	16
3	Literature Review: Collocation	19
3.1	Solving Boundary Value Problems (BVPs)	19
3.2	Method of Weighted Residuals	20
3.2.1	Galerkin Method	22
3.2.2	Collocation Method	22
3.3	Determining collocation points	23
3.3.1	Jacobi Polynomials	24
3.3.2	Hahn Polynomials	25
3.4	Finding the Roots of the Jacobi Polynomials	25
3.5	Collocation Method in Detail	27
3.5.1	Lagrange Interpolation Polynomials	27
3.5.2	Derivative Matrices	27
3.6	Orthogonal Collocation on Finite Elements (OCFE)	29
3.7	Collocation and Process Design	30
3.8	Collocation and Distillation	31
3.8.1	Staged Columns	31
3.8.2	Dealing with Steep and Flat Profiles	33
3.8.3	Collocation and Reactive Distillation	37
3.8.4	Packed Columns	37
3.8.5	Orthogonal Polynomial Choice	38

4	Literature Review: Process Intensification	41
4.1	Reactive Distillation	41
4.1.1	Industrial Use of RD	42
4.1.2	Advantages and Disadvantages of RD	44
4.1.3	Modelling RD Columns	45
4.1.4	Comparisons between RD Columns and Conventional Systems	47
4.2	Integrated Side Reactor Systems	47
4.2.1	Modelling Side Reactor Systems	50
4.2.2	Comparisons with RD	50
4.2.3	Advantages and Disadvantages of the Side Reactor System over RD	52
5	Literature Review: Distillation Column Optimisation	55
5.1	Mixed Integer Non-Linear Programming	56
5.2	Generalised Disjunctive Programming	58
5.3	Comparisons between MINLP and GDP for Distillation Optimisation	59
5.4	Collocation in Distillation Column Optimisation	60
5.5	Genetic Algorithms	60
5.5.1	Algorithm Structure	61
5.5.2	Dealing with Constraints	64
5.5.3	GAs used to Optimise Distillation Columns	65
6	Model Development and Methodology	67
6.1	Program Structure	67
6.1.1	Overall Structure	67
6.1.2	Model Structure	69

6.2	Optimisation	70
6.2.1	NLP	70
6.2.2	Genetic Algorithms	72
6.3	Distillation Collocation Model	75
6.3.1	Collocation Method Applied to a Packed Distillation Column Model	75
6.3.2	Boundary Conditions	76
6.4	Reactor Model	78
6.4.1	Toluene Disproportionation Case Study	79
6.4.2	Methyl Acetate Case Study	80
6.5	Thermodynamics, Mass and Heat Transfer Coefficients	81
7	Results: Preliminary Results	83
7.1	Model Accuracy	83
7.2	Collocation Model	86
7.2.1	Choosing the number of interior points	89
7.3	Choice of Optimisation Routine	89
7.3.1	DONLP2	89
7.3.2	SolvOpt	95
7.3.3	Genetic Algorithms	96
7.3.4	Advantages and disadvantages of using GAs	98
8	Results: Toluene Disproportionation	101
8.1	Overall Toluene Conversion	101
8.2	Total Annual Cost	107
8.2.1	Comparison with RD and Conventional Systems in Literature	107
8.2.2	Comparison with Conventional Two Column System	115

9 Results: Methyl Acetate Synthesis	123
9.1 Overall Conversion	123
9.1.1 Comparability	124
9.1.2 Results	124
9.1.3 Multiple Steady States	126
9.2 Total Annual Cost	126
10 Future Work	137
10.1 Improvements to the program	137
10.2 Directions for future work and applications	138
11 Conclusions	141
11.1 Toluene Disproportionation Case Study	141
11.2 Methyl Acetate Case Study	142
11.3 Concluding Remarks	143
11.4 Summary of contributions	144
A Mass and Heat Transfer Derivations	147
A.1 Mass Transfer	147
A.1.1 Structured Packing	147
A.1.2 Random Packing	149
A.1.3 Packing Characteristics	150
A.2 Heat Transfer	150
B Physical Properties	153
B.1 Component Temperature Dependent Properties	153

C Cost Calculations	155
C.1 Capital Costs	155
C.2 Utility Costs	156
D Flooding calculations	157
Nomenclature	159
Bibliography	165
Index	175

University Of Cape Town

List of Figures

2.1	Film theory model for mass transfer	3
2.2	Example of a McCabe-Thiele Diagram	7
2.3	Example of a McCabe-Thiele Diagram using Murphree vapour efficiency	8
2.4	Equilibrium stage model	10
2.5	Two-film theory model	12
2.6	Nonequilibrium stage model	13
2.7	Raschig rings used in packed distillation columns	15
3.1	Collocation points showing order reduction	31
3.2	Discontinuity in the liquid flow rate due to a liquid feed at stage N_F	32
3.3	OCFE distillation model using two finite elements per section and two collocation points per element	35
3.4	Order reduction using Orthogonal Collocation on Finite Elements	36
4.1	Conventional reactor-separator system	42
4.2	Reactive Distillation column	43
4.3	Integrated side reactor system	48
4.4	Side reactor configurations (a) co-current (b) counter-current (c) reactor-separation unit (d) local stage side reactor (adapted from Baur and Krishna (2004))	49

4.5	Coupled reactor system used by Chiang et al. (2002)	51
5.1	Feed location optimisation problem using MINLP	57
5.2	MINLP using variable reflux and reboil stream location	57
5.3	MINLP using variable reboiler location	58
5.4	GDP model with permanent and conditional trays	59
5.5	Replacement strategies for GAs	64
5.6	Constraint handling method by Deb (2000)	66
6.1	Overall Program Structure	68
6.2	Model Structure	69
6.3	Single external reactor column showing boundary condition positions	77
6.4	Toluene Disproportionation Reaction	79
7.1	Liquid composition profiles of the staged model and Chemsep using 20 stages	84
7.2	Liquid composition profiles of the staged model using 10, 20 and 40 stages	85
7.3	Liquid composition profiles of the collocation model using 4 sections and 9 interior points compared to the 40 stage model	87
7.4	Liquid composition profiles of the collocation model using 4 sections and 1, 3 and 9 interior points	88
7.5	Side reactor system used in the optimisation studies	90
7.6	DONLP2 optimisation progress for optimising R and Rb for maximum $X_{Toluene}$	92
7.7	Overall toluene conversion as a function of reflux and boilup ratios	93
7.8	DONLP2 progress for optimising the feed location for maximum toluene conversion	94
7.9	Overall toluene conversion as a function of the feed location using DONLP2	94

7.10	SolvOpt optimisation progress for optimising R and Rb for maximum $X_{Toluene}$	95
7.11	Overall toluene conversion as a function of the feed location using SolvOpt	96
7.12	GA optimisation progress for optimising R and Rb for maximum $X_{Toluene}$	97
7.13	GA progress for optimising the feed location for maximum toluene conversion	98
8.1	Optimal configurations for maximum toluene conversion using (a) one external side reactor, (b) two external side reactors and (c) three external side reactors	104
8.2	Liquid composition in 1 Reactor system	105
8.3	Fraction of Flooding in column in 1 Reactor system	105
8.4	Liquid and Vapour flow rates in column in 1 Reactor system	106
8.5	Optimal configurations for minimum TAC using (a) one external equilibrium side reactor, (b) two external equilibrium side reactors and (c) three external equilibrium side reactors	110
8.6	Capital cost breakdown for 1, 2 and 3 external equilibrium side reactor systems with ethyl benzene side reaction	112
8.7	Utility cost breakdown for 1, 2 and 3 external equilibrium side reactor systems with ethyl benzene side reaction	113
8.8	Conventional System used by Stitt (2002)	114
8.9	RD system used by Stitt (2002)	114
8.10	Two column conventional system used in optimisation comparison	116
8.11	Optimal configurations for minimum TAC using (a) one external side reactor, (b) two external side reactors and (c) three external side reactors	117
8.12	Capital cost breakdown for 1, 2 and 3 external kinetic side reactor systems compared to the conventional system	120
8.13	Utility cost breakdown for 1, 2 and 3 external kinetic side reactor systems compared to the conventional system	121

8.14	Cost trends using side reactor systems for toluene disproportionation . . .	121
9.1	Comparison between Baur and Krishna (2004) and the collocation model for various optimum configurations	125
9.2	Three column system to produce Methyl Acetate from Acetic Acid and Methanol	127
9.3	Optimal configurations for minimum TAC using the side reactor systems with (a) one, (b) two, (c) three, (d) four and (e) five external reactors . .	129
9.4	Fraction of flooding with the column with 5 external reactors	131
9.5	Cost trends using side reactor systems and the conventional system for methyl acetate production	134
9.6	Comparison of capital costs for the side reactor systems and the conventional 3 column system for the production of methyl acetate	135
9.7	Comparison of utility costs for the side reactor systems and the conventional 3 column system for the production of methyl acetate	136
10.1	Various configurations of distillation columns to separate four components	139
A.1	Geometry of structured packing (a) Flow channel cross section (b) Flow channel arrangement	148

List of Tables

5.1	Example of a binary encoding of 3 variables to a single individual	61
5.2	Example of a Point and Random Crossover operations	63
6.1	Boundary conditions used in a single reactor column shown in Figure 6.3 .	78
7.1	Distillation column parameters used for comparison	84
7.2	Computational times required for staged model comparison	86
7.3	Computational times required for collocation model comparison	88
7.4	Fixed side reactor parameters used in the optimisation studies for the NLP solvers	91
7.5	Parameters for DONLP2 optimisation of Reflux and Boilup ratios for maximum toluene conversion	92
7.6	Results for Optimisation routine comparisons	99
8.1	Fixed side reactor system parameters used in the overall conversion op- timisation	102
8.2	Optimum systems to achieve maximum overall toluene conversion	103
8.3	External reactor details for the configurations to achieve maximum overall toluene conversion	103
8.4	Fixed side reactor system parameters used in the minimisation of Total Annual Costs using and equilibrium reactor and taking the ethylbenzene side reaction into account	109

8.5	Optimum systems to achieve minimum TAC using equilibrium reactors with ethylbenzene side reaction	109
8.6	External reactor details for the configurations to achieve minimum TAC using equilibrium reactors	110
8.7	Capital and Utility cost breakdown for TAC optimum systems using equilibrium reactors and taking into account the ethylbenzene side reaction (\$'000)	112
8.8	Capital costs obtained by Stitt (2002) - updated to 2008 values (\$'000) .	113
8.9	Fixed side reactor system parameters used in the minimisation of Total Annual Costs	115
8.10	Optimum systems to achieve minimum TAC	116
8.11	External reactor details for the configurations to achieve minimum TAC using kinetic reactors	117
8.12	Optimum two column conventional system to achieve minimum TAC . .	119
8.13	Capital and Utility cost breakdown for TAC optimum systems (\$'000) . .	120
9.1	Fixed system parameters used in the minimisation of Total Annual Costs for the side reactor system in the Methyl Acetate study	128
9.2	Fixed system parameters used in the minimisation of Total Annual Costs for the conventional system in the Methyl Acetate study	128
9.3	Optimisation parameters used in the minimisation of Total Annual Costs for the Methyl Acetate study	129
9.4	Optimum systems to achieve minimum TAC for methyl acetate synthesis	130
9.5	External reactor details for the configurations to achieve minimum TAC for the methyl acetate system	131
9.6	Optimum three column conventional system to achieve the minimum TAC of \$7.924 million for producing 50mol/s of methyl acetate	134
A.1	Random and Structured Packing Characteristics	151

B.1 Correlations used for Temperature Dependent properties 153

C.1 Utility cost coefficients 156

University Of Cape Town

University Of Cape Town

Chapter 1

Introduction

1.1 Optimisation of Distillation Columns

Distillation columns are an integral part of a chemical processing facility. They allow for the separation of reaction products to produce them in high enough concentrations for sale. The ability to optimise the design of a single distillation column or a sequence of multiple columns is critical to reduce the costs involved and maximise the production of the desired product in the process.

1.2 Collocation

The majority of distillation column optimisation is performed using simple equilibrium models that allow the optimisation process to be achieved quickly. This is usually justified when performing early phase designs, but as the design process develops, it would be more useful to use more rigorous non equilibrium models that have been proven to model the processes more accurately. The disadvantage of using these rigorous models is that they inevitably take a long time to solve and are therefore not particularly suited to optimisation studies as these require multiple instances of the model to be solved.

A technique has been used to reduce the order of the model system without an appreciable loss in accuracy. This technique is known as Orthogonal Collocation and has been proven to be effective in distillation column modelling. This allows for the use of rigorous models to be used in optimisation studies as it reduces the time required to solve

the system.

1.3 Catalytic Distillation and Side Reactor Systems

To test the use of these rigorous models in distillation optimisation, a test case was required. Recently, the subject of process intensification has seen a lot of interest as it has the potential to reduce costs, lower emissions and reduce energy usage. One of the most promising of these is Reactive Distillation (RD). However, the reaction needs to take place in the liquid phase and the conditions for the reaction need be such that distillation and reaction are similar. This has limited the application in industry to a few select reaction types.

A possible alternative to these systems is a hybrid form of using external reactors integrated into the distillation column system to achieve similar, if not better performance, without having the limitations associated with RD. By using this separate, yet integrated approach, it is possible to optimise both the reactor and distillation column without having to compromise as much as in RD systems.

When looking at the optimisation of distillation column systems, the ability to apply multiple feeds and side streams is vital. Therefore, using an integrated side reactor system allows for the scope of testing various configurations of feeds and side streams going to and from reactors.

1.4 Objectives & Key Questions

Therefore, the aim of this research is:

- to develop a rigorous distillation column model using orthogonal collocation to be used in optimisation studies
- to incorporate this model in an optimisation tool for distillation column optimisation
- to use this tool to investigate optimum configurations of integrated side reactor systems
- to compare these optimum configurations with more conventional process systems and RD systems.

Chapter 2

Literature Review: Mass Transfer and Distillation

In separation systems, the understanding of the mass transfer effects is critical. In contacting devices such as distillation columns, there are usually two or more phases and mass transfer occurs between them. The flow of these phases is usually highly turbulent to achieve a high degree of mixing. This mixing allows for a reasonably homogeneous bulk phase that have very small concentration and temperature differences. However, near the interface between the phases, this turbulence is reduced and one can assume that a film exists where the only mechanisms for transport are molecular diffusion, convective transport (due to a displacement of matter), and conduction (for heat transport) (Nernst (1904)). This theory was extended to two films in series by Whitman (1923) and

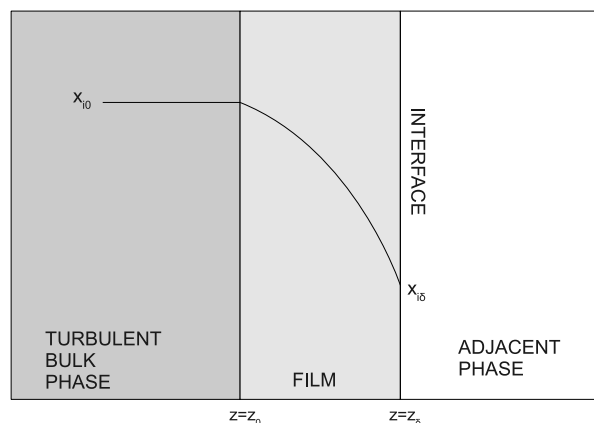


Figure 2.1: Film theory model for mass transfer

stated that all the resistance to mass transfer was present in the two films and that the concentrations at the interface are in thermodynamic equilibrium.

2.1 Fick's Law

In the 1850s, Adolf Fick was working on experimental studies on binary mixtures to investigate basic diffusion equations. This work (Fick 1855a, 1855b) resulted in Fick's first law. The law states that the flux of a component is proportional to concentration of that component in a binary mixture and its diffusivity. There is also a convective portion to the flux due to the displacement of matter. Therefore, the flux of a component in a binary mixture is given by

$$N_i = -c_t D_i \frac{dx_i}{dz} + x_i N_t. \quad (2.1)$$

However, this approach is less suited to multicomponent mixtures as it does not take into account the interactions between the components.

When applying Fick's law to multicomponent systems (Bird et al. (2002)), the number of independent equations is $c - 1$ where c is the number of components. Therefore, for a ternary system, one would have two independent equations

$$J_1 = -c_t D_{1,1} \nabla x_1 - c_t D_{1,2} \nabla x_2 \quad (2.2)$$

and

$$J_2 = -c_t D_{2,1} \nabla x_1 - c_t D_{2,2} \nabla x_2. \quad (2.3)$$

However, the $D_{i,j}$ values are multicomponent diffusivities that do not share the same characteristics of their binary equivalents. They can be positive or negative, are not usually symmetric (i.e. $D_{i,j} \neq D_{j,i}$) and do not reflect the interactions between the two components.

2.2 Maxwell-Stefan Relations

At the same time as Fick was investigating diffusion in binary mixtures, Scottish physicist James Clerk Maxwell and Austrian scientist Josef Stefan were developing equations to model multicomponent diffusion. Their work (Maxwell (1866) and Stefan (1871)) resulted in Equation 2.4 for multicomponent systems.

$$\mathbf{d}_i = - \sum_{j=1}^n \frac{x_i x_j (\mathbf{u}_i - \mathbf{u}_j)}{D_{i,j}} \quad (2.4)$$

The first recognisable form of these equations were found in an article titled "Diffusion", in the Encyclopaedia Britannica (Maxwell (1878)). If the definition of the molar fluxes is used ($N_i = c_i \mathbf{u}_i$), then

$$\mathbf{d}_i = - \sum_{j=1}^n \frac{x_j \mathbf{N}_i - x_i \mathbf{N}_j}{c_t D_{i,j}} \quad (2.5)$$

and if the mixture is ideal and the pressure is constant, then $\mathbf{d}_i = \nabla \mathbf{x}$. But if the mixture is nonideal, then

$$\mathbf{d}_i = \frac{x_i}{RT} \nabla_{T,P} \mu. \quad (2.6)$$

Due to the difficulty of using chemical potentials, it is possible to convert equation 2.6 into a form that uses mole fractions (Taylor and Krishna (1993))

$$\mathbf{d}_i = \sum_{j=1}^{n-1} \Gamma_{i,j} \nabla x_j \quad (2.7)$$

where

$$\Gamma_{i,j} = \delta_{i,j} + x_i \left. \frac{\partial (\ln \gamma_i)}{\partial x_j} \right|_{T,P,x_k, k \neq j=1, \dots, n-1} \quad (2.8)$$

2.3 Binary Distillation

Distillation is a widely used unit operation in the chemical processing industry. It allows for the separation of a mixture based on the differences in the individual component volatilities. As early as the first century AD, evidence of the use of distillation has been found and so this technology is not new (Forbes (1970)). However, the design and operation of these units has only been a relatively recent focus, but is still a mature separation operation when comparing it to some of the more recent developments.

2.3.1 McCabe-Thiele Diagram

Binary distillation is the simplest case for distillation. A large amount of work has been done using binary mixtures to investigate distillation systems. One advantage of looking at binary systems is that they are easy to visualise on a two dimensional graph. In 1925, McCabe and Thiele developed an approximate graphical technique to combine the equilibrium curve with the operating lines. Figure 2.2 shows an example of a McCabe-Thiele diagram. The use of McCabe-Thiele diagrams is somewhat restricted in that there are a number of assumptions that are used to achieve the graph. These are:

- that the liquid and vapour phases are perfectly mixed
- that the column operates isobarically and adiabatically
- that Constant Molar Overflow (CMO) is in effect
- that the exiting streams of each stage are in thermodynamic equilibrium.

The CMO assumption calls for the liquid and vapour from each stage to remain constant within each column section. This is very unlikely in practice, but this method does allow for a quick and visual method to determine the number of equilibrium stages and the reflux ratio required for a given binary feed and operating pressure.

2.3.2 Murphree Efficiency

As highlighted in Section 2.3.1, the McCabe-Thiele method assumes that the exiting streams on each stage are in thermodynamic equilibrium. In industry, this is usually not

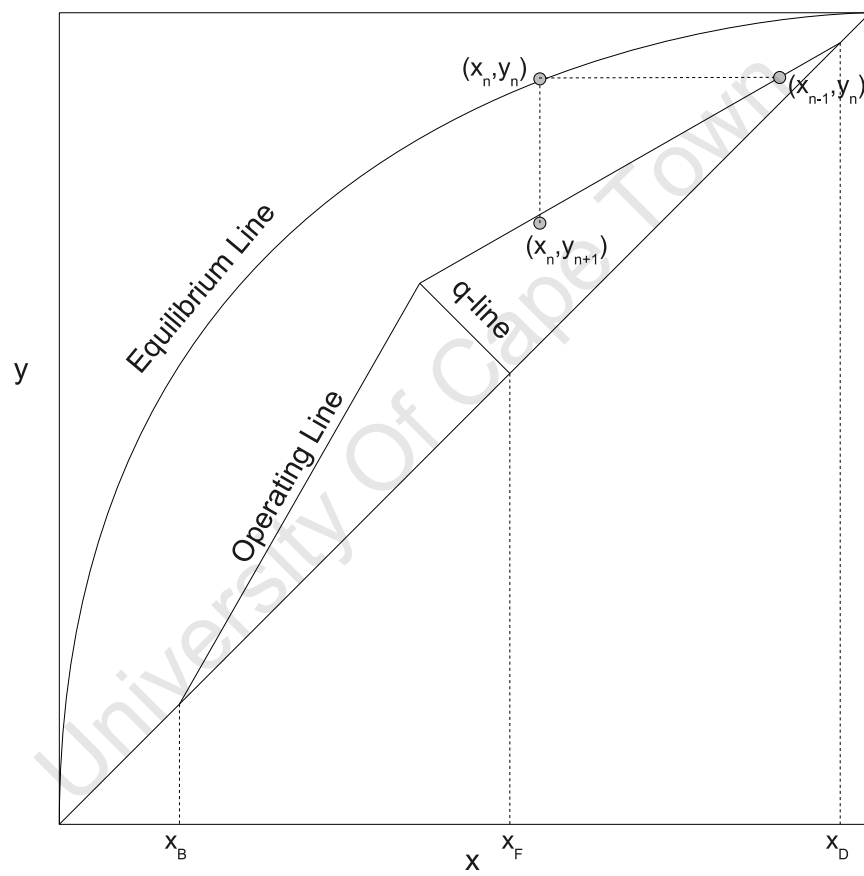


Figure 2.2: Example of a McCabe-Thiele Diagram

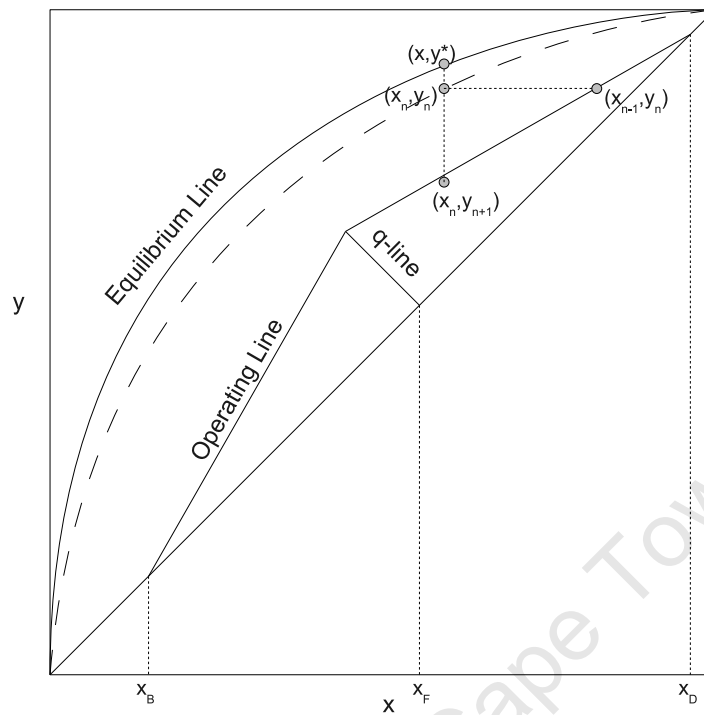


Figure 2.3: Example of a McCabe-Thiele Diagram using Murphree vapour efficiency

possible and so the changes in concentration are usually less than those predicted by the equilibrium. A common method to account for this difference is the use of a stage efficiency, and more specifically, a Murphree plate efficiency (Murphree 1925a, 1925b).

This efficiency can be defined for a given component on a vapour or liquid basis. Equation 2.9 shows the Murphree vapour efficiency definition.

$$E^{MV} = \frac{y_n - y_{n+1}}{y_n^e - y_{n+1}} \quad (2.9)$$

Figure 2.3 shows the use of a Murphree vapour efficiency in the construction of a McCabe-Thiele diagram. By using the efficiency, it effectively creates a new “equilibrium” curve and the technique is largely unchanged.

2.4 Multicomponent Distillation

2.4.1 Pseudo McCabe-Thiele Diagrams

It is possible to extend McCabe-Thiele diagrams for use with multicomponent systems (Kooijman and Taylor (2001)). They are not as useful in terms of taking all the components into account, but can still provide some insights into the operation of the column (e.g. optimal feed placement). They are usually constructed using two key components and ignoring the others. Then the y -axis will be defined as

$$y = \frac{y_{LK}}{y_{LK} + y_{HK}} \quad (2.10)$$

and the x -axis as

$$x = \frac{x_{LK}}{x_{LK} + x_{HK}} \quad (2.11)$$

where LK represents the lighter of the two key components, while HK , the heavier. These are then normalised to range from 0 to 1.

2.4.2 Equilibrium Models

When modelling multicomponent distillation systems, most studies involve the use of MESH equations (see Wang and Henke (1966)). These equations represent an equilibrium stage as shown in Figure 2.4. They include the Mass balances (including the overall mass balance)

$$M_j^T \equiv V_j + W_j + L_j + U_j - V_{j+1} - L_{j-1} - F_j = 0 \quad (2.12)$$

$$M_{ij} \equiv (V_j + W_j)y_{i,j} + (L_j + U_j)x_{i,j} - V_{j+1}y_{i,j+1} - L_{j-1}x_{i,j-1} - F_j z_{i,j}^F = 0 \quad (2.13)$$

the Equilibrium equations

$$E_{ij} \equiv K_{i,j}x_{i,j} - y_{i,j} = 0 \quad (2.14)$$

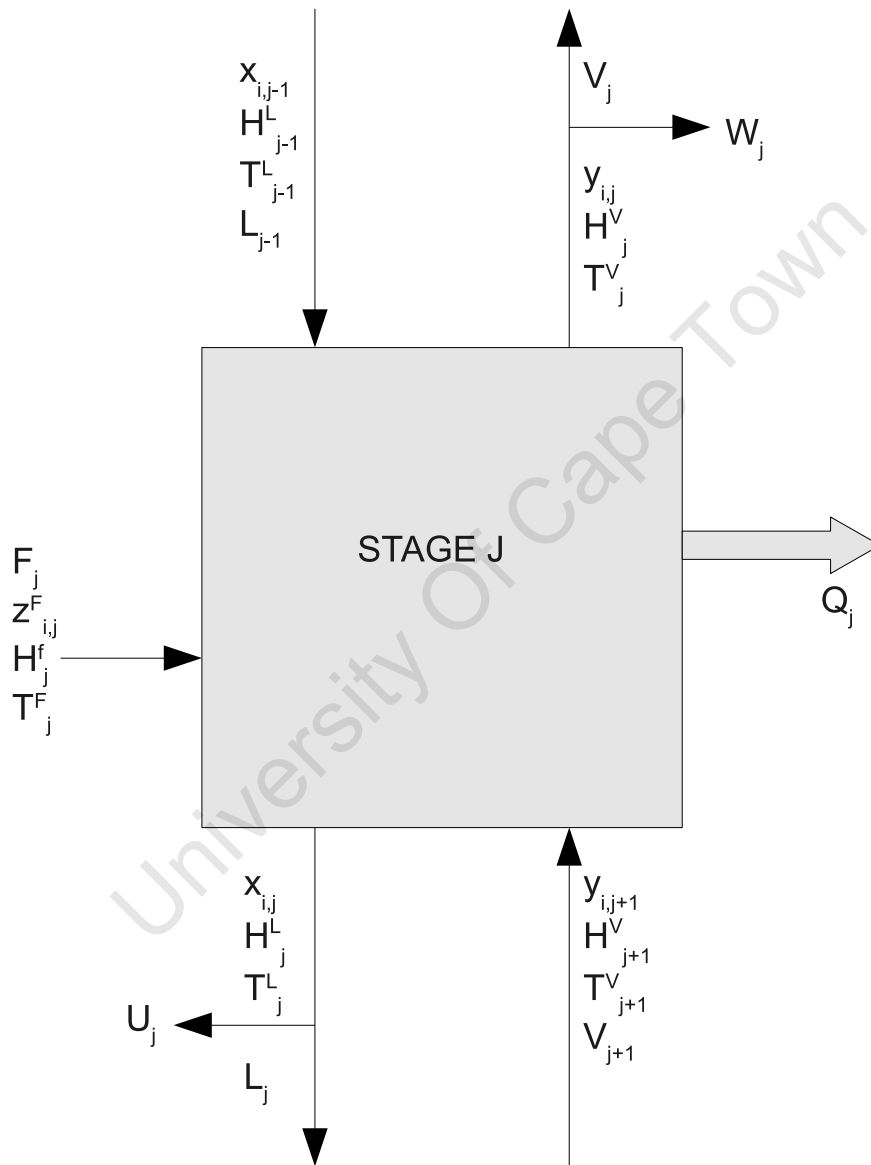


Figure 2.4: Equilibrium stage model

the Summation of mole fractions in both phases

$$S_j^V \equiv \sum_{i=1}^c y_{i,j} - 1 = 0 \quad (2.15)$$

$$S_j^L \equiv \sum_{i=1}^c x_{i,j} - 1 = 0 \quad (2.16)$$

and the entHalpy balance

$$H_j \equiv (V_j + W_j)H_j^V + (L_j + U_j)H_j^L - V_{j+1}H_{j+1}^V - L_{j-1}H_{j-1}^L - F_jH_j^F + Q_j = 0. \quad (2.17)$$

This results in $2c + 5$ equations, but only $2c + 3$ of these equations are independent and so normally the c component mass balances, the c equilibrium equations, the enthalpy equation and two of either the two summation equations or the total mass balance would be used.

In 1893, Sorel published the fundamental equations for this equilibrium model. Unfortunately, these equations were relatively complex at that time and were only put into practice using a graphical technique by Ponchon (1921) and Savarit (1922). Thiele and Geddes (1933) and Lewis and Matheson (1932) developed iterative numerical methods to obtain a solution to Sorel's model. These techniques were first implemented using computers by Amundsen and Pontinen (1958) and have been improved upon and applied to a large number of column configurations and systems. They have been implemented in ChemSep and the RADFRAC algorithm of Aspen Plus™.

2.4.3 Efficiency Models

The use of stage efficiencies (see Section 2.3.2) can be implemented and Equation 2.18 shows the effect of this on the equilibrium equation (Equation 2.14).

$$E_{ij} \equiv E_{i,j}^{MV} K_{i,j} x_{i,j} - y_{i,j} - (1 - E_{i,j}^{MV}) y_{i,j+1} = 0 \quad (2.18)$$

The use of Murphree efficiencies has been shown to be effective for binary systems or close boiling ideal multicomponent mixtures, but its use in general multicomponent mixture systems is problematic. E^{MV} values are not the same for each component and

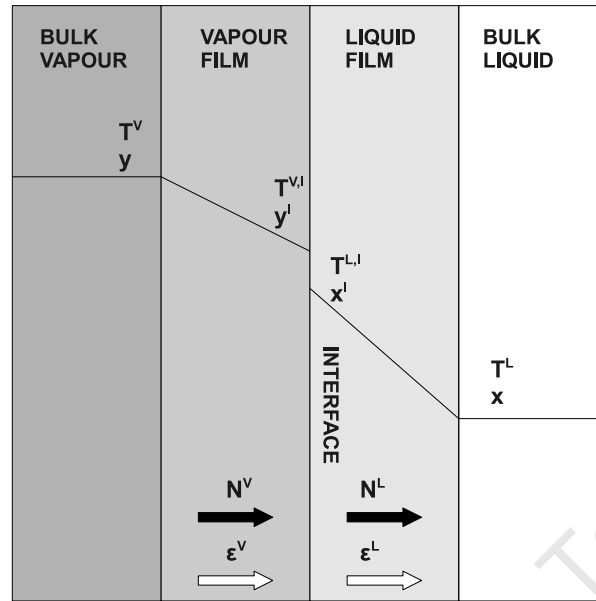


Figure 2.5: Two-film theory model

differ from stage to stage. Additionally, E^{MV} values for binary systems lie between 0 and 100%, while multicomponent E^{MV} values have no such restrictions.

2.4.4 Rigorous Rate-based Model

In a series of papers, Krishnamurthy and Taylor (1985a, 1985b, 1985c) developed a rate based nonequilibrium distillation model that extends the equilibrium model discussed in Section 2.4.2. It applies the two-film theory shown in Figure 2.5 and requires correlations of mass- and heat-transfer coefficients. The number of equations and variables increases from $2c + 5$ to $6c + 8$. Figure 2.6 shows an example of a nonequilibrium stage and the variables associated with it.

The equations include the component *Mass* balances in each phase

$$M_{ij}^V \equiv (1 + r_j^V)V_j y_{i,j} - V_{j+1} y_{i,j+1} - (1 - q_j^F)F_j y_{i,j}^F + N_{i,j}^V = 0 \quad (2.19)$$

$$M_{ij}^L \equiv (1 + r_j^L)L_j x_{i,j} - L_{j-1} x_{i,j-1} - q_j^F F_j x_{i,j}^F - N_{i,j}^L = 0 \quad (2.20)$$

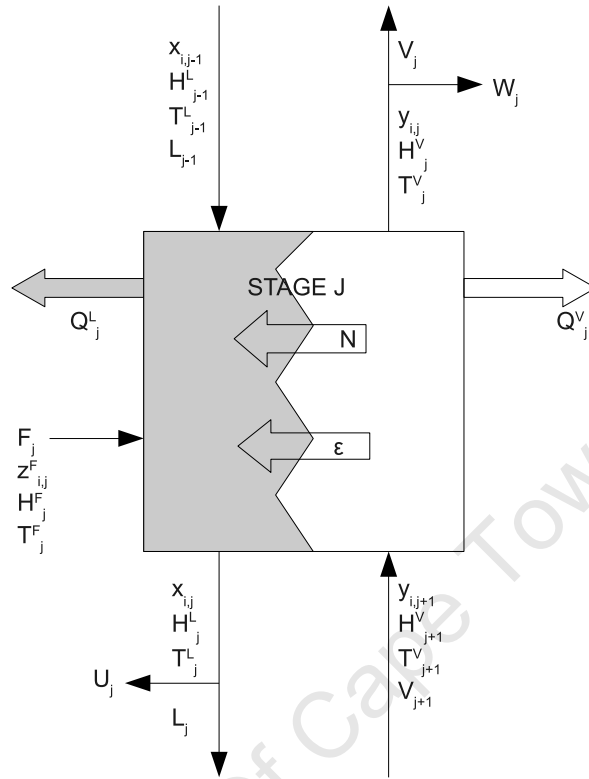


Figure 2.6: Nonequilibrium stage model

the overall Mass balances for each phase

$$M_{t,j}^V \equiv (1 + r_j^V)V_j - V_{j+1} - (1 - q_j^F)F_j + N_{t,j}^V = 0 \quad (2.21)$$

$$M_{t,j}^L \equiv (1 + r_j^L)L_j - L_{j-1} - q_j^F F_j - N_{t,j}^L = 0 \quad (2.22)$$

the Energy balance over each phase

$$E_j^V \equiv (1 + r_j^V)V_j H_j^V - V_{j+1} H_{j+1}^V - (1 - q_j^F)F_j H_j^{VF} + \epsilon_j^V = 0 \quad (2.23)$$

$$E_j^L \equiv (1 + r_j^L)L_j H_j^L - L_{j-1} H_{j-1}^L - q_j^F F_j H_j^{LF} - \epsilon_j^L = 0 \quad (2.24)$$

and at the interface

$$E_j^I \equiv \epsilon_j^V - \epsilon_j^L = 0 \quad (2.25)$$

the Rate equations for each component in each phase

$$R_{i,j}^V \equiv N_{i,j} - N_{i,j}^V = 0 \quad (2.26)$$

$$R_{i,j}^L \equiv N_{i,j} - N_{i,j}^L = 0 \quad (2.27)$$

where the mass transfer rates are given by

$$(N_{i,j}^V) = c_t^V [k_j^V] a_j^I (y_j - y_j^I) - (y_j) N_{t,j}^V \quad (2.28)$$

$$(N_{i,j}^L) = c_t^L [k_j^L] a_j^I (x_j^I - x_j) - (x_j) N_{t,j}^L \quad (2.29)$$

the mole fraction Summation equations for each phase at the interface

$$S_j^{VI} \equiv \sum_{i=1}^c y_{i,j}^I - 1 = 0 \quad (2.30)$$

$$S_j^{LI} \equiv \sum_{i=1}^c x_{i,j}^I - 1 = 0 \quad (2.31)$$

and finally the phase eQuilibrium equation for each component at the interface

$$Q_{i,j}^I \equiv K_{i,j} x_{i,j}^I - y_{i,j}^I = 0. \quad (2.32)$$

A good reference to this method is Taylor and Krishna (1993), which is a textbook that reviews and summarises the model. It has been implemented in ChemSep and the RATEFRAC algorithm in Aspen PlusTM and used extensively to model distillation columns using non-equilibrium stages.



Figure 2.7: Raschig rings used in packed distillation columns

2.5 Packed Columns

Columns containing a form of packing can be used as an alternative to trayed towers. These consist of a vertical column filled with either random (or dumped) packing, or structured packing. Random packing may be made of either metal, ceramic or plastic materials and are usually between 10 and 50mm in size. Figure 2.7 shows one type of these random packings called Raschig rings.

Structured packing is a newer alternative that allows for a lower pressure drop and has better mass transfer characteristics than random packing. Packed columns are used mainly in absorption or distillation with low flow rate requirements.

2.5.1 Modelling

To model a packed column, a section of the height is analysed and differential forms of the Rate-based model defined in Section 2.4.4 are then developed. The vapour component mass balance over the differential element is given by

$$y_i V|_{z+\Delta z} - y_i V|_z - N_i^V \Delta z = 0 \quad (2.33)$$

Dividing by Δz and taking the limit as Δz goes to zero, the equation becomes

$$\frac{d(y_i V)}{dz} = N_i^V \quad (2.34)$$

and if this equation is summed over all components, then

$$\frac{dV}{dz} = N_t^V \quad (2.35)$$

Similarly, the liquid mass balances are given by

$$\frac{d(x_i L)}{dz} = N_i^L \quad (2.36)$$

and

$$\frac{dL}{dz} = N_t^L. \quad (2.37)$$

The energy balance for the vapour phase over the element is

$$VH^V|_{z+\Delta z} - VH^V|_z + \epsilon^V \Delta z = 0 \quad (2.38)$$

and dividing by Δz and taking the limit as Δz goes to zero

$$\frac{d(VH^V)}{dz} = \epsilon^V \quad (2.39)$$

similarly, for the liquid phase

$$\frac{d(LH^L)}{dz} = \epsilon^L. \quad (2.40)$$

The other equations remain the same as in Section 2.4.4.

2.5.2 HETP

Packed columns by definition are continuous differential contacting devices and are best analysed as such. However, in practice, most packed columns are modelled using the Equilibrium model defined in Section 2.4.2 using an equivalent height of packing to

represent a single equilibrium stage. This height is defined as

$$HETP = \frac{H}{N_{eq}} \quad (2.41)$$

where N_{eq} is the number of equilibrium stages required to represent the same degree of separation attained using a height H of packing.

There is no theoretical basis for this concept (Seader and Henley (1998)), and the values of HETP for a system should be obtained using experimental data and backcalculating. Once the value of HETP is known for a specific system, it is possible to then model the system using the equilibrium stage model.

University Of Cape Town

University Of Cape Town

Chapter 3

Literature Review: Collocation

3.1 Solving Boundary Value Problems (BVPs)

Boundary Value Problems are systems of ordinary differential equations that have their solution and derivative values specified at more than one point. The most common of these is the two-point BVP

$$\frac{d^2y}{dx^2} = f(x, y, y'), \quad x \in (a, b) \quad (3.1)$$

with the boundary conditions

$$y(a) = \alpha \quad \text{and} \quad y'(b) = \beta. \quad (3.2)$$

It is not possible to integrate the equation directly and so this usually means that some sort of approximation method is required to solve these problems. One way of doing this is to use what is known as the shooting method. This effectively converts a BVP into an Initial Value Problem (IVP). It does this by changing the boundary conditions to be

$$y(a) = \alpha \quad \text{and} \quad y'(a) = \theta. \quad (3.3)$$

The value of θ is solved for iteratively until $y'(b) = \beta$ using conventional IVP solution strategies. Unfortunately, this method's success is based on the stability of the derived IVP. If a small change to the ODE results in a large change in the solution, then the IVP is said to have a low stability. The other problem associated with this method is

the choice of θ (the initial guess) and its effect on the iterative solver (e.g. Newton's Method).

Another method that is used to solve BVPs is the finite difference method. This method involves discretising the problem's domain into a grid or mesh. Then the derivatives are approximated as follows:

$$y'(a) = \lim_{h \rightarrow 0} \frac{y(a+h) - y(a)}{h} \quad (3.4)$$

becomes

$$y'(a) \approx \frac{y(a+h) - y(a)}{h} \quad (3.5)$$

if the distance between each point (h) is very small. This is the forward difference approximation, but other approximations can be used. The boundary conditions are also treated the same, so that a ODE system becomes a system of algebraic equations that can be solved using conventional linear or nonlinear equation solvers.

This method is very simple to program and usually results in a banded matrix which is fast to solve. Unfortunately, for high accuracy, a large number of points are needed (i.e. the space between points is small) and this results in a very large system of equations to solve.

The third method for solving BVPs is the method of weighted residuals (see Section 3.2).

3.2 Method of Weighted Residuals

The method of weighted residuals is an approximation technique for solving differential equations. It actually encompasses various methods including collocation, Galerkin and integral methods. Each method is defined by their test (or weighting) function. However they all have the same basic form.

If the system to be solved is of the form

$$\frac{d^2y}{dx^2} = f\left(x, y, \frac{dy}{dx}\right) \text{ with } p < x < q \quad (3.6)$$

and boundary conditions

$$y(p) = \eta \quad y'(q) = \theta \quad (3.7)$$

then a trial (approximate) solution is given by

$$\hat{y}(x, \mathbf{a}) = \sum_{i=1}^n a_i \phi_i(x) \quad (3.8)$$

where $\phi_i(x)$ are trial functions and by choosing the values of a_i , it is possible to satisfy the boundary conditions. A number of collocation points can be chosen between p and q and the trial solution forced to satisfy Equation 3.6 at each of these points, however this is the method of *weighted* residuals and so to determine the values of a_i , an average residual is set to zero.

Firstly a residual is defined by substituting the trial solution into the Equation 3.6

$$R(x, \hat{y}) = \frac{d^2 \hat{y}}{dx^2} - f\left(x, \hat{y}, \frac{d\hat{y}}{dx}\right) \quad (3.9)$$

then the weighted integrals of the residual are forced to zero

$$\int_p^q R(x, \mathbf{a}) w_k(x) dx = 0 \quad (3.10)$$

where $w_k(x)$ are the test (or weighting) functions. This integral is defined as an inner product

$$(u, v) = \int_z u v dz \quad (3.11)$$

and if it equals zero, then the two functions are orthogonal.

This then results in a set of n algebraic equations of inner products that are solved to obtain the coefficients a_i .

$$(R, w_k) = 0. \quad (3.12)$$

The test (or weighting) functions can be chosen in many different ways, and this is what defines the different types of methods. These include

- the collocation method

- the subdomain method
- the least squares method
- the moment method
- the Galerkin method.

3.2.1 Galerkin Method

In 1915, a Russian engineer Galerkin (1915) developed one of these methods. In this method the test function is the same as the trial function and so

$$w_k = \phi_k(x) \quad (3.13)$$

The Galerkin method is often the most accurate of the five methods mentioned above (Finlayson (1972)). However, as one increases the number of terms in the trial solution, it becomes more difficult to apply analytically.

The other challenge with all the methods is that they all require the integration of Equation 3.10. This may require numerical integration, if an analytical solution is not possible. However, one of the features of the collocation method described next is that the method uses Dirac delta functions and allows for easier integration. Therefore, the collocation method is the most widely applied method and still achieves a relatively high accuracy.

3.2.2 Collocation Method

The collocation method is relatively easy to apply and can achieve high accuracy. Its test function is the Dirac delta function at the n collocation points

$$w_k = \delta(x - x_k) \quad (3.14)$$

with the useful properties of

$$w_k = \delta(x - x_k) = \begin{cases} 1, & x = x_k \\ 0, & x \neq x_k \end{cases} \quad (3.15)$$

and

$$\int_z w_k R dz = R(x_k). \quad (3.16)$$

The method was first applied by Slater (1934) looking at electronic energy bands in metals and was developed by numerous researchers over the years. However, the position of the collocation points were initially chosen arbitrarily, but this leads to difficulties in solving the system.

3.3 Determining collocation points

The number of collocation points may not increase the accuracy of the solution, however, the placement of these points can have a significant effect on the accuracy of the solution (Rice and Do (1995)). In the orthogonal collocation method, the collocation points are taken as the roots of orthogonal polynomials. These functions are convenient as they are compact and contain only a few terms.

The first use of the roots of an orthogonal polynomial as the collocation points was done by Lanczos (1938) in which he used the roots of a Chebychev polynomial, which is the solution to the Chebychev equation.

$$(1 - x^2) \frac{d^2 y}{dx^2} - x \frac{dy}{dx} + n^2 y = 0 \quad (3.17)$$

This work was further developed, but was primarily used for initial-value problems. Villadsen and Stewart (1967) helped advance the method significantly when they developed orthogonal collocation for boundary-value problems. They did this by choosing the trial functions to be polynomials that satisfied the boundary conditions. The roots of these orthogonal polynomials were then the collocation points.

3.3.1 Jacobi Polynomials

Jacobi polynomials are one of these orthogonal polynomials. They are solutions to the Jacobi equation

$$x(1-x)\frac{d^2y}{dx^2} + [\alpha - (1-\beta)x]\frac{dy}{dx} + n(\beta+n)y = 0. \quad (3.18)$$

The solution to this equation would be the n -th order Jacobi polynomial $J_n^{(\alpha,\beta)}(x)$, which can be represented as a power series

$$J_n^{(\alpha,\beta)}(x) = \sum_{k=0}^n (-1)^{n-k} \gamma_{n,k} x^k, \quad (3.19)$$

where $\gamma_{n,k}$ are constant coefficients and α and β characterise the polynomial with respect to the weighting function

$$w(x) = x^\beta(1-x)^\alpha. \quad (3.20)$$

The Jacobi polynomials are given explicitly by the Rodrigues formula

$$J_n^{(\alpha,\beta)}(x)[x^\beta(1-x)^\alpha] = \frac{(-1)^n \Gamma(\beta+1)}{\Gamma(n+\beta+1)} \frac{d^n}{dx^n} [x^{n+\beta}(1-x)^{n+\alpha}] \quad (3.21)$$

where Γ is the Gamma function

$$\Gamma(x) = \int_0^\infty t^{x-1} e^{-t} dt \quad (3.22)$$

and since they are orthogonal polynomials, they satisfy the orthogonality condition

$$\int_0^1 [x^\beta(1-x)^\alpha] J_k^{(\alpha,\beta)}(x) J_n^{(\alpha,\beta)}(x) dx = 0. \quad (3.23)$$

3.3.2 Hahn Polynomials

Another type of orthogonal polynomial often used are the Hahn polynomials. These are defined as

$$Q(x, \alpha, \beta, n) = {}_3F_2 \left(\begin{matrix} -n, n + \alpha + \beta + 1, -x \\ \alpha + 1, -n \end{matrix}; 1 \right) \quad (3.24)$$

where ${}_3F_2()$ is a generalised hypergeometric function. They are the discrete analogue of Jacobi polynomials and as the number of collocation increases, it tends toward the Jacobi polynomials.

3.4 Finding the Roots of the Jacobi Polynomials

Orthogonal collocation requires the n roots of the Jacobi polynomial $J_n^{(\alpha, \beta)}$ defined in Section 3.3.1. Villadsen and Michelsen (1978) developed a technique given by the FORTRAN subroutine *JCOBI*. In this subroutine, the Jacobi polynomial, given below:

$$J_n^{(\alpha, \beta)}(x) = \sum_{k=0}^n (-1)^{n-k} \gamma_{n,k} x^k \quad (3.25)$$

is rescaled to form a node polynomial

$$p_n(x) = (x - x_1)(x - x_2)(x - x_3) \cdots (x - x_n) = \frac{J_n^{(\alpha, \beta)}(x)}{\gamma_{n,n}}. \quad (3.26)$$

This equation is not suited to computational programming and is calculated using the recursive formula

$$p_n(x) = (x - g_n)p_{n-1} - h_n p_{n-2} \quad (3.27)$$

where

$$g_1 = \frac{\beta + 1}{\alpha + \beta + 2}, \quad g_n = \frac{1}{2} \left(1 - \frac{\alpha^2 - \beta^2}{(2n + \alpha + \beta - 1)^2 - 1} \right) \quad (3.28)$$

and

$$h_1 = 0, \quad h_2 = \frac{(\alpha + 1)(\beta + 1)}{(\alpha + \beta + 2)^2(\alpha + \beta + 3)}$$

$$h_n = \frac{(n-1)(n+\alpha-1)(n+\beta-1)(n+\alpha+\beta-1)}{(2n+\alpha+\beta-1)(2n+\alpha+\beta-2)^2(2n+\alpha+\beta-3)}. \quad (3.29)$$

The Newton-Raphson method is used to solve for the roots using an initial guess of $x = 0$. This will result in the first root being x_1 and it is possible to find the next root by suppressing the previously determined zero. If $x_1, x_2, x_3, \dots, x_k$ previously determined roots have been found, then the following function can be constructed to suppress these roots

$$G_{n-k} = \frac{p_n(x)}{\prod_{i=1}^k (x - x_i)} \quad (3.30)$$

then the Newton-Raphson formula becomes

$$x_{k+1}^{(i)} = x_{k+1}^{(i-1)} - \left[\frac{G_{n-k}(x)}{G'_{n-k}(x)} \right]_{x_{k+1}^{(i-1)}} \quad (3.31)$$

to determine the root, x_{k+1} at the i -th iteration with the initial guess being

$$x_{k+1}^{(0)} = x_k + \varepsilon \quad (3.32)$$

where ε is a small quantity.

The derivative of the node polynomial is calculated using the recursive formula

$$p'_n(x) = (x - g_n)p'_{n-1} - h_n p'_{n-2}. \quad (3.33)$$

3.5 Collocation Method in Detail

3.5.1 Lagrange Interpolation Polynomials

An interpolation polynomial passing through a set of data points $(x_1, y_1), (x_2, y_2), \dots, (x_{n+1}, y_{n+1})$, can be expressed as an n -th degree polynomial

$$y_n(x) = \sum_{i=1}^{n+1} y_i l_i(x) \quad (3.34)$$

where $l_i(x)$ is the Lagrange interpolation polynomial defined as

$$l_i(x_j) = \begin{cases} 0 & i \neq j \\ 1 & i = j \end{cases} \quad (3.35)$$

or as

$$l_i(x) = \frac{p_{n+1}(x)}{(x - x_i)p'_{n+1}(x_i)}. \quad (3.36)$$

3.5.2 Derivative Matrices

Taking the first and second derivatives of the interpolation polynomial, one obtains

$$\frac{dy_n(x)}{dx} = \sum_{i=1}^{n+1} y_i \frac{dl_i(x)}{dx} \quad (3.37)$$

$$\frac{d^2 y_n(x)}{dx^2} = \sum_{i=1}^{n+1} y_i \frac{d^2 l_i(x)}{dx^2} \quad (3.38)$$

and at the interpolation points

$$\frac{dy_n(x_i)}{dx} = \sum_{j=1}^{n+1} y_j \frac{dl_j(x_i)}{dx} \quad (3.39)$$

$$\frac{d^2 y_n(x_i)}{dx^2} = \sum_{j=1}^{n+1} y_j \frac{d^2 l_j(x_i)}{dx^2}. \quad (3.40)$$

A first derivative vector can be defined as the $n+1$ derivatives at the $n+1$ interpolation points

$$\mathbf{y}'_n = \left[\frac{dy_n(x_1)}{dx}, \frac{dy_n(x_2)}{dx}, \dots, \frac{dy_n(x_n)}{dx}, \frac{dy_n(x_{n+1})}{dx} \right]^T \quad (3.41)$$

and the second derivative vector as

$$\mathbf{y}''_n = \left[\frac{dy_n^2(x_1)}{dx^2}, \frac{dy_n^2(x_2)}{dx^2}, \dots, \frac{dy_n^2(x_n)}{dx^2}, \frac{dy_n^2(x_{n+1})}{dx^2} \right]^T \quad (3.42)$$

with the function vector defined as

$$\mathbf{y}_n = [y_1, y_2, \dots, y_n, y_{n+1}]^T. \quad (3.43)$$

This allows the first and second derivative vectors to be written in terms of the function vector as follows

$$\mathbf{y}'_n = \mathbf{A} \cdot \mathbf{y}_n \quad (3.44)$$

$$\mathbf{y}''_n = \mathbf{B} \cdot \mathbf{y}_n \quad (3.45)$$

where the coefficient matrices are defined as

$$\mathbf{A} = \left\{ A_{i,j} = \frac{dl_j(x_i)}{dx}; \quad i, j = 1, 2, \dots, n, n+1 \right\} \quad (3.46)$$

$$\mathbf{B} = \left\{ B_{i,j} = \frac{d^2 l_j(x_i)}{dx^2}; \quad i, j = 1, 2, \dots, n, n+1 \right\}. \quad (3.47)$$

These values $A_{i,j}$ and $B_{i,j}$ can be obtained using the *DFOPR* subroutine by Villadsen and Michelsen (1978) using the derivatives obtained in the *JCOBI* subroutine.

3.6 Orthogonal Collocation on Finite Elements (OCFE)

If the profile being approximated is very steep, then collocation may struggle to fit the profile. One method of overcoming this is to increase the number of collocation points, but this often leads to oscillations in the solution. Another possible way to overcome steep profiles is to choose different values of α and β in the Jacobi or Hahn polynomials. This can place more points in the area of the domain where the profile is changing rapidly.

It is also possible to deal with steep profiles in another way. If the domain is divided into smaller finite elements and collocation is applied to each of these elements individually, then the method is called Orthogonal Collocation on Finite Elements (OCFE). It was first used to predict the effectiveness factor in a catalyst pellet by Paterson and Cresswell (1971). Effectiveness factors can have very steep profiles within catalyst pellets in chemical reactors.

OCFE can be summarised as follows. If the problem is of the form:

$$\frac{d^2y}{dx^2} = f\left(x, y, \frac{dy}{dx}\right) \quad \text{with } 0 < x < 1 \quad (3.48)$$

and boundary conditions

$$y(0) = \eta \quad y'(1) = \theta \quad (3.49)$$

then the domain is split into elements, for example

$$(0, 1) \rightarrow (0, w) \quad \text{and} \quad (w, 1). \quad (3.50)$$

Each of these domains is normalised, for example for the n -th element

$$u = \frac{x - x_n}{\Delta x_n} \quad \text{where} \quad \Delta x_n = x_{n+1} - x_n \quad (3.51)$$

then the differential equation becomes:

$$\frac{1}{\Delta x_n^2} \frac{d^2y}{du^2} = f\left(u, y, \frac{dy}{du}\right) \quad \text{with } 0 < u < 1. \quad (3.52)$$

The boundary conditions have to increase due to the increase in the number of equations.

Continuity equations fulfil the boundary conditions, as at the end of each element

$$y(x_n^-) = y(x_n^+) \quad (3.53)$$

and

$$\frac{dy}{dx}\bigg|_{x_n^-} = \frac{dy}{dx}\bigg|_{x_n^+}. \quad (3.54)$$

What this method allows for is different interpolating polynomials to be used in each element with differing number of collocation points. For steep profiles, the element in that part of the domain could have a high order polynomial, while in flatter sections, a low order polynomial will be sufficient. Another approach using OCFE would be to divide the domain where the steep profile is present into many elements and then have lower order polynomials in each of those elements.

3.7 Collocation and Process Design

Collocation has found a number of uses in the design and modelling of chemical processes. The main driver for its use is the reduction in the model order that collocation can attain. Figure 3.1 shows how the collocation method reduces the order of the system by interpolating the profile. The varied applications include fixed bed absorption columns (Kaczmarski et al. (1995)) and reactive absorption column superstructures (Algusune et al. (2006)).

Collocation has also been applied to packed bed reactors at the microscopic level, looking at the heat and mass transfer into the catalyst pellet (Finlayson (1972)) and where steep profiles are encountered, OCFE has been used (Carey and Finlayson (1975)). Packed bed reactors have also been investigated using collocation at a macroscopic level, looking at axial dispersion, interphase mass and heat transfer, as well as reaction kinetics (Gardini et al. (1985)).

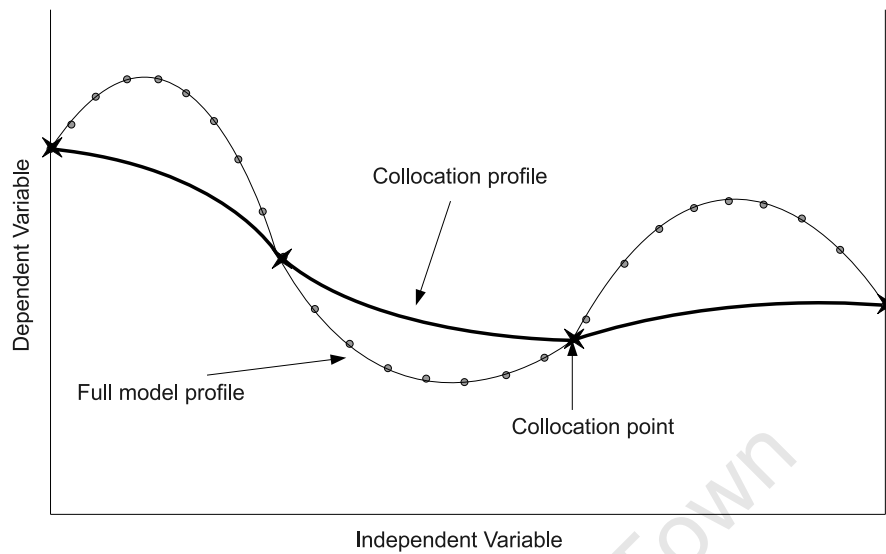


Figure 3.1: Collocation points showing order reduction

3.8 Collocation and Distillation

It is clear from Sections 2.4.2 and 2.4.4 that modelling separation systems, and distillation systems in particular, results in a system of many equations and variables (a high order system). The application of the collocation method to these systems has the potential to reduce the order of the system and allow for easier and faster solution of the systems without a significant decrease in the accuracy. This reduction in the order is due to the number of collocation points being fewer than the number of stages.

3.8.1 Staged Columns

Distillation columns consisting of trays as the contacting devices are the most widely used in industry. Therefore, it is not surprising that this is where most of the work using collocation on these systems has been focused.

The first work of collocation applied to a separation system was by Wong and Luus (1980). They developed a simple dynamic staged absorber model by converting the differential algebraic equations into partial differential equations and then applying the orthogonal collocation method to these new equations. Unfortunately, they found that the method they used did not preserve the mass balance in the steady state.

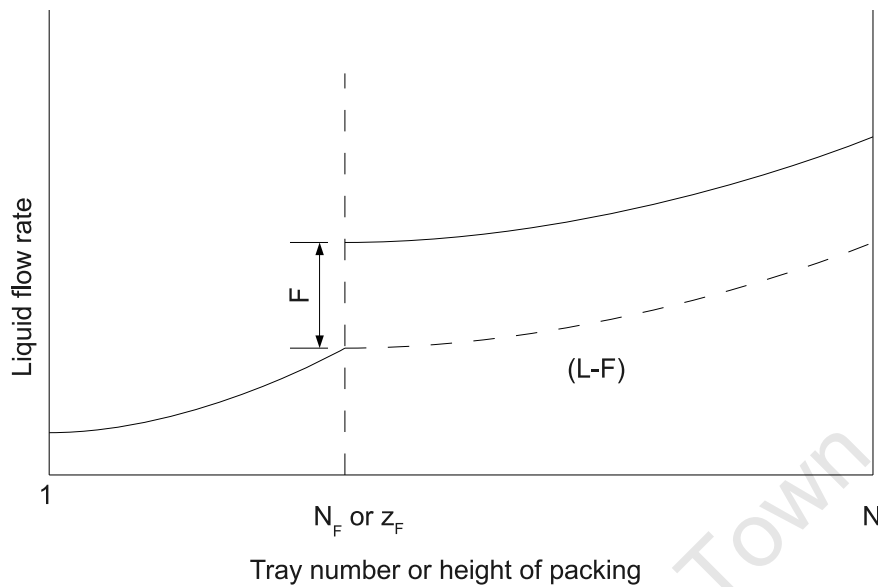


Figure 3.2: Discontinuity in the liquid flow rate due to a liquid feed at stage N_F

Later, Cho and Joseph (1983a) developed the idea further and in their second paper in a series (Cho and Joseph (1983b)) extended it to nonlinear multicomponent systems. They were also able to preserve the component and total mass balances over the column, unlike the earlier work.

Work by Stewart et al. (1985) also looked at the modelling of distillation columns using orthogonal collocation, treating the number of stages as a continuous variable.

Multiple Feeds and Sidestreams

In their third paper in the series, Cho and Joseph (1984) extended their model to take into account multiple feeds and sidestreams. They allowed for the discontinuities associated with these streams by redefining variables so that the column profiles could be fitted using a single polynomial over the entire column. Figure 3.2 shows this process where the liquid flow rate is redefined below a liquid feed stage.

They found that the resulting model was fairly accurate, but that the accuracy seemed to deteriorate as the collocation points were positioned further away from the feed and sidestream locations.

Srivastava and Joseph (1987a) continued the series of papers on the topic, with this

study focusing on multiple feeds and sidestreams again. However, in this case, they looked at using a spline fitting method to deal with the stream discontinuities instead of the variable redefinition approach. They decided to look at this as an alternative as the previous method had some drawbacks. They stated that the introduction of a feed into the column results in two types of discontinuities

$$L(z_F^-) \neq L(z_F^+) \quad (3.55)$$

$$\left. \frac{dL}{dz} \right|_{z_F^-} \neq \left. \frac{dL}{dz} \right|_{z_F^+}. \quad (3.56)$$

The previous method dealt with the first discontinuity by redefining the variable and approximating the whole profile by a single polynomial. Unfortunately, this does not deal with the second discontinuity and results in an oscillatory behaviour in the approximating polynomial.

The other problem given by Srivastava and Joseph (1987a) is that the first type of discontinuity was only accounted for at the collocation point nearest to the feed location and not at the exact location. The spline fitting method accounts for both of these discontinuities, by placing one of the collocation points exactly at the feed location and then approximating the entire profile by splines. They found that this method can greatly reduce the number of equations required as it only requires one additional equation for each feed stream, compared to the original model developed by Stewart et al. (1985).

3.8.2 Dealing with Steep and Flat Profiles

One problem that Srivastava and Joseph (1985) found when selecting the points for collocation was how to deal with steep and flat profiles within a column. Steep profiles need a higher order polynomial to approximate them, but if the same polynomial is used for flat profiles, then the profile obtained tends to oscillate. They were developing an Order Reduction Parameter (ORP), which is a function of how steep or flat the profile is in the column. For a binary system, the ORP is defined as

$$ORP = N \ln \left(\frac{L}{KV} \right). \quad (3.57)$$

and can be extended to a multicomponent system by

$$ORP(i) = N \ln A_E(i) \quad (3.58)$$

where $A_E(i)$ is usually given as some average of all the $A_j(i)$'s defined as

$$A_j(i) = \frac{L_j}{K_{i,j} V_j} \quad (3.59)$$

Unfortunately, this method, when applied to a rigorous model with all the variables changing down the column, will require an initial solution to calculate the values of the $A_j(i)$'s. However, if the collocation model is being used for dynamic studies, it is possible to use an initial solution at steady state to determine these values. This then allowed them to determine, *a priori*, whether many collocation points were needed or only a few. This is useful information as it allows for the best reduction of the system without compromising on accuracy.

By using the ORP, they were able to determine how many collocation points were necessary. At high ORP values, a large number of collocation points were needed (and hence reducing the effectiveness of the collocation method to reduce the order of the model). The problem still remained that some component profiles had high ORP values, while others had low ORP values in the same column. Since the number of collocation points is the same for all the component profiles, it was decided to use the highest ORP as the deciding factor. Unfortunately, this does not result in the optimal number of points for all the component profiles.

Srivastava and Joseph (1987b) attempted to overcome this problem by fitting the composition profiles with different polynomials for each component. They then developed a rather complex approach using global and local collocation points for non-step and steep profiles respectively. This results in a much more complicated model, but does result in a reduction in the number of equations and computational time required to solve the system.

Orthogonal Collocation on Finite Elements (OCFE)

To overcome the problem of using high order polynomials, the use of OCFE was suggested (Stewart et al. (1985)). This already is in effect when multiple feeds and sidestreams are present as it breaks the column up into elements (Srivastava and Joseph (1987a)).

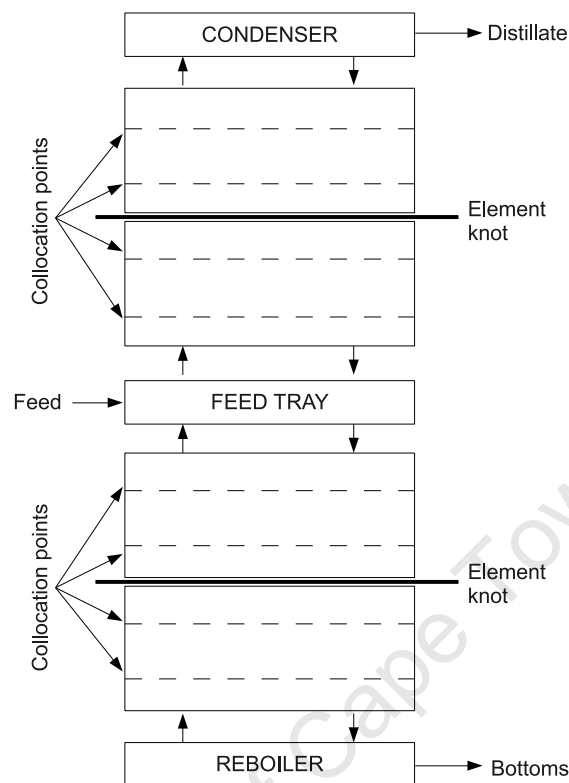


Figure 3.3: OCFE distillation model using two finite elements per section and two collocation points per element

However, it is possible to split each section into further elements that do not have these discontinuities at their boundaries. Figure 3.3 shows how this can be incorporated into a distillation model using two elements per section and two collocation points per element. The effect of using these elements on the collocation profile can be seen in Figure 3.4

Seferlis and Hrymak (1994) used this method to model distillation columns for use in optimisation studies. They were able to divide each column up into a number of elements and then apply a number of collocation points to each element. This keeps the order of the polynomials low and therefore reduces the oscillatory effect of using a higher order polynomial. At points in the column, where the profiles are changing rapidly, more collocation points can be applied.

Variable Transformations

Apart from the variable transformations described in Section 3.8.1, other transformations have been proposed to deal with the steep and flat profiles that can occur in distillation

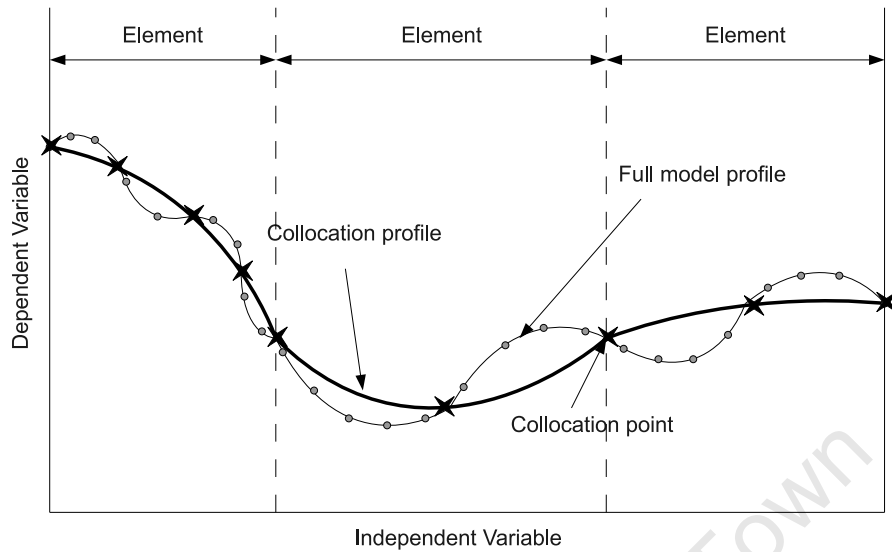


Figure 3.4: Order reduction using Orthogonal Collocation on Finite Elements

columns. Huss and Westerberg (1996) developed a collocation model for columns with flat profiles by using variable transformations. As the number of stages in a column increase, the profiles within the column flatten out. Huss and Westerberg (1996) used the following variable transformation to deal with this sort of problem

$$z = 1 - e^{-as} \quad (3.60)$$

where z is the transformation variable, s is the stage number, and a is some parameter. This transformation straightens out the trajectory by the fact that when $s = 0$, $z = 0$ and when s tends to infinity, then z tends to 1.

The other case for flattened profiles is when mole fractions tend towards 0 or 1 due to high purity distillation. To transform this asymptotic approach, Huss and Westerberg (1996) used the following transformation

$$2x_i - 1 = \tanh(\hat{x}_i) \quad (3.61)$$

where x_i is the mole fraction of component i and \hat{x}_i is the transformation variable. As the mole fraction goes to 0 or 1, the transformation variable goes to $-\infty$ and $+\infty$ respectively. The authors found that using these variable transformations had more effect in increasing the accuracy of the solution than the placement of the collocation points themselves.

3.8.3 Collocation and Reactive Distillation

Reactive distillation (RD) is a form of process intensification (see Section 4) that combines reaction and separation into a single unit to enhance the conversion or selectivity of a reaction. OCFE has been applied to RD column design by Seferlis and Grievink (2001) in which they used MESH equations to model the RD column. They looked at the production of ethyl acetate and divided the column into three sections due to the two feeds of acetic acid and ethanol. By using OCFE, they were able to transform the system into a set of algebraic equations that were then suitable for a Non-Linear Programming technique (see Section 5). They were also able to perform a sensitivity analysis.

3.8.4 Packed Columns

Due to their differential nature, packed distillation column models would seem like the ideal system to apply the orthogonal collocation method. Some of their attributes are:

- Their models can result in stiff problems when solving them by integration alone
- They result in Boundary Value Problems that require special methods to solve them (e.g. Shooting methods)
- Their independent variable (the height of the column (z)) is already continuous and therefore, there is no need to transform a discrete system, as with staged columns, into a continuous differential system, before applying the collocation method.
- The placement of the collocation points is not as crucial as with staged systems as the profiles are already continuous in each section.

It is surprising then to find that there has been very little application of orthogonal collocation on packed distillation columns of any form.

Continuous Operation

The first use of the collocation method on packed distillation columns was by Srivastava and Joseph (1984). They restricted their studies to modelling the rectifying section of a distillation column. In most of their case studies, they made a number of simplifying assumptions, particularly Constant Molar Overflow, and that the resistance to mass

transfer is only in the gas phase. They found that the method worked well in all the test cases, but stated that further work needed to be done using liquid and gas phase mass transfer resistance as well as looking at the effect of intermediated feed streams.

Karacan et al. (1998) modelled steady state and dynamic packed bed distillation columns using OCFE. Their research showed good results when compared to experimental data obtained for a methanol/water system.

Torres et al. (2000) conducted a comparison between a reduced order model using collocation for a packed distillation column and a rigorous nonequilibrium stage model. They found that the distillate and bottoms products agreed very well with the rigorous model, but found that the internal profiles were only reasonably predicted (especially when the system included steep and flat profiles). They did, however, find that the reduced order model was much more robust than the full model and converged to a solution in much less time.

Batch Operation

Due to the dynamic nature of batch distillation column models, their equations are not steady state equations, but include dynamic terms that change with time. Wajge et al. (1997) used the finite difference method and the collocation method to model a batch distillation column system. They found that the finite difference method was computationally intensive when compared to the collocation method. However, the collocation method required careful choosing of the polynomial order to obtain reasonable accuracy and efficiency.

Wajge et al. (1997) also looked at reactive distillation in a batch packed column. The production of ethyl acetate was used as a case study. They looked at various reflux configurations, but stated that a more rigorous optimisation method was necessary to fully ascertain the optimum operation of the batch system.

3.8.5 Orthogonal Polynomial Choice

Knowing that the accuracy of the collocation method increases when the collocation points are chosen as the roots of orthogonal polynomials, a number of these polynomials have been applied to distillation.

The original work by Wong and Luus (1980) used the roots of shifted Legendre polynomials to find the collocation points. However, Cho and Joseph (1983a) used the roots of the Jacobi polynomials as the collocation points for their staged model. They stated that these gave similar accuracy to the Galerkin method.

Stewart et al. (1985) performed extensive analysis of both Jacobi and Hahn polynomials with respect to staged distillation modelling and found that the roots of the Hahn polynomials were 10 times more accurate. However, Srivastava and Joseph (1985) also performed similar tests and found that there was no significant difference between using either polynomial. They did concede that for smaller columns, Hahn polynomials were more accurate. They stated that this was likely due to the discrete nature of Hahn polynomials and that the points tended to be located at the stage locations as the number of points increased.

It appears that it is accepted that for staged distillation models, Hahn polynomials are better than Jacobi polynomials. However, for packed continuous columns, either should produce similar results as their accuracy is not based on discrete stages. Therefore, Jacobi polynomials tend to be used for packed distillation modelling using the orthogonal collocation method.

University Of Cape Town

Chapter 4

Literature Review: Process Intensification

Process intensification has come under the spotlight in recent years as the cost of energy increases and resources become more scarce. By intensifying processes, one is able to minimise the capital costs of construction as fewer units need to be produced. One of the methods proposed is to combine the two most fundamental functions of chemical engineering into one unit. These two functions are namely reaction and separation.

In the petrochemical industry, reaction is usually done in a reactor using solid catalysts to speed up the reaction. Separation is conducted using distillation which takes advantage of the fact that each component has a different volatility. The conventional process involves the reactants being partially converted in a reactor and then the product mixture is separated in the distillation column, with the unreacted reactants usually recycled back through the reactor to achieve a viable overall conversion. An example of this type of system can be seen in Figure 4.1

4.1 Reactive Distillation

Reactive Distillation (RD) is one of the proposed methods of combining these two functions into one unit. The reaction can either be catalysed homogeneously or heterogeneously. For homogeneously catalysed reactions, the catalyst is usually some form of acid (e.g. sulphuric acid) that is added to the distillation mixture and the reaction then takes place inside the distillation column as the separation is occurring. This type of

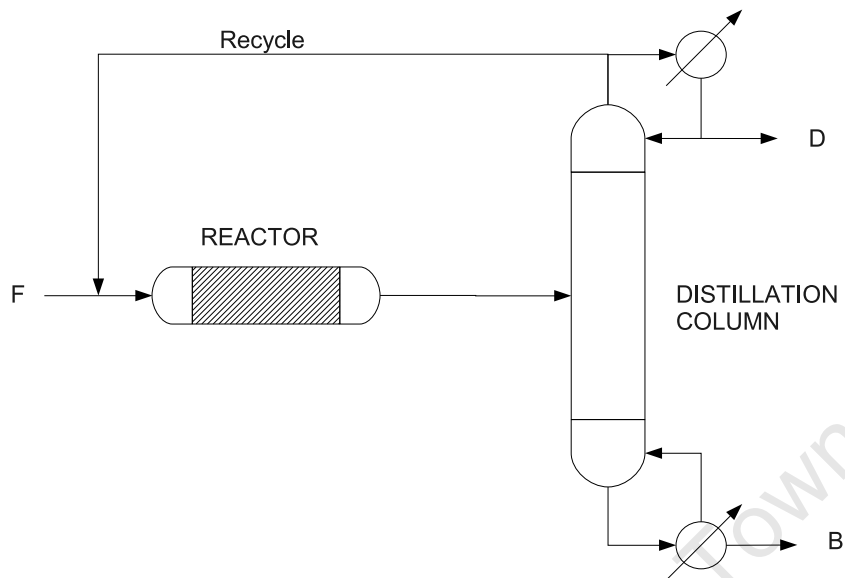


Figure 4.1: Conventional reactor-separator system

reactive distillation was first patented in the 1920s (Backhaus (1921)) and further work was done by Keyes (1932) and Leyes and Othmer (1945).

The use of heterogeneous catalysts in RD is more recent, with the first description by Spes (1966). A RD column using a heterogeneous catalyst usually consists of a reactive section in the middle of the column filled with catalyst particles suspended in envelopes of wire-mesh in a variety of shapes. In the case of structured packing, specially designed catalyst packing is available (e.g. KATAPAK-S by Sulzer and KATAMAX by Koch-Glitsch). Other options are to put the catalyst in the downcomers of trayed columns, or to actually make the packing out of the catalyst itself (e.g. in the shape of Raschig Rings - see Figure 2.7).

The RD column has conventional rectifying and stripping sections above and below the reactive section as shown in Figure 4.2. In the figure, the reaction $A + B \rightleftharpoons C + D$ occurs in the reactive section with the product C being the most volatile and removed in the distillate, while the product D is the least volatile and is removed in the bottoms.

4.1.1 Industrial Use of RD

A successful implementation of the use of RD columns was in the synthesis of methyl acetate by esterification of acetic acid with methanol (Agreda and Partin (1984)). This

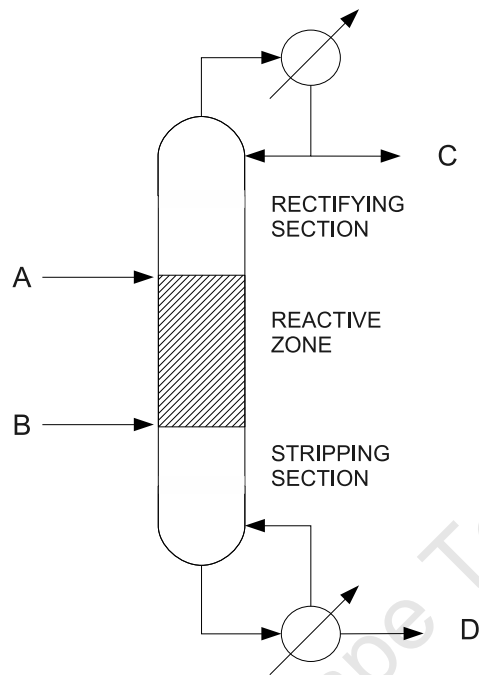


Figure 4.2: Reactive Distillation column

was developed by Eastman Kodak in the 1980s and has proved very successful in reducing capital and energy requirements by a factor of 5 (Sirola (1996)) when compared to the conventional process. The conventional process consisted of a reactor followed by a train of nine distillation columns while the RD system is a single column that is able to achieve nearly 100% conversion of the reactant.

Another important application of RD in industry is the acid catalysed reaction between iso-butene and methanol to form methyl tert-butyl ether (MTBE). This was developed by CDTECH in 1981 at Charter Oil in the USA (Harmsen (2007)). The traditional configuration of a reactor followed by a train of distillation columns is very complex due to the product mixture from the reactor forming three minimum boiling azeotropes (Taylor and Krishna (2000)). The RD system only requires a single column fed by a butene feed (non-reactive n-butene and reactive iso-butene) and a methanol feed near the bottom of the reactive section. It is able to convert nearly 100% of the iso-butene and methanol and reduce the formation of unwanted side products (Sundmacher (1995)).

Other potential applications of RD are:

- Hydration reactions, such as the hydration of ethylene oxide to mono-ethylene glycol ($EO + H_2O \rightarrow EG$) (Ciric and Gu (1994)). Using RD suppresses the side

reaction to di-ethylene glycol and utilises the high heat of reaction to vaporise the liquid on the trays.

- Alkylation reactions, for example, the alkylation of benzene with propene to form cumene (Shoemaker and Jones (1987)). RD allows for the suppression of the formation of the side product di-isopropylbenzene and reduces the problems of hotspots (can lead to runaway reactions) forming in the reaction zone.
- Hydrogenation reactions, such as the hydrogenation of benzene to form cyclohexane. It is possible to perform this reaction at moderate temperatures and pressures using RD to produce 99.9% pure cyclohexane (Gildert (2001)).

4.1.2 Advantages and Disadvantages of RD

From integrating the two functions of reaction and separation into a single unit, there are various advantages. These include:

- a reduction of capital costs due to the simplification of the overall system (especially the separation system)
- an improvement in conversion of the reactant (which can reduce the cost of recycling unused reactants)
- an improvement in selectivity by removing the desired product from the reaction mixture
- a reduction in the amount of catalyst for the same conversion (thus reducing the cost)
- avoiding azeotrope formation by changing the composition of the mixture via reaction
- integrating the heat of reaction into the heat of vaporisation of the liquid on each tray
- avoiding hotspots and runaway reactions by vaporising the liquid (and therefore slowing the reaction).

However, using RD does not come without some limitations and problems. These include (Towler and Frey (2000)):

- the volatilities of the reactants and products must be such that the concentrations of the reactants are high in the reaction zone
- the reaction needs to take place in the liquid phase
- the residence time of the reaction needs to be low, otherwise large columns and large liquid holdups will be required
- difficulty in designing RD for large flow rates due to liquid distribution in packed bed columns
- the possibility of a mismatch between the optimal conditions for reaction and separation
- dealing with deactivated catalyst within a distillation column.

Of these disadvantages, the most problematic is a conditions mismatch. If the reaction needs to take place at a high temperature and pressure, this will be problematic, as high pressures will be required to keep the reactants in the liquid phase.

4.1.3 Modelling RD Columns

Taylor and Krishna (2000) performed a comprehensive review of RD and the modelling of these systems. They found that most of the models are extensions of the equilibrium (see Section 2.4.2) and nonequilibrium models (see Section 2.4.4).

The equilibrium model is essentially the same except for the material balances which have an extra term so that for the steady state on stage j , the overall mass balance becomes

$$M_j^T \equiv V_j + W_j + L_j + U_j - V_{j+1} - L_{j-1} - F_j - \sum_{m=1}^r \sum_{i=1}^c \nu_{i,m} R_{m,j} \varepsilon_j = 0 \quad (4.1)$$

where $\nu_{i,m}$ is the stoichiometric coefficient of component i in reaction m , $R_{m,j}$ is the reaction rate of reaction m and ε_j is the reaction volume on stage j .

The mass balance for component i becomes

$$M_{ij} \equiv (V_j + W_j)y_{i,j} + (L_j + U_j)x_{i,j} - V_{j+1}y_{i,j+1} - L_{j-1}x_{i,j-1} - F_j z_{i,j}^F - \sum_{m=1}^r \nu_{i,m} R_{m,j} \varepsilon_j = 0 \quad (4.2)$$

The MESH equations can be solved in a similar manner to the non-reactive distillation column models described previously. Aspen PlusTM also has an algorithm that can solve these equilibrium models (including RD) called RADFRAC (Venkataraman et al. (1990)). It has been used by Bezzo et al. (1999), amongst others, to model actual industrial RD columns. Bezzo et al. (1999) used it to model an RD column producing propylene oxide from propylene chlorohydrin and calcium hydroxide. They were able to achieve agreement between the model and plant data by adjusting the Murphree efficiency.

Nonequilibrium modelling of RD columns is not as simple as adding a term onto the liquid phase mass balances as in the equilibrium model. This requires a look at both cases of homogeneously and heterogeneously catalysed reactions. For homogeneous RD, the mass balance for component i in the liquid phase becomes

$$M_{ij}^L \equiv (1 + r_j^L)L_j x_{i,j} - L_{j-1}x_{i,j-1} - q_j^F F_j x_{i,j}^F - N_{i,j}^L - \sum_{m=1}^r \nu_{i,m} R_{m,j} \varepsilon_j = 0 \quad (4.3)$$

The liquid holdup ε_j needs to be obtained from column internals specifications and correlations. Other considerations that need to be taken into account are fast reactions occurring in the liquid film, and equilibrium relations at the interface being influenced by additional species being formed. Otherwise, the same procedure can be followed as in Section 2.4.4.

There are two options when modelling heterogeneous RD columns using nonequilibrium models. It is possible to treat the reaction as a pseudo-homogeneous one. This results in equation 4.3 above with the reaction volume ε_j being the volume of catalyst on the stage. The other method would be to take into account catalyst diffusion and reaction separately and this would require knowledge of catalyst geometry.

The algorithm RATEFRAC in Aspen PlusTM uses this nonequilibrium model to model RD columns by adding equations to account for reaction and chemical equilibrium.

4.1.4 Comparisons between RD Columns and Conventional Systems

In a series of papers by Kaymak and Luyben (2004b),(2004c) and Kaymak et al. (2004), they investigated numerous cases using a generic exothermic reaction $A + B \rightleftharpoons C + D$. They first performed an economic optimisation on an RD system alone, looking at the effect of the chemical equilibrium constant (K_{eq}) on the design. They used a generic reversible reaction $A + B \rightleftharpoons C + D$. They found that as the K_{eq} decreases, the required number of reactive trays increases and this in turn has a negative effect on the cost of the process.

In their second paper (Kaymak and Luyben (2004c)), they compared RD column systems with conventional systems of a reactor followed by a separation section. They employed a grid search optimisation strategy and found that the RD system was more economical than the conventional system for any value of K_{eq} .

Kaymak et al. (2004) took the comparison further and looked at the effect of the relative volatility on the design of both types of systems. They found that if the relative volatilities decreased as the temperature reached the optimum reaction temperature, then the conventional system showed better economic characteristics.

4.2 Integrated Side Reactor Systems

It has been proposed that using external reactors integrated into the distillation column can achieve similar, if not better, performance to RD columns without having the limiting condition of requiring the same conditions for reaction and separation. This allows for optimisation of the distillation and reaction conditions to achieve the desired conversion.

An example of what an integrated side reactor system consists of can be seen in Figure 4.3. The system is made up of a conventional tray or packed distillation column where a liquid side stream is drawn off at some point down the column height. This stream is fed into one or more conventional reactors where the reaction takes place at optimum conditions. The reaction products are returned to the column and separated and recovered in the distillate or bottoms.

Buehler and Schoenmakers (1982) were the first to propose the use of a side reactor coupled to a distillation. They looked at the homogeneously catalysed esterification reaction of carboxylic acid. They found that using mineral acids as catalysts resulted in

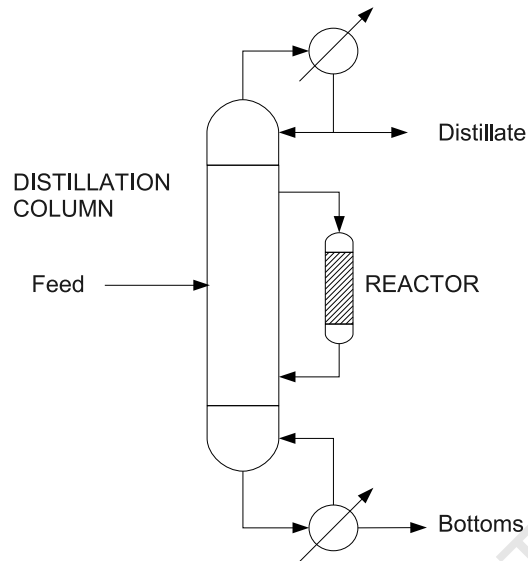


Figure 4.3: Integrated side reactor system

a loss of products in both systems. They suggested using ion exchange resins in external reactors to achieve equivalent conversion and energy consumption.

Various external reactor configurations were proposed by Baur and Krishna (2004). They can be seen in Figure 4.4 where 4.4(a) is a co-current configuration where liquid is drawn off at stage j and sent through the reactor and the products are returned to another stage further down the column. The amount of liquid withdrawn needs to be restricted to a limit of a certain fraction of the liquid flowing in the column. If that limit is exceeded, then the column can run dry in the intermediate stages between the sidestreams.

Figure 4.4(b) is the opposite of the previous configuration. The liquid is drawn off at a lower stage and then fed back into the column higher up. This configuration has the drawback that it can cause flooding and high flow rates in the stages between the sidestreams. This could also lead to increased energy requirements.

Both the co- and counter-current configurations have extreme cases illustrated in Figure 4.4(c) and (d) respectively. In the first case, all the liquid is removed from the stage and then the reactor products are returned to the stage immediately below. This case could be implemented using catalyst placed in the downcomers and then no external reactor would be necessary.

Figure 4.4(d) shows that some of the liquid from a stage can be sent to the reactor and

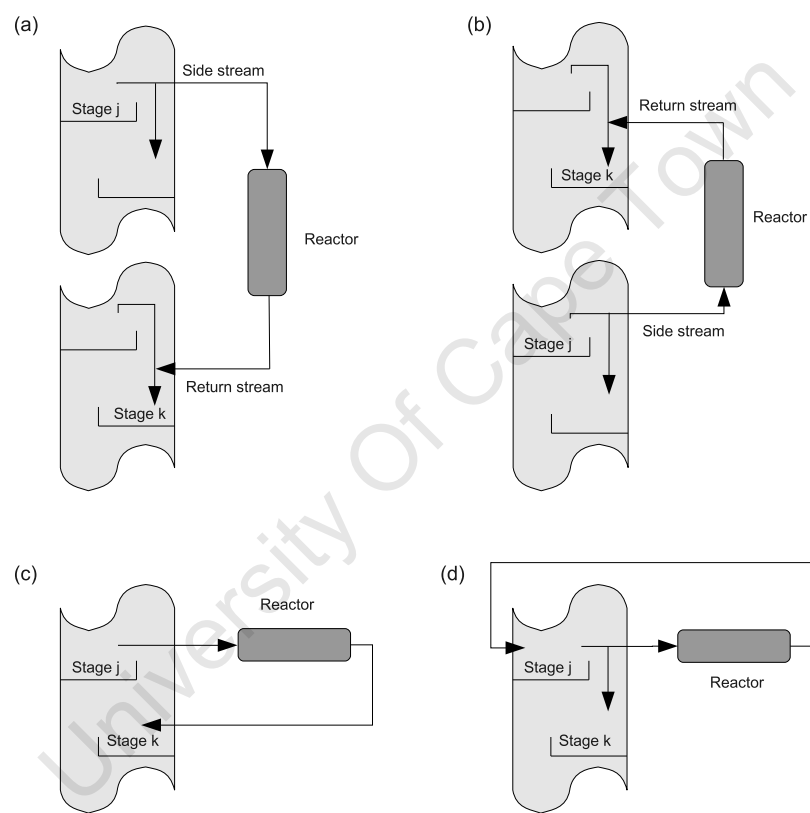


Figure 4.4: Side reactor configurations (a) co-current (b) counter-current (c) reactor-separation unit (d) local stage side reactor (adapted from Baur and Krishna (2004))

the products returned to the same stage. This could also result in a flooded stage as in the counter-current configuration above.

4.2.1 Modelling Side Reactor Systems

Side reactor systems are often modelled using the same methods as conventional process modelling. Distillation columns are modelled using either the Equilibrium or Nonequilibrium models described earlier. CSTR and PFR models are used to model the reactors. Often flowsheeting software, such as Aspen PlusTM, has been used to model the systems (Chiang et al. (2002), Citro and Lee (2004)). It is often difficult for these packages to converge to a solution when there is a recycle stream present. In the case of the side reactor systems at hand, there could be multiple reactors and therefore multiple recycle streams.

Jakobsson et al. (2002) used a novel approach and modelled the whole system as one unit and solved all the equations simultaneously. They used the simpler MESH approach using Murphree efficiency for the distillation column model. They tested their method on the production of MTBE and found that the system could achieve isobutene conversions of > 94% and solved the system efficiently.

To find the optimal placement of the side reactors, Baur and Krishna (2004) developed an algorithm using a one-dimensional line search. They decided to limit their search directions due to the high computational costs, but were able to investigate the methyl acetate synthesis system.

4.2.2 Comparisons with RD

Due to the similar nature of the two processes, side reactor systems and RD columns have been the subject of a number of comparison studies. Baur and Krishna (2004) used their algorithm to determine the optimum placement of the reactors to achieve the best conversion of acetic acid. They then compared their results with an RD system and found that for high conversions, RD columns are still favourable, but for more modest conversion levels, the side reactor system could achieve similar performance.

Chiang et al. (2002) studied the amyl acetate production and found that RD was better than a coupled reactor system in terms of economic considerations. However, the

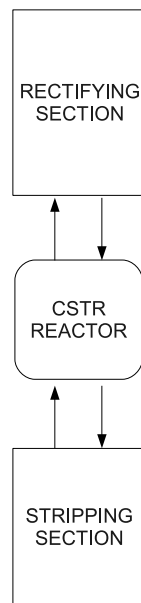


Figure 4.5: Coupled reactor system used by Chiang et al. (2002)

external reactor system was of a different configuration to those proposed previously (see Figure 4.5). They also looked at the dynamic control of RD columns and found it to be rather complex.

Kaymak and Luyben (2004a) extended their investigation (discussed in Section 4.1.4) to include an external side reactor system. They stated that if there is a significant mismatch between the optimum temperature for the reaction and distillation, then the external reactor system has much better steady state economics than RD or conventional systems.

Another comparison was conducted by Ouni et al. (2004), looking at optimising the reaction conditions in TAME production and isobutylene dimerisation. Both of these reaction systems have been proved to be viable in RD systems and if low internal flow rates are used, the side reactor system is not comparable. However, when they were able to optimise the reaction conditions in the external reactors, they found that the side reactor system can be a viable alternative to RD (in terms of conversion and selectivity).

Citro and Lee (2004) used a technique called the concurrent design method, based on partial control, to find alternative designs to RD systems. They found that the side reactor system is suitable for most reaction systems where there is a mismatch in conditions. They also state that these systems have a great potential to extend the applicability of RD.

In another comparative study, Nava et al. (2004) compared the production of TAME using RD and a side reactor system. In both cases a pre-reactor was necessary and they found that the side reactor system had higher energy requirements due to high reflux ratios. They did not conduct an economic study, but did find that to achieve comparable conversions, only one external reactor would be necessary.

In an interesting investigation, Bisowarno et al. (2004) looked at the use of side reactors applied to a reactive distillation column. They used the ETBE process as a case study and found that by adding a side reactor to an RD system can reduce the number of reactive stages required, and this has the potential to reduce costs.

4.2.3 Advantages and Disadvantages of the Side Reactor System over RD

From the discussion above, it is clear that using integrated side reactors has some potential advantages over RD systems. These include:

- being able to optimise conditions in both the distillation column and the reactors
- catalyst deactivation can be dealt with much more easily due to the reactor being outside the columns
- the reaction is not limited to the liquid phase
- conventional modelling techniques can be used to model the reactor and distillation column
- in some cases, it is clear that the side reactor system is more economical than RD or conventional systems.

The disadvantages include:

- the side reactor system is not always more economical
- the effect of removing products from the reactive zone is less pronounced than in RD
- modelling the system is difficult in some cases due to the recycle streams

- high internal and external recycle flow rates are often necessary to achieve reasonable conversions.

University Of Cape Town

University Of Cape Town

Chapter 5

Literature Review: Distillation Column Optimisation

Optimising a distillation column is an important part of designing a chemical process. They contribute a large portion of the operating and capital costs and by minimising these, large savings can be made. To optimise a staged distillation column, the number of trays and feed location need to be selected. Other operating conditions such as reflux ratios and heat duties need to be considered.

The operating conditions can be considered as continuous decision variables, but the feed location and the number of trays are discrete variables. It is these discrete variables that cause complications in the optimisation of the columns and, therefore, special optimisation techniques need to be employed to deal with these issues. There are two major representations of problems involving discrete and continuous variables. These are Mixed Integer Non-Linear Programming (MINLP) and Generalised Disjunctive Programming (GDP).

5.1 Mixed Integer Non-Linear Programming

Mixed Integer Non-Linear Programming problems are of the form

$$\begin{aligned}
 \min \quad & Z = f(x) \\
 \text{s.t.} \quad & h(x) = 0 \\
 & By + g(x) \leq 0 \\
 & x \in \mathbb{R}, \quad y \in (0, 1)^m
 \end{aligned} \tag{5.1}$$

and can be solved using a variety of methods that include branch and bound (solving NLP problems at each node), generalised Benders decomposition and outer approximation methods. The last two are iterative methods where the discrete 0-1 variables are fixed and then NLP subproblems are solved. A master MILP problem predicts bounds and new values of the 0-1 variables.

MINLP was first applied to chemical engineering applications by Grossmann and Kravanja (1995), with Novak et al. (1996) extending the method to apply it to a complete flowsheet of heat-integrated distillation columns.

The simplest optimisation problem for a single distillation column would be to find the optimum location of the feed stage with a fixed number of stages. This is represented in Figure 5.1 as a problem where the feed is split into as many streams as there are stages. This type of problem usually is solved as a relaxed NLP problem as the optimal solution is almost always where the feed is on a single tray (usually where the composition of the tray matches the feed composition).

Adding to the complexity of the problem is the optimisation of the number of trays. If a tray “disappears” and the flows go to zero in the stage, then convergence problems are likely. The first use of a MINLP formulation for optimising a distillation column was Viswanathan and Grossmann (1990), where they used a binary variable of 1 to denote the existence of a stage, while a 0 signified the absence of the stage.

However, this method is quite computationally intensive and another approach was proposed by Viswanathan and Grossmann (1993). In the new approach, the feed tray is fixed and then the reflux and reboil streams are returned to all possible stages above and below the feed stage respectively (see Figure 5.2). The discrete 0-1 variables are assigned to the existence of the reflux and reboil streams on each stage. The problem with this new method is that in the streams above the potential reflux, there is no liquid

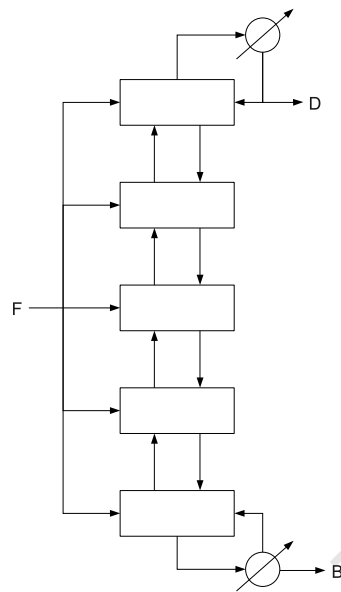


Figure 5.1: Feed location optimisation problem using MINLP

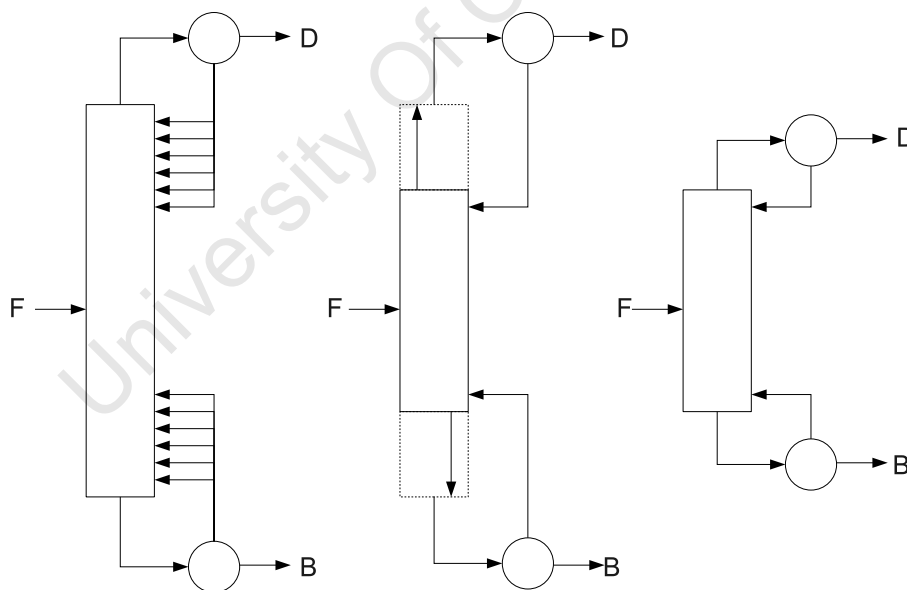


Figure 5.2: MINLP using variable reflux and reboil stream location

flow and this results in problems with the vapour-liquid equilibrium. It has however been applied successfully by Aguirre et al. (2001) and Bauer and Stichlmair (1998), amongst others.

Another alternative formulation proposed by Barttfeld et al. (2003) is shown in Figure

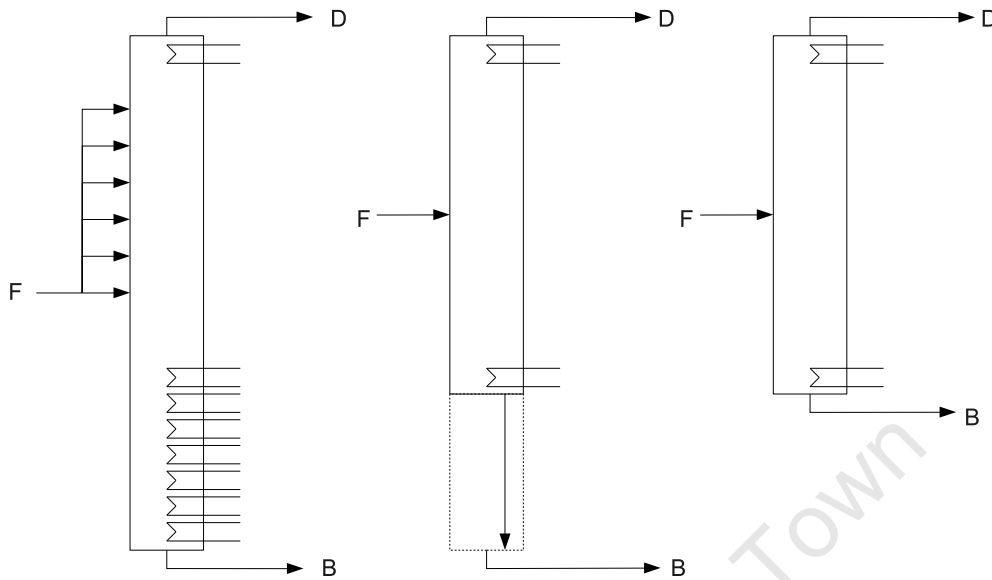


Figure 5.3: MINLP using variable reboiler location

5.3 where the condenser location is fixed and then the actual reboiler and feed location is variable. The other alternative of a fixed reboiler and variable condenser was also investigated, but found to be less effective. They found that they could potentially achieve more efficient energy designs using their new alternative formulation.

MINLP has also been used to optimise RD columns. Ciric and Gu (1994) applied MINLP to minimise the total annual cost (TAC) using the constraints formed by the MESH equations, modified as in Section 4.1.3. They applied it to the ethylene glycol synthesis reaction in a RD column.

Recently, Gangadwala and Kienle (2007) also applied MINLP to the synthesis of butyl acetate in a RD column and a side reactor system. They compared their results to those obtained using a single parameter optimisation and found that they could improve the heat duty in the reboiler by 5% in the RD column and 30% in the side reactor system.

5.2 Generalised Disjunctive Programming

Another way of solving the optimisation of distillation column problem was proposed by Yeomans and Grossmann (2000). It involves a Generalised Disjunctive Programming (GDP) model that is able to deal with the problems associated with the MINLP models.

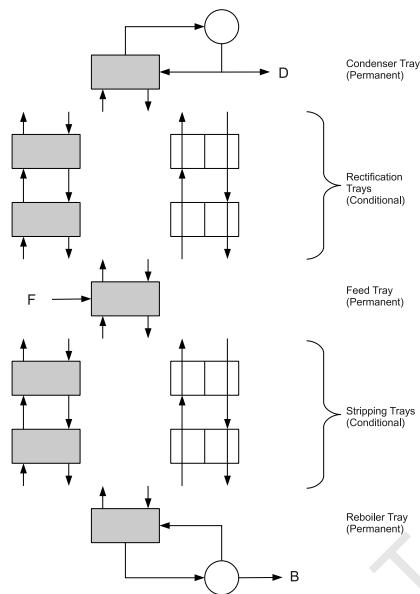


Figure 5.4: GDP model with permanent and conditional trays

It effectively “bypasses” the nonexisting trays by assuming no mass transfer occurs on them. This results in trivial material and energy balances on these trays. Figure 5.4 shows the structure of this GDP model where the shaded stages represent existing trays. For the equilibrium (MESH) model, the only difference between the existing and nonexisting stage would be the equilibrium equation (2.14).

5.3 Comparisons between MINLP and GDP for Distillation Optimisation

In a comparative study by Barttfeld et al. (2003), they compared the use of MINLP and GDP methods when optimising distillation columns. They found that the GDP formulations are more robust and less computationally intensive as the MINLP formulations. MINLP formulations are computationally intensive due to the fact that even if a tray does not exist, the relevant MESH equations still need to be solved. They also found that the GDP model is not as sensitive to the initial guess as MINLP.

5.4 Collocation in Distillation Column Optimisation

Collocation methods have been used previously in the optimisation of distillation columns. Swartz and Stewart (1986) extended the stagedwise orthogonal collocation method by Stewart et al. (1985) to optimisation of the design of distillation columns. They attempted to minimise the number of stages in a simple binary system using the golden section search method. They compared the results obtained to those from the McCabe-Thiele method and found the results to be comparable. An economic study was also conducted using a five component system. They used an SQP method and found that the collocation results matched those obtained using a full stagewise model.

To avoid using MINLP or GDP formulations to optimise a distillation column, Seferlis and Hrymak (1994) used OCFE to model a tray column. This resulted in a reduced order model that could be formulated as an NLP problem. They used two types of NLP solvers to solve the problem and compared the results to a tray-by-tray model and found that they converged to the same optimal solution. However, the collocation model reduced the model size and solution time considerably and was more robust as well.

5.5 Genetic Algorithms

The methods described above are classified as gradient based optimisation strategies to solving MINLP problems. MINLP problems are difficult to solve and conventional techniques often fail due to discontinuities and nonconvexities in the formulation. Rigorous models are often substituted by simplified ones to reduce the complexities of the problem, but this can result in the loss of many feasible solutions.

Stochastic algorithms have been used to solve these systems as well. These are usually adaptive random searches and have been used to successfully solve MINLP problems by Reklaitis et al. (1983) and Salcedo (1992), amongst others. The problem with these methods is that they are very computationally intensive.

Evolutionary algorithms, such as Genetic Algorithms (GAs) and Simulated Annealing (SA) have been applied to a wide variety of chemical engineering problems. These include heat exchange networks (Androulakis and Venkatasubramanian (1991)), mass exchange networks (Garrard and Fraga (1998)), heat exchangers (Tayal et al. (1999)) and heat integrated distillation column systems (Wang et al. (1998)). The reason for this is that

Table 5.1: Example of a binary encoding of 3 variables to a single individual

Variable	a	b	c
Real value	10	240	6000
Binary value	000001010	011110000	111110100
Chromosome (or individual)	000001010011110000111110100		

they only require the objective function value and no other information is necessary. This results in them not being restricted to a specific type of problem.

5.5.1 Algorithm Structure

The term Genetic Algorithm was first used by Goldberg (1989) and they were inspired by natural selection and genetics. They were first proposed by Holland (1975), not to solve specific problems, but to study the adaption in nature and import these into computer systems. To apply a genetic algorithm to optimise a problem, the following are required:

- a genetic representation of the solution domain (often in the form a binary strings)
- a fitness function to evaluate the quality of the solution.

A genetic algorithm takes a randomly generated population of potential solutions to the problem and then, by applying genetic operators to this population, finds the best solution.

The genetic representation of the solution is called a *chromosome* or *individual*, traditionally represented by a binary string of 0s and 1s. Each of these chromosomes represents one of a number of possible solutions to the problem. They are made up of each component of the solution vector that has been converted to a binary encoding and then combined (in order) to form a string. This can be visualised in Table 5.1 where three variables are converted and combined to form a single individual.

The convenience of using these chromosomes, is that they are easily aligned due to their fixed size. This makes it easy for the crossover operation (described later) to take place.

Initialisation

For the GA to start the evolutionary process, it needs to generate an initial population of solution vectors. This is most commonly done randomly in which a population of n individuals (or chromosomes) are produced.

Selection

The selection strategy decides which individuals are going to be the parents for particular newborn individuals. This is usually done to favour the fitter individuals by a number of methods. These include:

- The so-called *roulette wheel selection*, where each individual's probability of being selected as a parent is proportional to its fitness
- *Rank-based selection*, where the individual's probability of being selected is based on its fitness ranking in the population, rather than the actual value.

Crossover

This genetic operator is the basic operation in genetic algorithms. It attempts to combine the best features of two individuals (the parents) to form two (hopefully) better individuals. This can be done in many ways, but two examples are (see Table 5.2):

- *Point crossover*: This operator aligns up both parents and uses a randomly selected crossover position to define which parts of each parents are carried over to the new individuals. The part of the first parent before the position is carried over to the first individual, while the part of the second parent after the position is transferred to the first individual.
- *Random crossover*: This method randomly selects each bit in the newborn individuals from either of the parents at that position.

Table 5.2: Example of a Point and Random Crossover operations

	Starting Population	Point Crossover	Random Crossover
Parent 1	1001100101	1001 100101	1 0 0 1 1 0 0 1 0 1
Parent 2	0100010110	0100 010110	0 1 0 0 0 1 0 1 1 0
Child 1		1001010110	1101010111
Child 2		0100100101	0000100100

Mutation

Mutation allows for new genetic material to enter the GA population to explore new regions and maintain diversity. This can also be implemented in a variety of ways, but two of the most common are:

- *Uniform mutation*: This acts to replace each component of the individual with a random value using a uniform probability. The mutation probability is usually kept low.
- *Non-uniform mutation*: This type of mutation acts as above, but the probability of mutation reduces as the optimisation progresses.

Replacement

To keep the population size constant, the generation of a new individual must be accompanied by the death of another. Choosing which to replace can be done in a variety of ways (see Figure 5.5):

- *Generational replacement*: This forms the same number of new individuals as a previous generation. The new individuals form a new generation that is hoped to have increased in fitness due to the choice of the “fitter” parents.
- *Elitist replacement*: This form of replacement places a certain fraction of the parent generation into the new generation. They are chosen on their fitness and so the best individuals are preserved from generation to generation. The other individuals are replaced as usual by crossover and mutation.

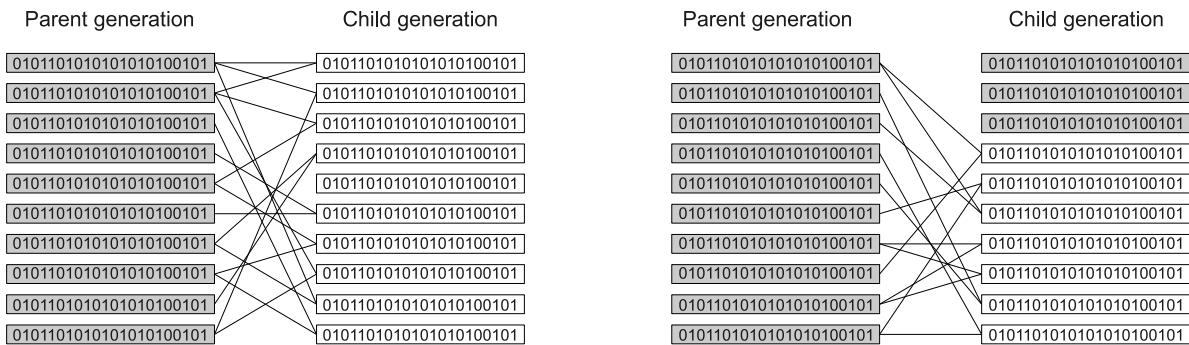


Figure 5.5: Replacement strategies for GAs

Overall Algorithm

Combining all the strategies described above, a simple genetic algorithm can be summarised as follows:

1. Initialise the population
2. Evaluate the fitness of each individual chromosome in the population
3. Repeat the following steps until a new population of the same number is produced:
 - Select a pair of chromosomes to be parents of a new generation via a selection strategy
 - Perform crossover and/or mutation to generate new individuals
4. Replace old generation with new generation
5. Go back to step number 2.

5.5.2 Dealing with Constraints

Most GA applied to constrained optimisation problems use a form of penalty function (Goldberg (1989)) to deal with constraints. This is usually simple and easy to implement by transforming the fitness function into

$$F(x) = f(x) + R \left(\sum_{k=1}^p [\max\{0, g_k(x)\}]^2 + \sum_{l=1} [h_l(x)]^2 \right). \quad (5.2)$$

The problem with this approach is that one needs to set the value of R , the penalty coefficient. This usually requires some experimentation to find a value that results in satisfactory performance.

Deb (2000) proposed a new constraint handling method that does not need a penalty coefficient. The basic idea behind the method is a tournament selector operator that enforces the following:

- Any feasible solution is preferred to an infeasible solution
- Between two feasible solutions, the one with the better objective function is preferred
- Between two infeasible solutions, the one with the smaller violation of the constraint is preferred.

The penalty function is then defined as

$$F(x) = \begin{cases} f(x) & \text{if } g(x) \leq 0 \text{ and } h(x) = 0 \\ f_{min} - (\sum_{k=1}^p [\max\{0, g_k(x)\}] + \sum_{l=1} |h_l(x)|) & \text{otherwise} \end{cases} \quad (5.3)$$

which can be better understood from Figure 5.6 when finding the maximum feasible solution.

5.5.3 GAs used to Optimise Distillation Columns

Because of the difficulty of dealing with the complexities of rigorous distillation models in MINLP or GDP formulations, they are usually avoided and simpler models are used. By only requiring the objective function value, GAs are able to use the rigorous models very easily.

Gross and Roosen (1998) and Leboeiro and Acevedo (2004) used a process simulator (Aspen PlusTM) coupled to a genetic algorithm to optimise a wide variety of distillation

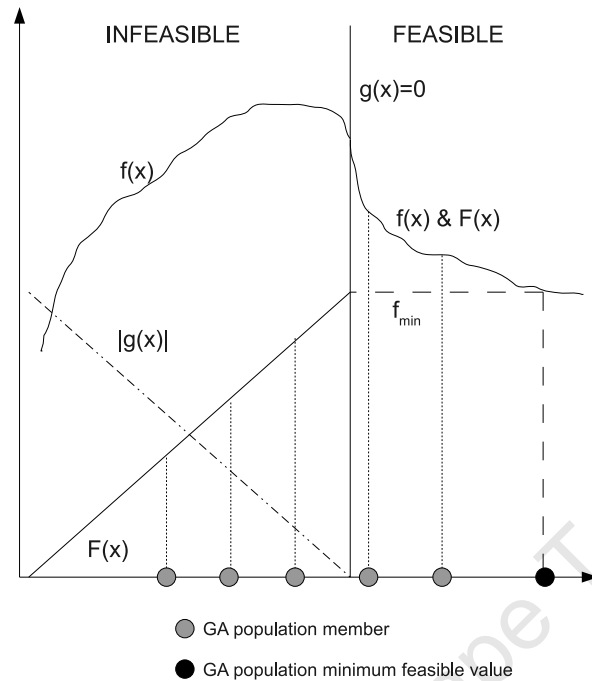


Figure 5.6: Constraint handling method by Deb (2000)

systems. Gross and Roosen (1998) looked mainly at column superstructures, while Leboeiro and Acevedo (2004) included extractive distillation, Petlyuk (Petlyuk et al. (1965)) configurations and complex superstructures.

Leboeiro and Acevedo (2004) also developed a new convergence criterion that involved evaluating the population's fitness. When 90% of the population is within 10% of the best solution found so far, a "mutation shock" is executed, causing the mutation probability to be 0.5 for one generation. This speeds up the process by introducing new genetic material to the population, but still keeps the best solutions through elitism.

When the population converges again, the best solution is compared to the previous best solution and if they are within a certain tolerance, the algorithm ends. Otherwise another mutation shock is applied. They found that the computational requirements were large and recommended finding new ways to reduce those requirements.

Chapter 6

Model Development and Methodology

6.1 Program Structure

6.1.1 Overall Structure

The FORTRAN program developed to optimise the side reactor systems consists of various modules and subroutines that are linked together to generate a result. The overall program structure can be seen in Figure 6.1. The user supplies various *input* parameters that include:

- Collocation input variables such as the number of collocation points within each section
- Distillation input such as the feed details, the packing type and (depending on what the optimisation parameters are) the reflux ratios, boilup ratios, sidestream ratios etc
- Cost data needed to calculate the capital and utility costs (e.g. CEPCI, types of heat exchangers)
- Optimisation details - these include the optimisation routine to be used, various parameters to be optimised, the formulation of the fitness function.

The *Optimisation* routine can be any one of the three routines described in Section 6.2. The fitness function needs to be developed, depending on the objective of the

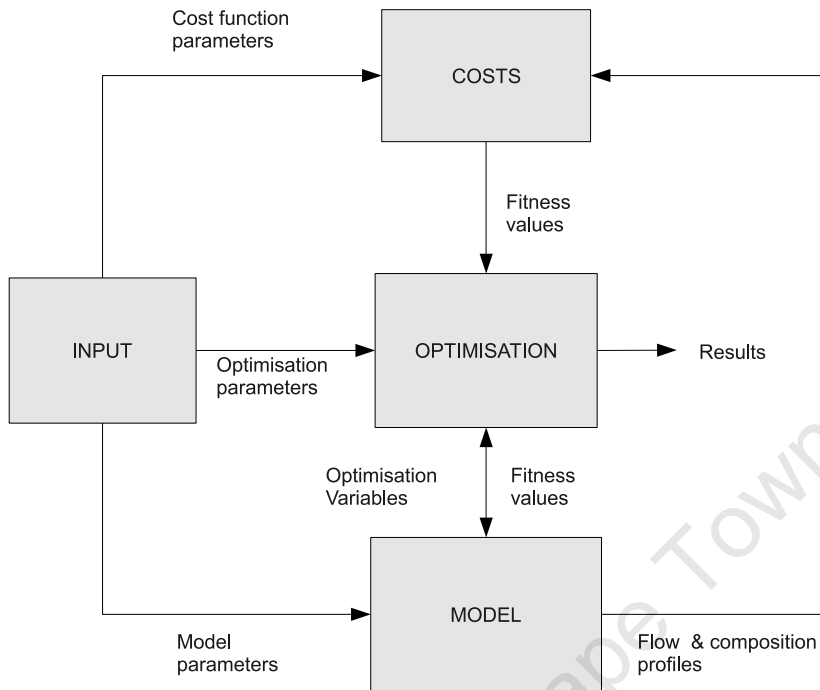


Figure 6.1: Overall Program Structure

optimisation study. Other choices to consider are the limits and ranges of the optimisation variables as well as the specific optimisation routine's operating parameters.

The *Model* routine will be described extensively in Section 6.1.2, but it effectively solves the side reactor system as a whole and produces column profiles and stream flows. These can be used in the *Optimisation* and *Cost* routines.

The *Cost* routine uses the results obtained from the *Model* routine and calculates the capital and utility costs. These values are used by the *Optimisation* routine to use in fitness functions when optimising various cost parameters (e.g. Total Annual Costs (TACs), capital and utility costs).

Once the *Optimisation* routine has all the information to calculate the fitness function from the *Cost* and *Model* routines, the optimisation parameters are altered and the whole procedure is repeated until a stopping criterion has been reached and a result is produced.

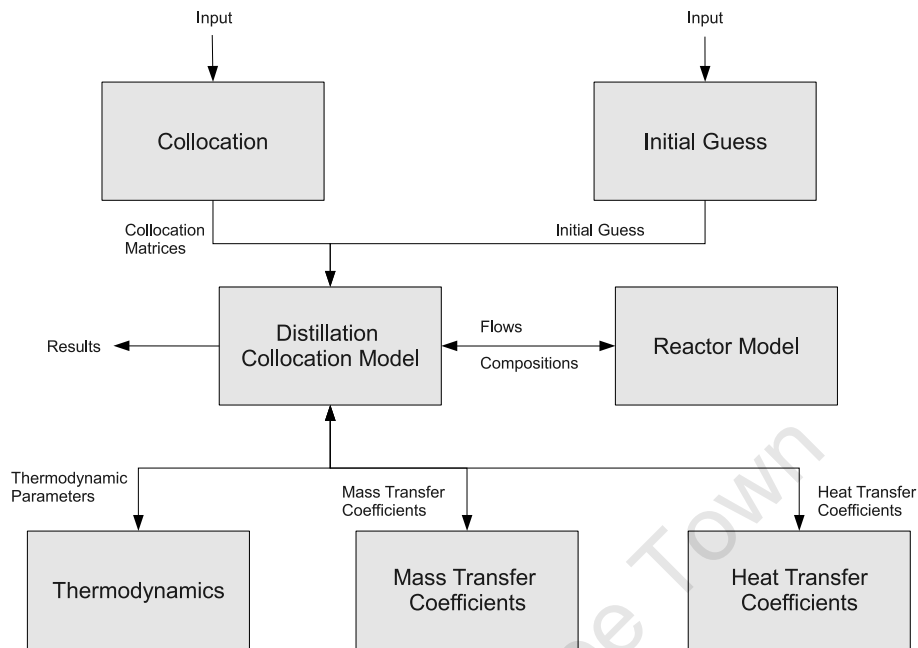


Figure 6.2: Model Structure

6.1.2 Model Structure

The *Model* routine described in Section 6.1.1 actually consists of a number of subroutines that act together to model the side reactor system (see Figure 6.2). These subroutines include:

- *Collocation* - This subroutine uses the information provided by the user and the *Optimisation* routine to calculate the collocation first derivative matrices ($A_{i,j}$).
- *Initial Guess* - The distillation column model is reduced to a set of non-linear algebraic equations that are solved in the *Distillation Collocation Model*. This is done using a Newton-Raphson method and requires an initial guess. This is done by solving a simple MESH equation model using the Constant Molar Overflow assumption. The results of this initial guess give composition profiles in the liquid and vapour phases as well as stage temperatures. The interfacial compositions and temperatures are assumed to be the same as the bulk values.
- *Distillation Collocation Model* - This is the main distillation model where the equations from Section 6.3.1 are solved by a Newton-Raphson method (the *HYBRD* routine from Minpack) using the boundary conditions described in Section 6.3.2.

It uses the collocation matrices and initial guess calculated above and solves the system. It calls on the *Reactor Model* during each iteration to obtain the reactor products. Other vital information is obtained from the *Thermodynamics*, *Mass Transfer Coefficients* and *Heat Transfer Coefficients* subroutines.

- *Reactor Model* - This is the model of the reactor that can be modified according to the reaction system being studied, as well as the type of reactor being used. Depending on the number of side reactors, this subroutine can be called a number of times in each iteration.

6.2 Optimisation

6.2.1 NLP

Due to the collocation method applied to the differential equations, and the fact that each section of the column was considered to have continuous profiles within them, it was thought that a Non-Linear Programming technique would be used to optimise the system. Two different NLP techniques were used in this research. One of these was the Sequential Quadratic Programming (SQP) method. This is a gradient based method that is similar to the Newton-Raphson method in one dimension.

DONLP2

The implementation of the SQP method was chosen as the software *DONLP2*, by Spelucci (1998). SQP methods find the search direction towards the optimum by minimising the quadratic approximation of the Lagrangian. The constraints are approximated linearly. The problem is usually defined as

$$\begin{aligned} \min \quad & Z = f(x) \\ \text{s.t.} \quad & h(x) = 0 \\ & g(x) \leq 0 \end{aligned} \tag{6.1}$$

which can be converted to a Lagrangian function

$$L(x) = f(x) + \lambda^T h(x) + \mu^T g(x) \tag{6.2}$$

where λ and μ are multiplier vectors for the constraints. The Quadratic Programming (QP) problem resulting from the above formulation is given by

$$\begin{aligned} \min \quad & Q = \nabla f^T \mathbf{s} + \frac{1}{2} \mathbf{s}^T (\nabla^2 L) \mathbf{s} \\ \text{s.t.} \quad & \nabla h^T \mathbf{s} + h = 0 \\ & \nabla g^T \mathbf{s} + g \leq 0. \end{aligned} \quad (6.3)$$

The solving of this problem results in the direction vector \mathbf{s} . This is then used to solve for the stepsize σ by solving a one-dimensional problem using a penalty function method. For example,

$$\min \quad \phi = f(x) + \sum_{j=1}^m \lambda_j |h_j(x)| + \sum_{k=1}^p \mu_k \max(0, g_k(x)). \quad (6.4)$$

This will allow for the calculation of the new x value by using the value of σ obtained from the above equation as follows

$$x_{k+1} = x_k + \sigma \mathbf{s}. \quad (6.5)$$

If the value of x_{k+1} is within some tolerance of x_k , then the iteration would end, otherwise the Hessian matrix ($\nabla^2 L$) would need to be updated and then the QP problem would need to be repeated.

SolvOpt

Some non-smooth functions were encountered when trying to optimise the systems and so the solver *SolvOpt* was used to overcome this problem. This solver uses Shor's r -algorithm (Shor et al. (1985)) to solve almost differentiable functions. This method effectively makes steps in the opposite direction to a subgradient at the current point in a transformed space. The algorithm is as follows:

Let $f(\cdot)$ be the almost differentiable function, then $g_f(x)$ is the gradient at point x . Assuming that k iterations have been performed, then x_k is the point where the transformation matrix is given by B_k and the transformed point is given by $\tilde{y}_k = B_k^{-1} x_{k-1}$. At the transformed point, a transformed function can be defined as $\phi_k(y) = f(B_k y)$ with its subgradient defined as \tilde{g}_k . For the $k + 1$ -th iteration, the following steps need to be taken:

1. Calculate $g_f(x_k)$
2. Calculate $g_k^* = B_k^T g_f(x_k)$, a subgradient of ϕ_k at the point $y_k = B_k^{-1}x_k$
3. Calculate $r_k = g_k^* - \tilde{g}_k$, the difference of the two subgradients of ϕ_k at y_k and \tilde{y}_k
4. Set $\xi_{k+1} = r_k/|r_k|$, the direction of the next space dilation to be performed
5. Calculate $B_{k+1} = B_k R_\alpha^{-1}(\xi_{k+1})$, where the space dilation matrix is given by

$$R_\alpha(\xi_{k+1}) \cdot x = x + (\alpha + 1)(x^T \xi_{k+1})\xi_{k+1} \quad (6.6)$$

6. Calculate $\tilde{g}_{k+1} = B_{k+1}^T g_f(x)$, another subgradient of the function $\phi_{k+1}(y) = f(B_{k+1}^T y)$ at the transformed point $\tilde{y}_{k+1} = B_{k+1}^{-1}x_k$.
7. Choose the stepsize h_{k+1}
8. Calculate $x_{k+1} = x_k - h_{k+1}B_{k+1}\tilde{g}_{k+1}$
9. Check convergence and repeat if necessary

6.2.2 Genetic Algorithms

Due to encountering discontinuities when optimising the systems, a GA was used to overcome this and optimise the system. The particular Genetic Algorithm used in this study was one developed by Carroll (1996), who developed it to model chemical lasers. The algorithm proceeds in the following way:

1. *Initialisation* - This initialises the population by distributing the parameters in the individuals randomly.
2. *Evaluation* - This calculates the fitness of each individual and assigns the best and average values.
3. *Niching* - This implements the sharing method by Holland (1975) and Goldberg and Richardson (1987), where the fitness is shared out between the number of similar individuals.
4. *GA Loop* - The following methods are repeated until the number of predefined generations is completed.

- *Selection* - Tournament selection is used to select the parents of the next generation.
 - *Crossover* - Either single point or uniform crossover can be applied.
 - *Mutation* - This mutates the child generation and can either be *Jump* or *Creep* mutation. *Jump* mutation is just another term for uniform mutation, while *Creep* mutation keeps the main merits of the parents by adding 1 to the last bit string.
 - *Replacement* - This can be done conventionally or with elitism applied so that the best parent is retained in a random slot.
5. *Micro-GA* - This is an option that starts out with a small population and evolves as a normal GA population. It converges quickly and then a new population is generated, keeping the best individual from the previously converged population and the process is repeated.

Stopping Criterion

The GA usually requires an input of how many generations are required to find a solution. This is often difficult to choose, as too few generations may result in a premature termination of the algorithm and the optimum solution not being found. Too many generations may result in very long computation times without an increase in the fitness of the best solution. Therefore, a stopping criterion was developed using the best individual fitness values from the *Micro-GA* routine. This stopping criterion consists of the following:

- The best individuals from the previous three *Micro-GA* generations are stored separately
- Each chromosome is compared with the other two using individual bits
- These differences are added up and divided by the number of bits in each chromosome
- If this value is below a certain tolerance then the algorithm stops. Otherwise the algorithm continues until the next best individual is attained using the *Micro-GA* method.

Constraint Handling

Most constraints encountered in this research were physical constraints of the system, such as the feed height being between 0.0m and the height of the column. These are easily dealt with in the GA's input parameters, but other constraints were encountered that required knowledge of the model results during the GA run. The constraint handling method described in Section 5.5.2, by Deb (2000) was used initially to deal with these types of constraints. However, the method requires that there be at least one feasible solution (adhering to the constraint) to be present in each generation. This was often not the case in many of the generations (especially when using the Micro-GA option) in a GA run and so the method was modified slightly.

The modification concerned the minimum feasible fitness value. Instead of using the minimum feasible fitness value per generation, the overall minimum feasible fitness value is used. This has the same effect on the overall fitness function as the previous unmodified method, but instead of the f_{min} value being zero for most of the run, it allows for all the infeasible solutions to have low fitness values quickly.

Convergence

Due to the different starting populations of each GA run, no two runs are identical. This is usually not a problem as multiple runs should reach the same global optimum solution. However, for these complex systems studied in this thesis, the GA runs often terminated (due to the stopping criterion described in Section 6.2.2 above) without even attaining a feasible solution (using the constraint handling method above).

Therefore, multiple runs were performed for each system to ensure that the global optimum solution was attained and, in the case of infeasible solutions, meaningful data could be obtained. By using the combination of the constraint handling method and the stopping criterion, the possibility of runs with very slow progression were minimised.

6.3 Distillation Collocation Model

6.3.1 Collocation Method Applied to a Packed Distillation Column Model

Using the method described in the Section 3.5, the equations discussed in Section 2.4.4 and 2.5.1 become

$$M_{i,j}^L \equiv \sum_{j=1}^N A_{i,j} (L_j x_{i,j}) - N_i \cdot \text{height}_{\text{section}} = 0 \quad (6.7)$$

$$M_{i,j}^V \equiv \sum_{j=1}^N A_{i,j} (V_j y_{i,j}) - N_i \cdot \text{height}_{\text{section}} = 0 \quad (6.8)$$

$$M_{t,j}^L \equiv \sum_{j=1}^N A_{i,j} L_j - N_t \cdot \text{height}_{\text{section}} = 0 \quad (6.9)$$

$$M_{t,j}^V \equiv \sum_{j=1}^N A_{i,j} V_j - N_t \cdot \text{height}_{\text{section}} = 0 \quad (6.10)$$

$$E_j^L \equiv \sum_{j=1}^N A_{i,j} (L_j H_j^L) - \epsilon_j^L \cdot \text{height}_{\text{section}} = 0 \quad (6.11)$$

$$E_j^V \equiv \sum_{j=1}^N A_{i,j} (V_j H_j^V) - \epsilon_j^V \cdot \text{height}_{\text{section}} = 0 \quad (6.12)$$

$$E_j^I \equiv h_j^V a_j^I (T_j^V - T_j^I) + \sum_{i=1}^c N_{i,j} (H_{i,j}^V - H_{i,j}^I) - h_j^L a_j^I (T_j^I - T_j^L) = 0 \quad (6.13)$$

$$R_{i,j}^L \equiv N_{i,j} - c_t^L [k_j^L] a_j^I (x_j^I - x_j) - x_{i,j} N_t^L = 0 \quad (6.14)$$

$$R_{i,j}^V \equiv N_{i,j} - c_t^V [k_j^V] a_j^l (y_j - y_j^l) - y_{i,j} N_t^V = 0 \quad (6.15)$$

$$S_j^{L,l} \equiv \sum_{i=1}^c x_{i,j} - 1 = 0 \quad (6.16)$$

$$S_j^{V,l} \equiv \sum_{i=1}^c y_{i,j} - 1 = 0 \quad (6.17)$$

$$Q_{i,j}^l \equiv K_{i,j} x_{i,j}^l - y_{i,j}^l = 0 \quad (6.18)$$

where i is for component i , while j represents collocation point j .

These equations are ordered into a vector with a corresponding variable vector, so that the Newton-Raphson method could be applied. Therefore, for each collocation point (j), the variables are ordered as follows

$$(\mathbf{x}_j)^T = \left(x_{1,j}, x_{2,j}, \dots, x_{c,j}, y_{1,j}, y_{2,j}, \dots, y_{c,j}, x_{1,j}^l, x_{2,j}^l, \dots, x_{c,j}^l, \right. \\ \left. y_{1,j}^l, y_{2,j}^l, \dots, y_{c,j}^l, N_{1,j}, N_{2,j}, \dots, N_{c,j}, L_j, V_j, T_j^L, T_j^V, T_j^l \right)^T \quad (6.19)$$

with the corresponding equation vector

$$(\mathbf{F}_j)^T = \left(M_{1,j}^L, M_{2,j}^L, \dots, M_{c,j}^L, M_{1,j}^V, M_{2,j}^V, \dots, M_{c,j}^V, Q_{1,j}^l, Q_{2,j}^l, \dots, Q_{c,j}^l, \right. \\ \left. R_{1,j}^V, R_{2,j}^V, \dots, R_{c-1,j}^V, S_j^{V,l}, R_{1,j}^L, R_{2,j}^L, \dots, R_{c-1,j}^L, S_j^{L,l}, M_{t,j}^L, M_{t,j}^V, E_j^L, E_j^V, E_j^l \right)^T. \quad (6.20)$$

6.3.2 Boundary Conditions

The modelling of packed distillation columns result in boundary value problems and so specific boundary conditions need to be defined on either side of a section or element. When using the system shown in Figure 6.3, the boundary conditions required are given in Table 6.1. They all apply to the equations that were originally in their differential form and have now been converted into an algebraic equation via collocation.

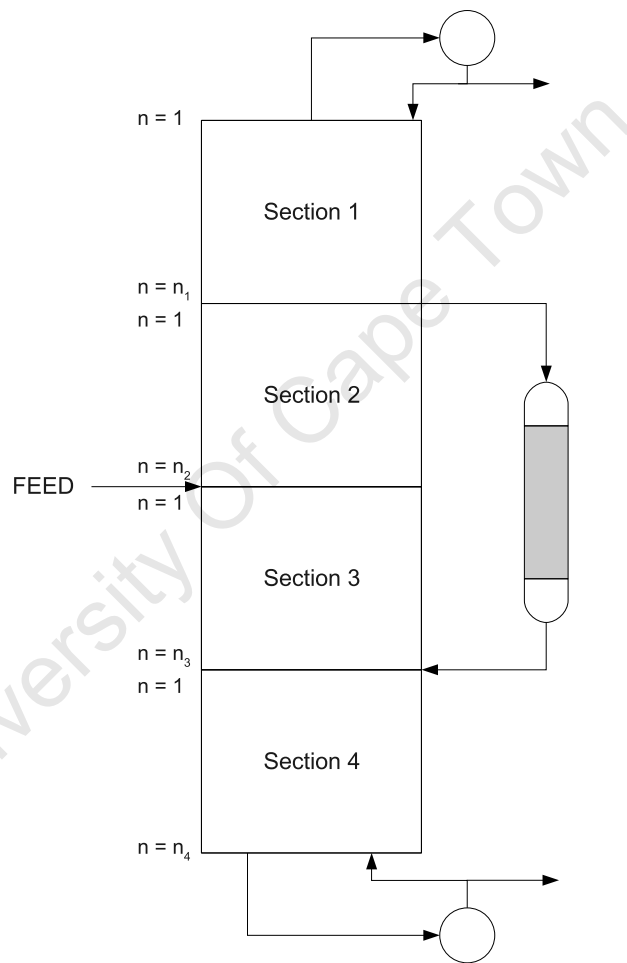


Figure 6.3: Single external reactor column showing boundary condition positions

Table 6.1: Boundary conditions used in a single reactor column shown in Figure 6.3

Profile	Position	Boundary Condition
Section 1		
x_i	$n = 1$	$x_{i,1}^{(1)} = y_{i,1}^{(1)}$
y_i	$n = n_1$	$y_{i,n_1}^{(1)} V_{n_1}^{(1)} = y_{i,1}^{(2)} V_1^{(2)}$
L	$n = 1$	$L_1^{(1)} (1 + \frac{1}{R}) = V_1^{(1)}$
V	$n = n_1$	$V_{n_1}^{(1)} = V_1^{(2)}$
T^L	$n = 1$	$L_1^{(1)} (1 + \frac{1}{R}) H_1^{L(1)} = V_1^{(1)} H_1^{V(1)}$
T^V	$n = n_1$	$V_{n_1}^{(1)} H_{n_1}^{V(1)} = V_1^{(2)} H_1^{V(2)}$
Section 2		
x_i	$n = 1$	$x_{i,1}^{(2)} L_1^{(2)} = x_{i,n_1}^{(1)} L_{n_1}^{(1)} (R_{sidestream} - 1)$
y_i	$n = n_2$	$y_{i,n_2}^{(2)} V_{n_2}^{(2)} = y_{i,1}^{(3)} V_1^{(3)} + y_i^F (1 - q^F) F$
L	$n = 1$	$L_1^{(2)} = L_{n_1}^{(1)} (R_{sidestream} - 1)$
V	$n = n_2$	$V_{n_2}^{(2)} = V_1^{(3)} + (1 - q^F) F$
T^L	$n = 1$	$L_1^{(2)} H_1^{L(2)} = L_{n_1}^{(1)} (R_{sidestream} - 1) H_{n_1}^{L(1)}$
T^V	$n = n_2$	$V_{n_2}^{(2)} H_{n_2}^{V(2)} = V_1^{(3)} H_1^{V(3)} + (1 - q^F) F H^{VF}$
Section 3		
x_i	$n = 1$	$x_{i,1}^{(3)} L_1^{(3)} = x_{i,n_2}^{(2)} L_{n_2}^{(2)} + x_i^F q^F F$
y_i	$n = n_3$	$y_{i,n_3}^{(3)} V_{n_3}^{(3)} = y_{i,1}^{(4)} V_1^{(4)}$
L	$n = 1$	$L_1^{(3)} = L_{n_2}^{(2)} + q^F F$
V	$n = n_3$	$V_{n_3}^{(3)} = V_1^{(4)}$
T^L	$n = 1$	$L_1^{(3)} H_1^{L(3)} = L_{n_2}^{(2)} H_{n_2}^{L(2)} + q^F F H^{LF}$
T^V	$n = n_3$	$V_{n_3}^{(3)} H_{n_3}^{V(3)} = V_1^{(4)} H_1^{V(4)}$
Section 4		
x_i	$n = 1$	$x_{i,1}^{(4)} L_1^{(4)} = x_{i,n_3}^{(3)} L_{n_3}^{(3)} + x_{i,return} Return$
y_i	$n = n_4$	$y_{i,n_4}^{(4)} = x_{i,n_4}^{(4)}$
L	$n = 1$	$L_1^{(4)} = L_{n_3}^{(3)} + Return$
V	$n = n_4$	$V_{n_4}^{(4)} (1 + \frac{1}{Rb}) = L_{n_4}^{(4)}$
T^L	$n = 1$	$L_1^{(4)} H_1^{L(4)} = L_{n_3}^{(3)} H_{n_3}^{L(3)} + Return \cdot H^{return}$
T^V	$n = n_4$	$V_{n_4}^{(4)} (1 + \frac{1}{Rb}) H_{n_4}^{V(4)} = L_{n_4}^{(4)} H_{n_4}^{L(4)}$

6.4 Reactor Model

The reactor can be modelled as a Plug Flow Reactor (PFR) using

$$\frac{dF_j}{dV} = r_j \quad (6.21)$$

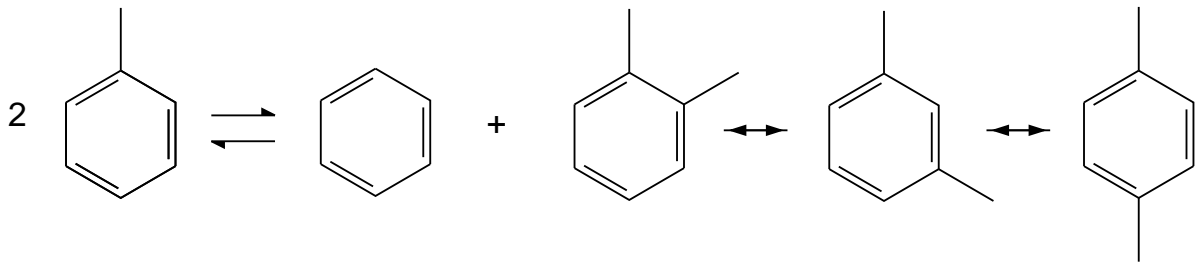


Figure 6.4: Toluene Disproportionation Reaction

a Packed Bed Reactor (PBR) using:

$$\frac{dF_j}{dW} = r_j \quad (6.22)$$

or a Continuously Stirred Tank Reactor (CSTR) using:

$$V = \frac{F_{j,0} - F_j}{-r_j} \quad (6.23)$$

6.4.1 Toluene Disproportionation Case Study

The first reaction to be studied was the toluene disproportionation (TDP) reaction. The reactor was modelled as a packed bed reactor using the following equation

$$\frac{dX}{dW} = \frac{r_{TDP}}{F_{Tol,0}} \quad (6.24)$$

The reaction is given by Figure 6.4, where two *toluene* molecules are reacted with each other to form a *benzene* molecule and one of three *xylene* isomers. The components have ideal characteristics for the system at hand as the products (benzene and xylenes) should be in higher concentrations at the top and bottom of the column (respectively), with the reactant (toluene) remaining in high concentrations in the centre of the column.

The reaction rate expression is taken from a study by Uguina et al. (1993), on the kinetics of the reaction over unmodified ZSM-5 zeolite catalysts. Their rate expression is a Langmuir-Hinshelwood expression, where the rate limiting step is the adsorption of

toluene onto the acid site. This is given by Equation 6.25

$$r_D = k_D \frac{P_T - \frac{P_B P_X}{K_D P_T}}{1 + \frac{K_T P_B P_X}{K_D P_T} + K_X P_X} \quad (6.25)$$

where k_D is the rate constant for the TDP reaction and P_T, P_B, P_X are the partial pressures of toluene, benzene and mixed xylenes respectively. K_D is the equilibrium constant for the TDP reaction, while K_T and K_X are the adsorption constants of toluene and xylenes respectively.

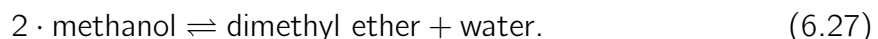
6.4.2 Methyl Acetate Case Study

Another reaction investigated was the reaction of *acetic acid* with *methanol* to form *methyl acetate* and *water*.



This reaction has been successfully applied to RD in industry (see Section 4.1.1) and has been used in a number of literature studies relating to RD columns. These include experimental studies (Song et al. (1998), Bessling et al. (1998) and Popken et al. (2001)) as well as design methods for reactive distillation that usually use the methyl acetate synthesis system as an example (Lee and Westerberg (2001), Chadda et al. (2001) and Huss et al. (2003)).

A potential side reaction can take place, producing *dimethyl ether* and *water* from *methanol*



However, Doherty and Malone (2001) state that this reaction has only a minor effect on the operation of a RD column at atmospheric pressure and so it was ignored in this study.

The reaction was modelled using two methods. The first being an adiabatic equilibrium reactor using the mass balance with *acetic acid* conversion (Equation 6.28) and the

energy balance to obtain the temperature (Equation 6.29).

$$K_{eq} = \frac{C_{MEAC}C_{H2O}}{C_{AA}C_{MEOH}} = \frac{(\theta_{MEAC} + X)(\theta_{H2O} + X)}{(1 - X)(\theta_{MEOH} - X)} \quad (6.28)$$

$$X = \frac{\sum_{i=1}^n \theta_i C_{p_i} (T - T_0)}{-\Delta H_{rxn}(T)} \quad (6.29)$$

The second method was modelling the reactor as a packed bed reactor using Amberlyst 15W as a catalyst. The kinetic data was obtained from Doherty and Malone (2001) and is given below.

$$r = c_t k_f \left(a_{AA} a_{MEOH} - \frac{1}{K_{eq}} a_{H2O} a_{MEAC} \right) \quad (6.30)$$

with the reaction constant (in s^{-1})

$$k_f = 2.7033 \times 10^5 \left(\frac{-6287.7}{T} \right) \quad (6.31)$$

and the equilibrium constant

$$K_{eq} = 2.32 \exp \left(\frac{782.98}{T} \right). \quad (6.32)$$

6.5 Thermodynamics, Mass and Heat Transfer Coefficients

All these properties are important to calculate when using a non-equilibrium rate-based distillation column model and so these need to be obtained at each iteration of the distillation model. The methods and correlations used to calculate these properties can be found in Appendix A.

University Of Cape Town

Chapter 7

Results: Preliminary Results

7.1 Model Accuracy

Two different packed distillation column models were developed for comparison purposes. These were the conventional staged rate-based model described in Section 2.4.4 and a model employing the collocation method described in Section 6.3.1. The first model approximates the differential nature of the continuous packed column by representing a section of the packing by a stage, while the second model uses the actual differential equations describing the column and converts these into nonlinear equations via collocation.

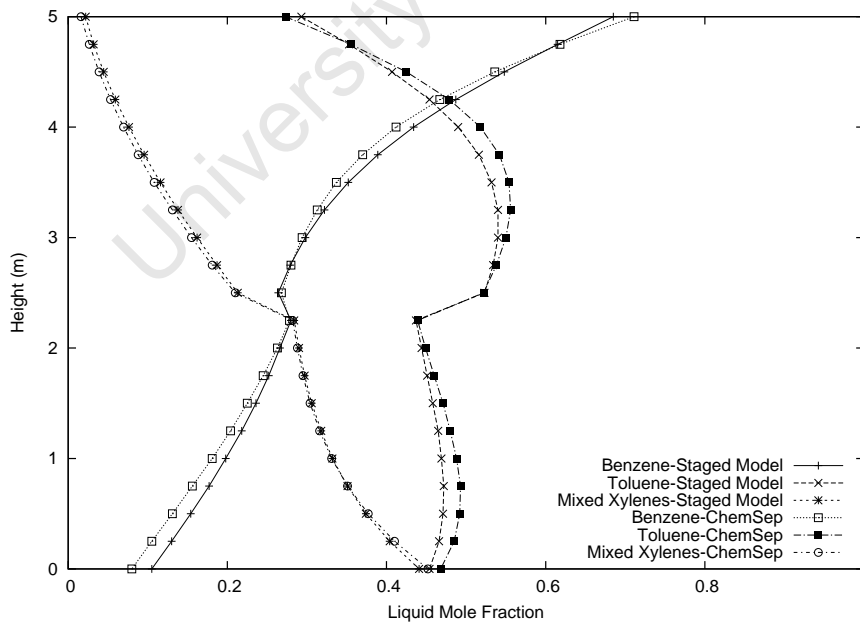
The first objective was to see if the rate-based staged model is accurate and comparable to an established commercial program. Therefore, the following simple distillation column system (Table 7.1) was modelled using the rate-based staged model and ChemSep. Twenty stages were used in the models and the liquid composition profiles were used to compare the results. The results can be seen in Figure 7.1 where the three xylene isomers have been combined for clarity purposes.

It is clear from Figure 7.1 that the staged model developed fits the results obtained by ChemSep very well. There are some slight discrepancies, but this is to be expected due to slightly different correlations and solvers. This result, however, is proof that the staged model does return valid results and can be used in other comparisons.

The issue with staged models is knowing how many stages to use to accurately describe the packed column effectively. Using staged models to model packed columns

Table 7.1: Distillation column parameters used for comparison

Parameter	Value	Parameter	Value
Height	5.0m	Reflux ratio	1.0
Diameter	0.2m	Boilup ratio	1.0
Feed flow rate	1.0mol/s	Packing type	2" Pall rings
Feed composition:		Condenser type	Total
Benzene	0.3	Reboiler type	Partial
Toluene	0.4	Feed height	2.5m
o-Xylene	0.1	Feed quality	1.0
m-Xylene	0.1		
p-Xylene	0.1		

**Figure 7.1:** Liquid composition profiles of the staged model and Chemsep using 20 stages

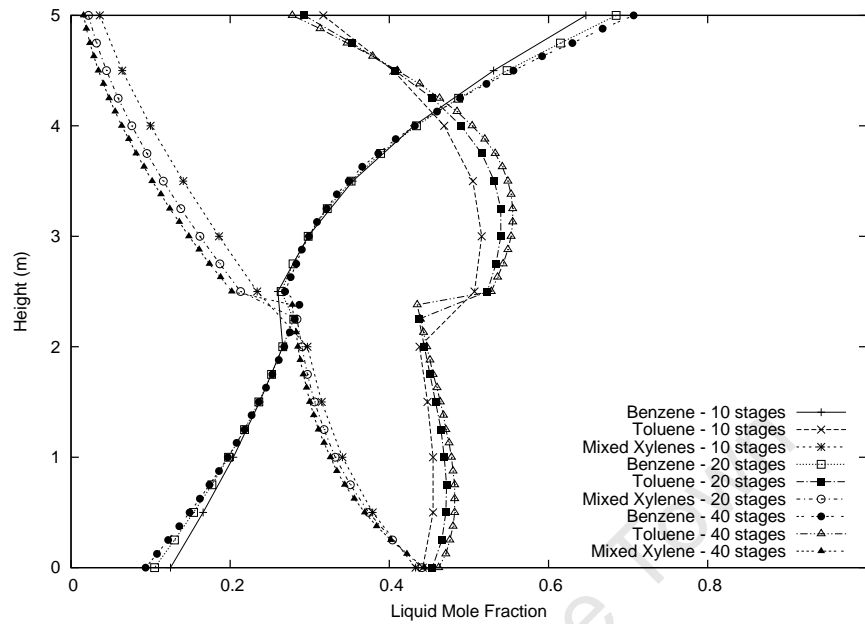


Figure 7.2: Liquid composition profiles of the staged model using 10, 20 and 40 stages

has been discussed in Section 2.5, where the HETP is used to estimate how many theoretical stages represent the column.

Another approach is employed by ChemSep, where a first order approximation is made of the differential equations described in Section 2.5. The resulting algebraic equations are solved using a Newton method. However this approach has a disadvantage in that the number of stages needs to be estimated beforehand. A low number of stages can be solved quickly, but is often inaccurate, while a large number of stages is usually more accurate, but can result in high computation times.

The distillation column defined by Table 7.1 was modelled using 10, 20 and 40 stages to show how the increase in the number of stages affects the accuracy of the solution and the computational effort. The results can be seen in Figure 7.2 and in Table 7.2.

The 40 stage model can be considered the most accurate, and it is clear that the 10 stage model has a lower accuracy. From Table 7.2, the results show that the complexity of more stages has a significant increase in the computational time required to solve the model.

Table 7.2: Computational times required for staged model comparison

Number of stages	Computational time (s)
10	4.688
20	7.578
40	55.47

7.2 Collocation Model

Now that the staged model has been verified to be reasonably accurate at modelling a simple distillation column system, the collocation model can be compared to this model. The reason for not using ChemSep directly, is that the methods and solvers are different and have been highly optimised for speed. This would not be a fair reflection on the collocation method in terms of computation time.

Therefore, in Figure 7.3, a collocation model using four sections (or elements) with 9 interior points per section was compared to the 40 stage model. The collocation model shows a very good fit to the staged model, but does show a few discrepancies.

Due to the different approaches, the stage model and the collocation model have their points at slightly different heights. This is as a result of the stage in the stage model taking up a certain volume, while the collocation model utilises points and calculations are performed around those points. This gives rise to the slight differences, noticed especially at the feed location. The staged model feed location is represented by a line connecting the mole fractions above and below the feed. The collocation model uses two points at the same location to represent the change in the mole fraction.

The other region where the differences are noticed are the top and bottom of the column. As the collocation model needs to perform the role of a condenser and a reboiler at two defined individual points, these values are slightly different to those obtained when using a full stage for those functions. However, as Figure 7.3 shows, these differences are very slight and the benefits of using fewer calculations in the model should outweigh the minor differences.

The key advantage of using the collocation model can be seen in Figure 7.4 where the liquid concentration profiles are plotted for the distillation column described in Table 7.1. In each case four sections were used and 1, 3 and 9 interior points were used for

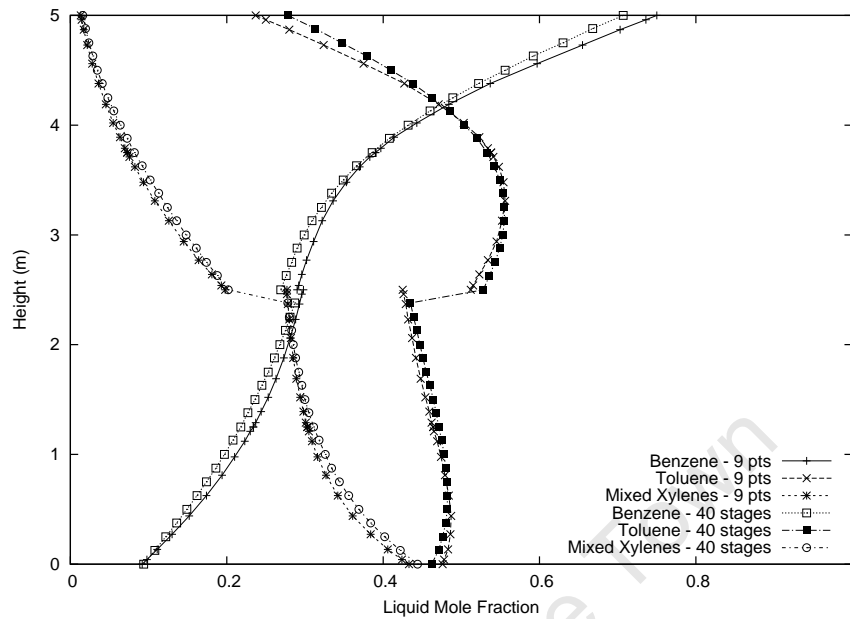


Figure 7.3: Liquid composition profiles of the collocation model using 4 sections and 9 interior points compared to the 40 stage model

each section. It is clear from the plot that the number of points does not have such a large affect on the accuracy of the collocation model as the number of stages had on the stage model (see Figure 7.2).

However, the number of points still has an influence on the computational time, as seen in Table 7.3 where the increase in points increases the computational time. Comparing these computational times with those of the staged model in Table 7.2, it is clear that the collocation model is faster than the staged model of 40 stages. Therefore, it is clear that collocation can be used with a few interior points and still achieve similar accuracy while reducing the computational time required to solve the model.

As an example, a collocation model using three interior points can achieve similar accuracy to a staged model with 40 stages in 7.3s, compared to 55.5s. This is an important benefit when performing optimisation studies, as the 48s difference can quickly add up over each iteration.

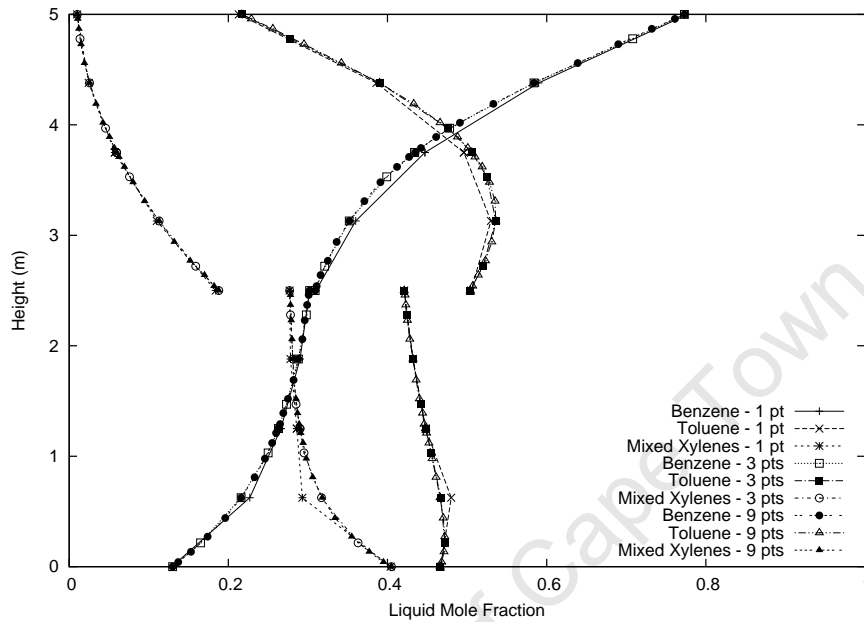


Figure 7.4: Liquid composition profiles of the collocation model using 4 sections and 1, 3 and 9 interior points

Table 7.3: Computational times required for collocation model comparison

Number of interior points	Total number of points	Computational time (s)
1	12	4.752
3	20	7.312
9	44	36.654

7.2.1 Choosing the number of interior points

From the previous section, it is clear that the number of interior points does not have a large impact on the accuracy of the solution. However, if the profiles are steep, or if fewer sections are used, this is less likely. The choice of the number of interior points is often a trial and error process, as it is difficult to determine before running the model.

As mentioned previously in Section 3.8.2, Srivastava and Joseph (1985) developed the Order Reduction Parameter (ORP) to calculate the optimum number of interior points. Unfortunately this method requires a previously calculated solution and is thus not practical in this study.

The number of interior points were chosen by trial and error, attempting to keep a reasonable accuracy, while minimising the computation time. These were generally between 1 and 5 interior points, depending on the situation.

7.3 Choice of Optimisation Routine

Turning to the optimisation of the side reactor system, the first thing was to look at suitable optimisation routines. These have been discussed in Section 6.2 and the results of these are presented in this section.

7.3.1 DONLP2

The first optimisation routine used was the SQP solver DONLP2 developed by Spellucci (1998). This is a relatively traditional SQP method and some of the results obtained using this method are given below.

Figure 7.5 shows the side reactor used in all the optimisation studies, though the number of reactors can be greater than the single one shown in the diagram. The definition of the *sidestream ratio*, S_{ratio} , is particularly important to note, as in other studies performed in literature there are various ways of defining and determining how much liquid is drawn off the column in the side stream. In this study the *sidestream ratio* is defined as the ratio of liquid drawn off in the sidestream to the liquid flow rate in the

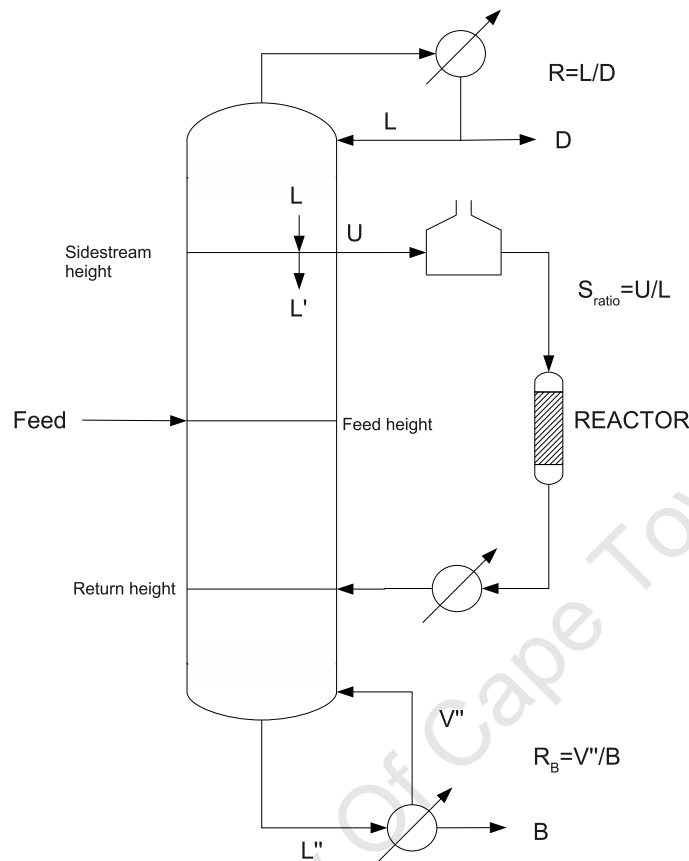


Figure 7.5: Side reactor system used in the optimisation studies

column just above the sidestream location.

$$S_{ratio} = \frac{U}{L} \quad (7.1)$$

By keeping this value lower than 1.0, it ensures that there is always liquid flowing within the column. There will be a sidestream ratio for each sidestream.

The most simple optimisation problem available is to determine the optimum reflux and boilup ratios. Usually this is done for a single distillation column for a specified separation, but as this study is focused on the side reactor system, the objective function is to find the maximum overall conversion of toluene. This is a good measure of the performance of both the reactor and separator and is often used in industry to evaluate the performance of systems.

The system investigated is given in Table 7.4 with a relatively small column and low

Table 7.4: Fixed side reactor parameters used in the optimisation studies for the NLP solvers

Parameter	Value	Parameter	Value
Height	3.0m	Sidestream ratio	0.9
Diameter	0.3m	Packing type	Sulzer BX
Feed flow rate	1.0mol/s	Condenser type	Total
Feed composition:		Reboiler type	Partial
Benzene	0.05	Feed quality	1.0
Toluene	0.98		
o-Xylene	0.05		
m-Xylene	0.05		
p-Xylene	0.05		

flow rates. The diameter of the column was chosen by looking at the maximum possible flow rates through the column and then using the percentage of flooding technique to find a suitable diameter.

The SQP solver performs very well in finding an optimum overall toluene conversion while being restricted as set out in Table 7.5, with the performance of the iterations seen in Figure 7.6. However, this is a relatively simple continuous surface to optimise, as seen in Figure 7.7 and so it should be easy for DONLP2 to obtain the optimum value. It is clear from Figure 7.7 that high reflux and boilup ratios are conducive to higher overall conversions. This is to be expected as this increases the amount of recycle through the reactor and thus increasing the conversion. Another advantage (inherent in the model) is that the size of the reactor is dependent on the flow through it as it is forced to have a Weight Hourly Space Velocity (WHSV) of $1.3h^{-1}$. Therefore, higher flows give rise to larger reactors to deal with the flow rates and thus the overall toluene conversion is increased.

Discontinuities

DONLP2 worked well for the continuous problem discussed above and would be very good for a conventional distillation column that does not have the type of discontinuities

Table 7.5: Parameters for DONLP2 optimisation of Reflux and Boilup ratios for maximum toluene conversion

Parameter	value
Feed height	1.50m
Sidestream height	2.25m
Return height	0.75m
Reflux ratio	$0.1 \leq R \leq 5.0$
Boilup ratio	$0.1 \leq R \leq 5.0$

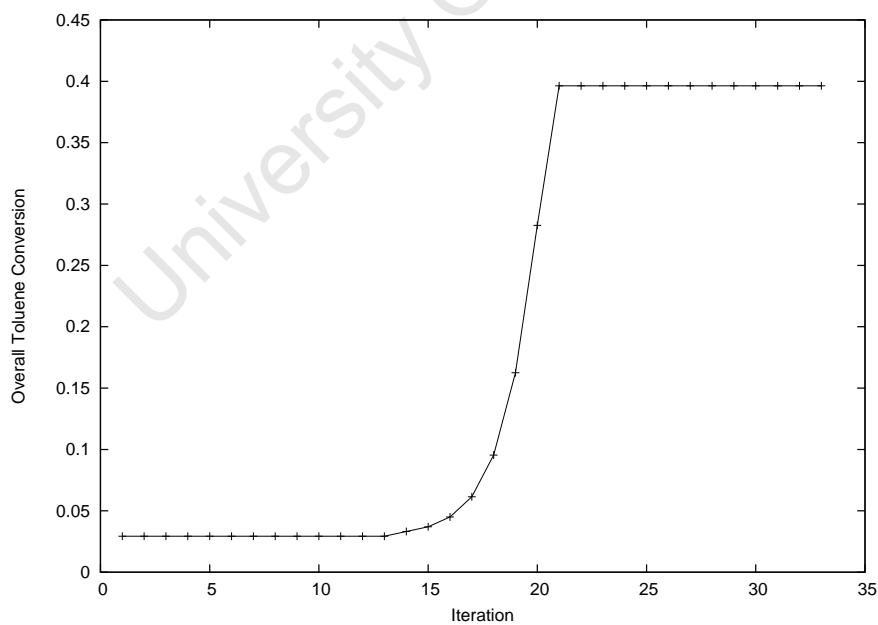


Figure 7.6: DONLP2 optimisation progress for optimising R and R_b for maximum $X_{Toluene}$

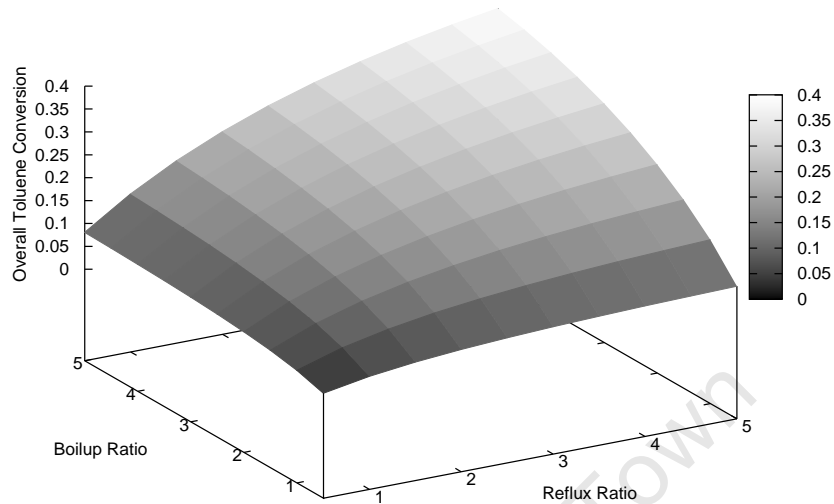


Figure 7.7: Overall toluene conversion as a function of reflux and boilup ratios

inherent in the side reactor system. Due to the multiple streams entering and leaving the column, conditions change abruptly with only a small change in the optimisation variables. This is evident when looking at the progress of the solver in trying to find the optimum feed location using the same parameters as in Table 7.5, but keeping the reflux and boilup ratios fixed at 5.0.

Figure 7.8 clearly shows that the optimisation routine struggled to find the optimum solution. The sharp jumps in the conversion coincide with the point when the solver is crossing over the discontinuity. To determine the cause of this problem, the column was modelled using a number of different feed positions and then observing the overall toluene conversion obtained. Figure 7.9 shows the results and it is clear that the discontinuities occur at the position where the other streams are located (the sidestream in particular).

This problem with the discontinuities will only increase with an increase in the number of optimisation variables and reactors. Another problem will be the cost functions used when optimising the column to minimise costs. These are usually highly nonlinear and will probably result in further discontinuities and more difficulties for the solver.

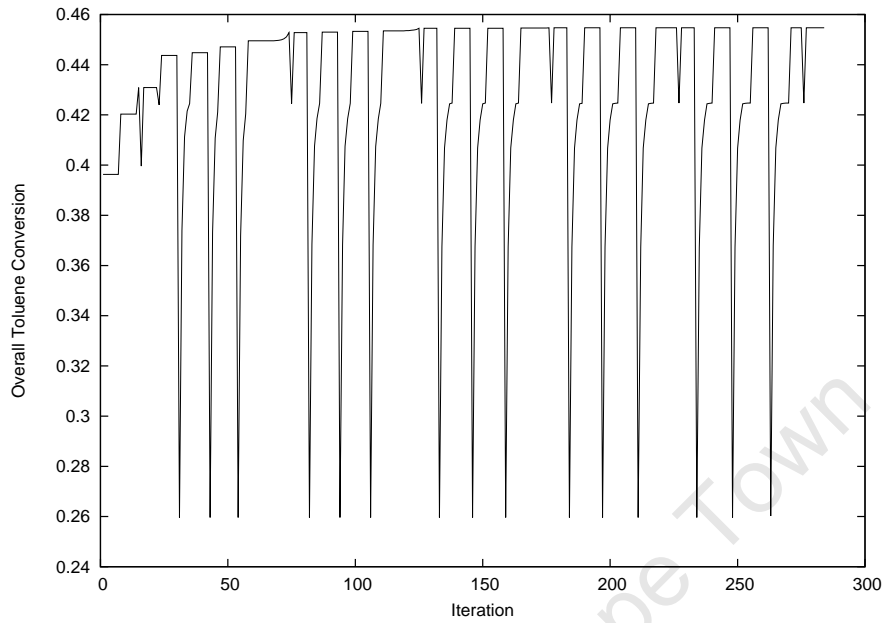


Figure 7.8: DONLP2 progress for optimising the feed location for maximum toluene conversion

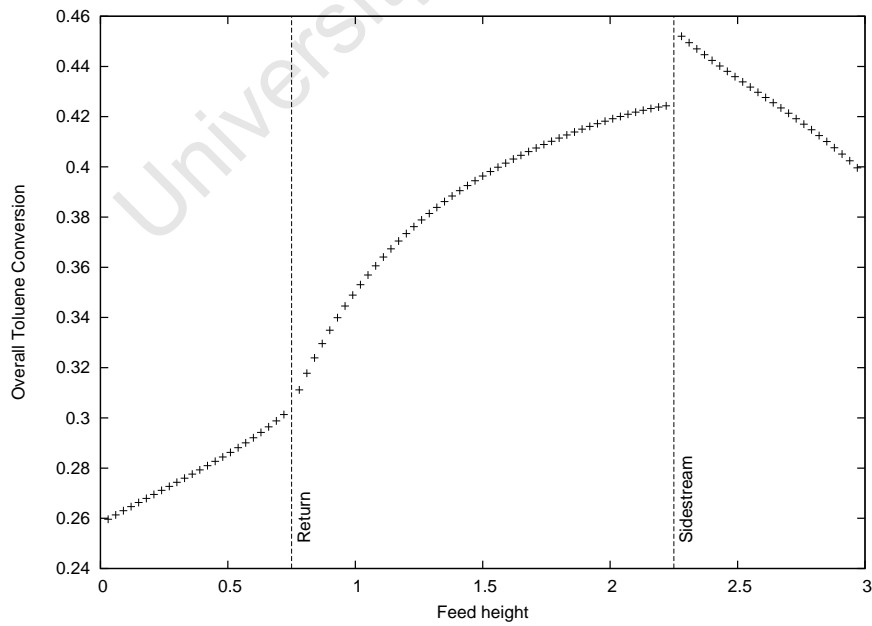


Figure 7.9: Overall toluene conversion as a function of the feed location using DONLP2

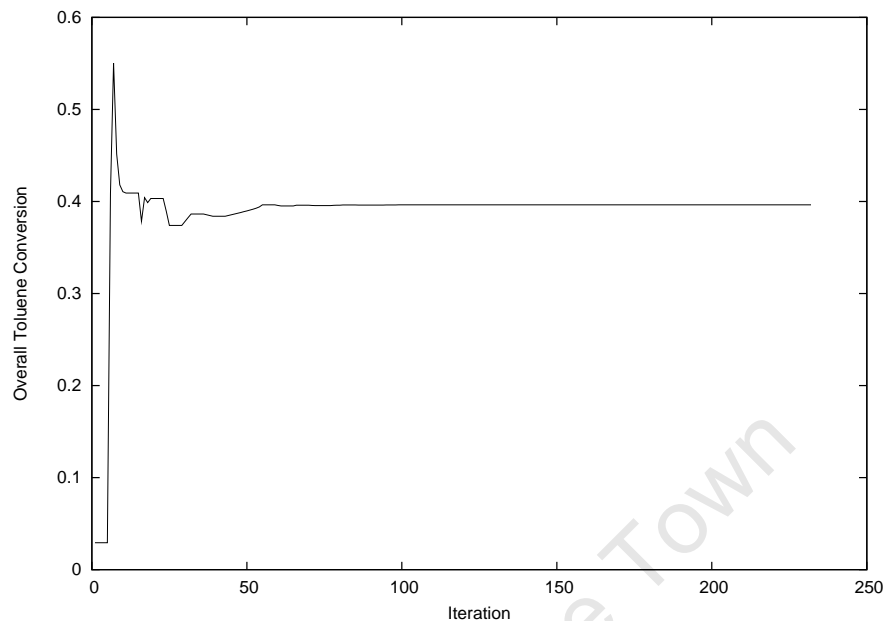


Figure 7.10: SolvOpt optimisation progress for optimising R and Rb for maximum $X_{Toluene}$

7.3.2 SolvOpt

SolvOpt utilises Shor's r-algorithm which is said to be one of the more efficient methods of optimising almost-differentiable (non-smooth) functions. Therefore, due to the discontinuities that occur at a few points in the function, it would seem that SolvOpt would be better equipped than DONLP2.

Looking at the same system as before, and using the same constraints, the following results were obtained. Firstly, the reflux and boilup ratios were optimised as before, using the overall toluene conversion as the objective function. The solver's progress using this method can be seen in Figure 7.10.

From Figure 7.10, it is clear that the solver manages to obtain a solution successfully and without much difficulty. It must be noted that when comparing the progress to that of the SQP solver (DONLP2) in Figure 7.6, SolvOpt requires a higher number of iterations to obtain a solution. This can be attributed to the fact that SolvOpt is a more general solver and is specifically aimed at non-smooth functions.

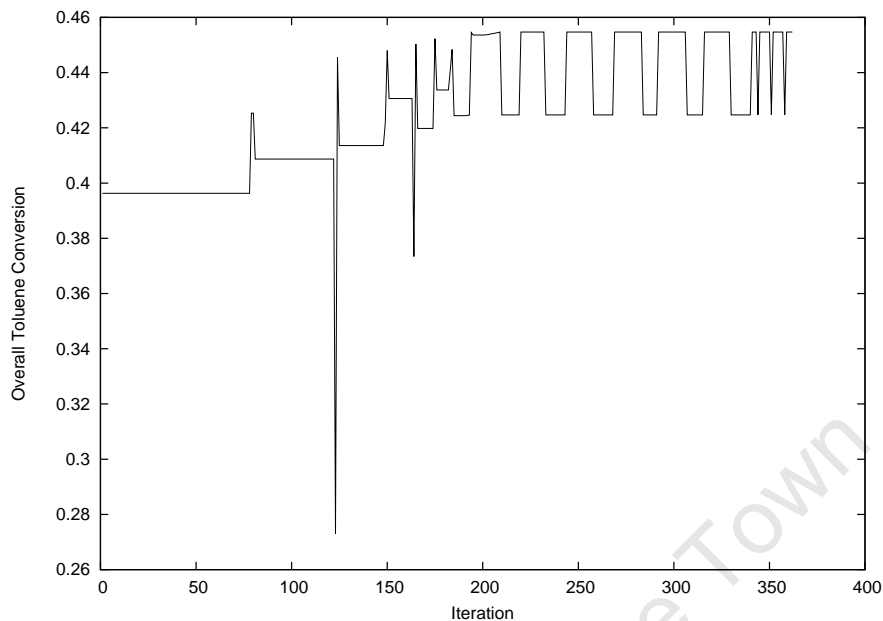


Figure 7.11: Overall toluene conversion as a function of the feed location using SolvOpt

Discontinuities

The optimal feed location was then considered as before, but this time using SolvOpt as the solver routine. It was hoped that this solver would be more robust and able to handle the problems of the discontinuities in the objective function, but from Figure 7.11, it is clear that this is not the case. The discontinuities associated with the feed location still affect the solver and result in very long computational times.

These problems with discontinuities led to the decision to apply a genetic algorithm to optimise the side reactor systems. Genetic algorithms are not gradient based methods and are thus not as affected by discontinuities in the objective function.

7.3.3 Genetic Algorithms

To test the performance of the genetic algorithm, the same tests were performed as with the two NLP solvers. Firstly the reflux and boilup ratios were optimised using the overall toluene conversion as the objective function. The progress of the GA can be seen in Figure 7.12. The average fitness (overall toluene conversion) changes rapidly as the GA progresses. This is due to the Micro-GA option being implemented in this case. This

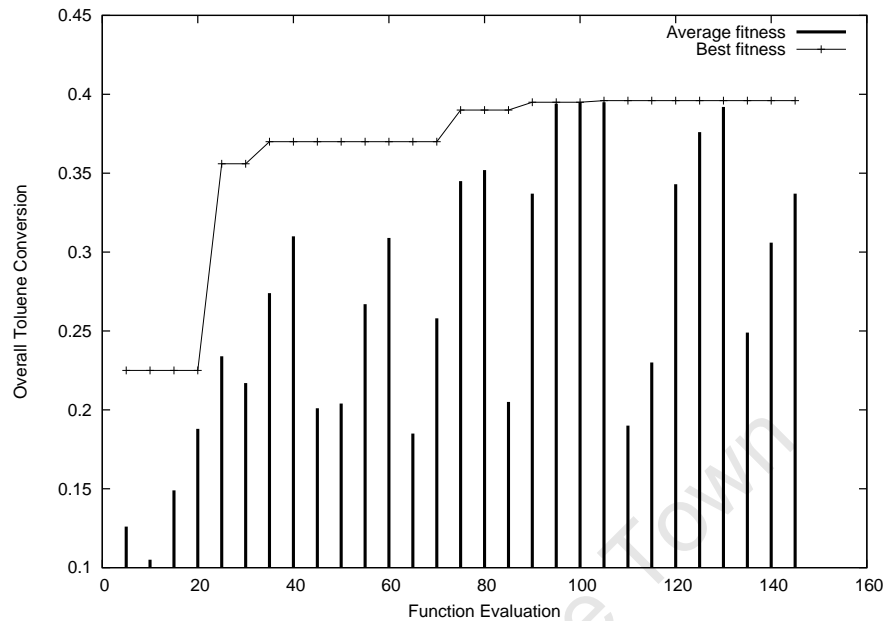


Figure 7.12: GA optimisation progress for optimising R and R_b for maximum $X_{Toluene}$

average will increase until it comes within a certain range of the best value and then a new population will be generated, keeping the best configuration from the previous population. Figure 7.12 shows that the GA achieves its optimum configuration in 145 function evaluations (or 29 generations of 5 individuals). However the configuration obtained is $R = 4.9904$ and $R_b = 4.9808$, not quite at the optimum of $R=5$ and $R_b=5$.

This difference can be minimised by running the GA multiple times to achieve a better result, but that would increase the number of function evaluations and hence minimise those advantages achieved. Another alternative available is to use the GA to find an approximate solution quickly and then use this as a starting point for the other NLP solvers to search a narrow range (with the aim of avoiding many of the discontinuities).

The discontinuity with the feed location optimisation is dealt with very well by the GA and the results can be seen in Figure 7.13. The GA only required 95 function evaluations (or 19 generations of 5 individuals), compared to the 284 and 362 for DONLP2 and SolvOpt respectively. The feed location obtained is 2.2545m, which compared to the other optimisation routines, is slightly less accurate. However, it still shows that the feed should be positioned just above the side stream. This would appear to be obvious as the toluene concentration is the highest here, but this might not be the case when multiple reactors are used.

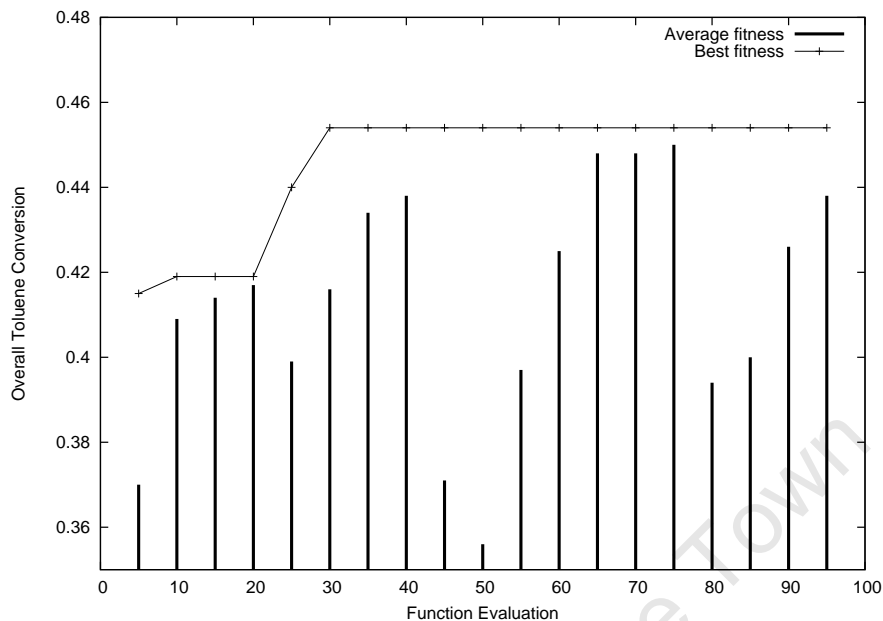


Figure 7.13: GA progress for optimising the feed location for maximum toluene conversion

Table 7.6 gives a comparison of the performance of the three optimisation routines. It is clear that the two gradient-based methods (DONLP2 and SolvOpt) are more accurate, but at the cost of high computational times, especially when dealing with discontinuities in the objective function. The GA is less accurate, but performs much better in terms of time and function evaluations. If this program is to be used in industry and by engineers in the field, then time is often more of a factor than absolute accuracy. Therefore, from the results achieved thus far, the GA was chosen as the optimisation routine for all further optimisation studies.

7.3.4 Advantages and disadvantages of using GAs

From the results in this Chapter, the advantages and disadvantages of using Genetic Algorithms in process design are clear. These can be summarised as follows

- GAs are able to seek a global optimum in the presence of discontinuous variables and objective functions
- They do not require much information regarding the system - only the fitness value

Table 7.6: Results for Optimisation routine comparisons

Parameter	DONLP2	SolvOpt	GA
Reflux ratio	5.0	5.0	4.9904
Boilup ratio	5.0	5.0	4.9808
Function Evaluations	33	232	145
Time (s)	167	1566	850
Feed height (m)	2.2500	2.2500	2.2545
Function Evaluations	284	362	95
Time (s)	1915	1535	643

(no derivatives required)

- GAs do not usually have stopping criteria and may not reach the global optimum
- They always reach a solution, but can sometimes get stuck and only reach suboptimal solutions (unless mutation is enforced)
- They tend to be slower in finding a solution to simple problems, where gradient-based methods are more suitable, but quicker at optimising complex problems (where gradient-based methods may get trapped in suboptimal regions for long periods of time)

The most useful attribute of GAs for this research is the fact that they do not require derivatives of the objective function and can optimise the problem, even when there are discontinuous variables and objective functions.

University Of Cape Town

Chapter 8

Results: Toluene Disproportionation

The toluene disproportionation reaction was used as a case study to see what information can be obtained when optimising these side reactor systems. The possible parameters to be optimised are given below:

- Reflux ratio ($0.1 \leq R \leq 5.0$)
- Boilup ratio ($0.1 \leq R_b \leq 5.0$)
- Sidestream ratio(s) ($0.01 \leq S_R \leq 0.99$)
- Feed height ($0.01 \leq F_{ht} \leq 0.99$ of the column height)
- Sidestream height(s) ($0.01 \leq S_{ht} \leq 0.99$ of the column height)
- Return height(s) ($0.01 \leq R_{ht} \leq 0.99$ of the column height)
- Number of reactors (performed manually to see the effects).

8.1 Overall Toluene Conversion

The first objective was to determine the maximum possible toluene conversion using the parameters given above. This results in the following objective function

$$\max f(x) = X_{overall} \quad (8.1)$$

Table 8.1: Fixed side reactor system parameters used in the overall conversion optimisation

Parameter	Value	Parameter	Value
Feed flow rate	1.0mol/s	Condenser type	Total
Feed composition:		Reboiler type	Partial
Benzene	0.005	Height	3.0m
Toluene	0.98	Diameter	0.3m
o-Xylene	0.005	Packing type	Sulzer BX
m-Xylene	0.005	Feed quality	1.0
p-Xylene	0.005		

with all the constraints being embedded within the system model. The overall conversion is a good indicator of performance of the system as a whole and is often used in industry when optimising processes.

The system considered is given by Figure 7.5 and is defined by Table 8.1. Due to the feed being fed directly to the distillation column, the model would struggle to solve the system with only a single component initially (a problem of all steady state models). Therefore, a small amount of the other components were added to the feed to allow the model to solve more easily.

The reactors were modelled as plug flow reactors using the kinetics described in Section 6.4.1 and each had a constant WHSV of 1.3. Thus, their sizes were allowed to increase and decrease according to the flow through them. The GA was used to optimise the systems, consisting of one, two and three side reactors for the maximum overall conversion of toluene.

The resulting optimum systems obtained are given in Table 8.2, with the respective heights measured from the bottom of the distillation column. Graphical representations of these optimum systems are given by Figure 8.1, with the locations of the sidestreams to scale with the height of the column.

Table 8.2 shows that the increase in the number of reactors actually decreases the maximum possible overall toluene conversion. This is likely due to the sidestream locations competing for the best positions in the column and finding suboptimal concentra-

Table 8.2: Optimum systems to achieve maximum overall toluene conversion

	1 Reactor	2 Reactors	3 Reactors
Reflux Ratio	3.759	4.602	3.894
Boilup Ratio	4.986	4.808	4.674
Feed Height (m)	1.688	0.976	1.846
Sidestream ratio 1	0.979	0.026	0.958
Sidestream height 1 (m)	1.401	0.820	0.703
Return height 1 (m)	1.892	1.913	0.806
Sidestream ratio 2	-	0.962	0.241
Sidestream height 2 (m)	-	0.904	1.467
Return height 2 (m)	-	1.197	2.228
Sidestream ratio 3	-	-	0.939
Sidestream height 3 (m)	-	-	1.108
Return height 3 (m)	-	-	1.384
Overall Toluene Conversion	0.939	0.885	0.886

Table 8.3: External reactor details for the configurations to achieve maximum overall toluene conversion

	1 Reactor	2 Reactors	3 Reactors
Reactor 1 flow rate (mol/s)	130.6	0.080	63.77
Reactor 1 toluene conversion	0.014	0.031	0.010
Reactor 2 flow rate (mol/s)	-	77.98	0.909
Reactor 2 toluene conversion	-	0.022	0.121
Reactor 3 flow rate (mol/s)	-	-	43.52
Reactor 3 toluene conversion	-	-	0.023

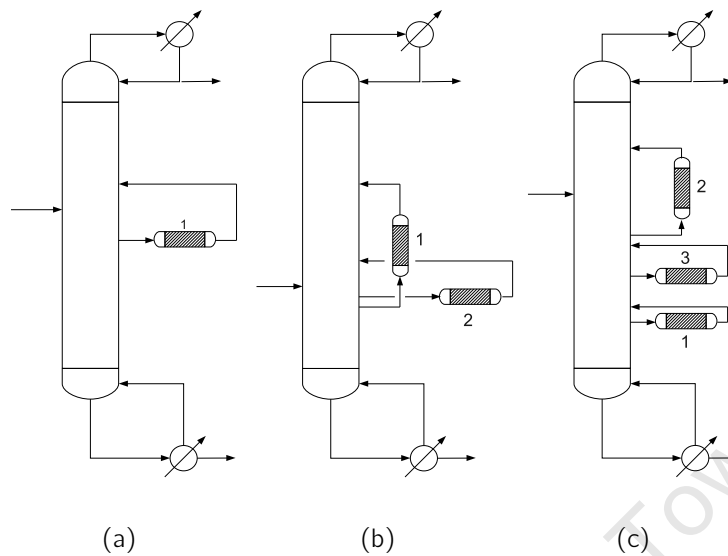


Figure 8.1: Optimal configurations for maximum toluene conversion using (a) one external side reactor, (b) two external side reactors and (c) three external side reactors

tions of toluene at the second or third location.

Table 8.3 shows that high flow rates are necessary (considering that the feed to the column is only 1mol/s) to achieve the high overall conversions and that the conversion of toluene per pass is actually very low. This is mostly due to the high concentrations of the products in the reactor and this reduces the forward reaction. Unfortunately, these high internal flow rates in certain sections of the column lead to flooding. This can be seen in Figure 8.2, where the composition of liquid does not change much between the reactor return and the sidestream location.

Further evidence of flooding can be seen in Figure 8.3, where the fraction of flooding is very high in the sections between the reactor inlet and outlet. The fraction of flooding is the ratio between the superficial vapour velocity and the superficial vapour velocity at flooding (calculated from the flood pressure drop - see Appendix for further information).

The reason for the high superficial velocity is shown in Figure 8.4, where the high liquid flow rate in the sections between the reactor inlet and outlet causes the flooding superficial vapour velocity to be much smaller. Because the vapour flow rate is not proportionally high in these sections, the fraction of flooding is much greater than desired

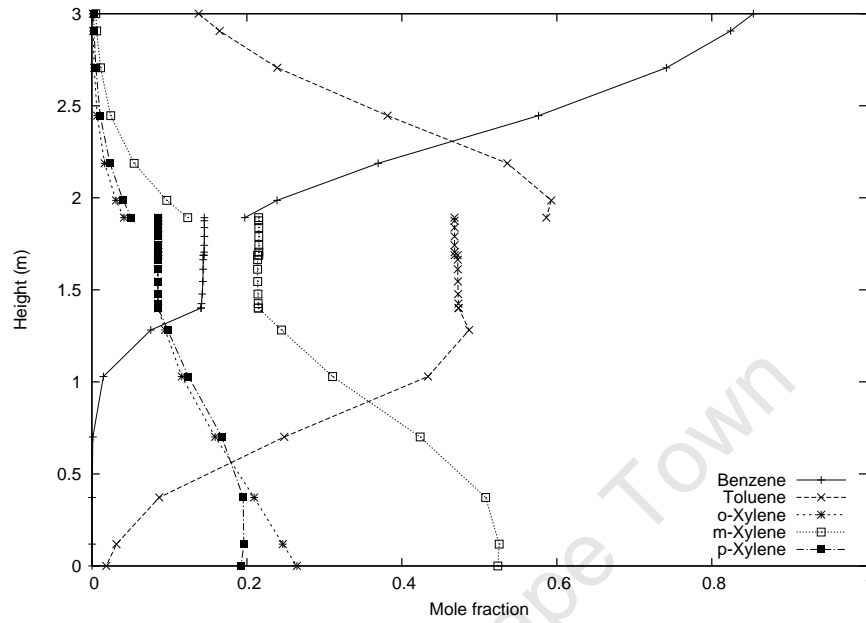


Figure 8.2: Liquid composition in 1 Reactor system

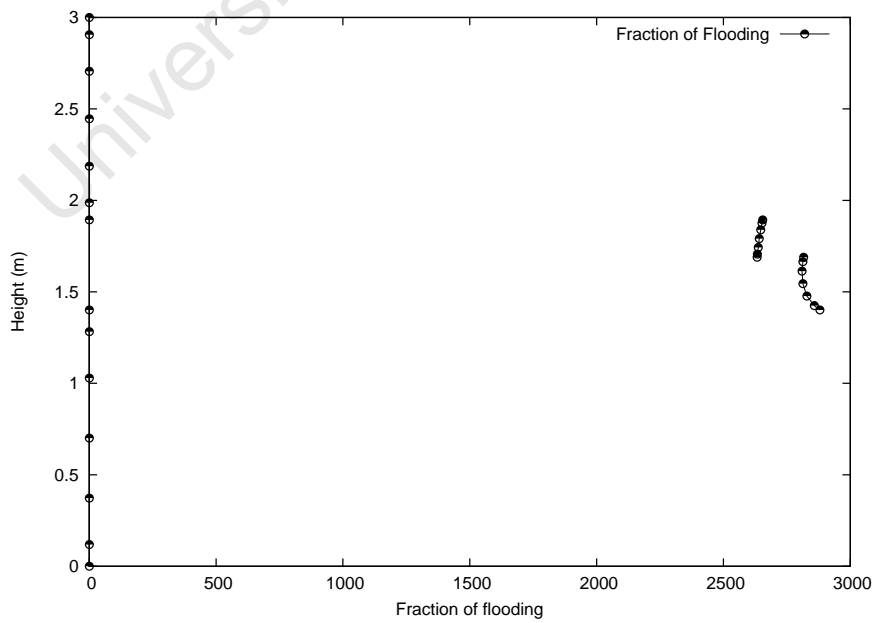


Figure 8.3: Fraction of Flooding in column in 1 Reactor system

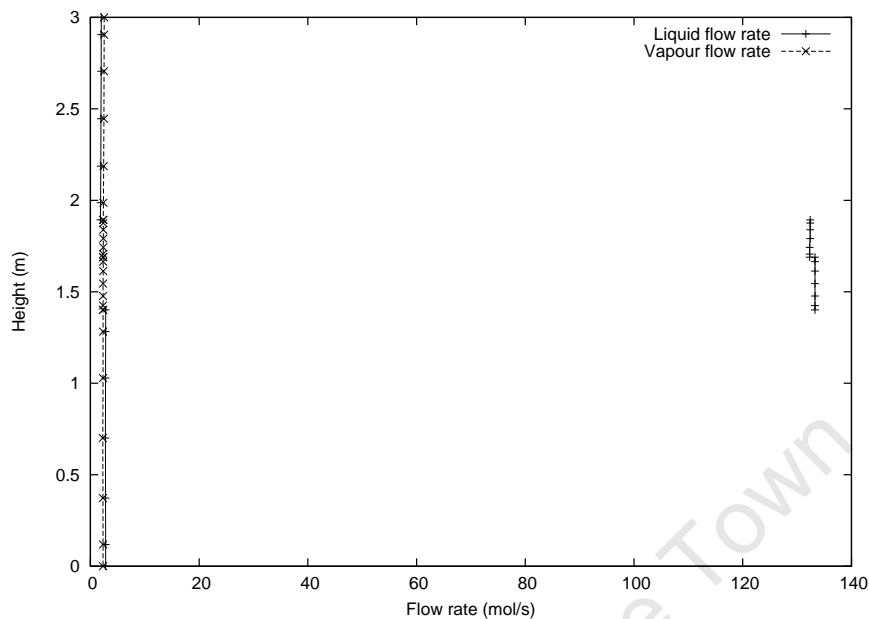


Figure 8.4: Liquid and Vapour flow rates in column in 1 Reactor system

and so flooding is inevitable.

This observation highlights the need to take flooding into account when designing systems of this nature. However, the way that the optimisation system is set up requires a single diameter column and this would result in very wide columns to minimise flooding. Future work could include optimising the diameter of the columns, or having different diameter sections.

Another interesting observation is the fact that the reactor with the higher conversion per pass is not usually favoured in terms of the flow rate through it. This shows that the whole system needs to be treated as a whole, as the implication of the changes in the composition profiles by the reactor streams is large. It appears that the separation of the products in the distillation column is of more importance than the actual individual conversions within each reactor when maximising overall toluene conversion.

Figures 8.1(a) and 8.1(b) show a trend of having the feed to the side reactors drawn from below the feed location and returning the reaction products to a location above the feed. This *counter-current* flow through the reactor (with respect to the flow in the column) tends to result in higher flow rates through the reactor. Having the sidestream located just below the feed should allow for a higher toluene concentration in the reactor feed and result in higher conversions in the reactor. A number of other interesting

observations can be seen from these results.

- In most cases, high reflux and boilup ratios are required to achieve maximum toluene conversions. However, there appear to be optimum values in each case that are not the maximum in the range (in this case, R and $R_b \leq 5.0$).
- It appears that, in some cases, one of the reactors might be favoured over another - this can be seen in the two reactor system in Table 8.2, where the first reactor only has a sidestream ratio of 0.026 (resulting in a flow rate of 0.08mol/s), while the second reactor has a a sidestream ratio of 0.962 (resulting in a flow rate of 77.98mol/s). However, in the three reactor system, there is less of a disparity between the reactor sidestream ratios, but still results in two of the reactors being favoured in terms of flow through them.

8.2 Total Annual Cost

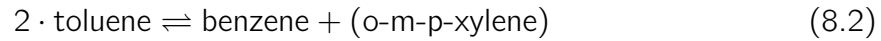
8.2.1 Comparison with RD and Conventional Systems in Literature

In 2002, Stitt performed a technical and economical evaluation of using a RD system for toluene disproportionation. The study compared a RD system to a conventional system consisting of three reactors followed by a series of distillation columns to separate out the various products. The author concluded that the RD system was not more economically attractive than a conventional system, due mainly to the high operating pressures required to keep the reactants in the liquid phase in the RD column.

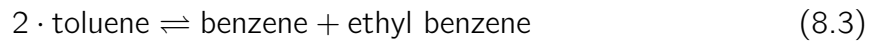
Therefore, a comparison of the side reactor systems with the systems evaluated by Stitt (2002) was considered. It was thought that the use of the side reactor systems would allow optimum operating conditions in the reactors and separators and reduce the cost of the high pressure columns experienced by Stitt (2002) in the RD column.

In the literature study, a plant producing 150,000 tons/year of mixed xylenes was considered using a feed of toluene of between 37.5 and 41.2 tons per hour. This translates into a feed of 113mol/s of toluene feed and becomes the basis of the following comparison. Side reactor systems consisting of one, two and three external reactors, were considered and the specification of 150,000 tons/year of mixed xylenes was an additional constraint. The objective function was to minimise the TAC.

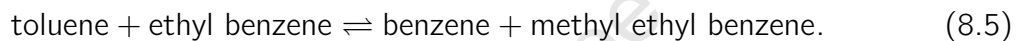
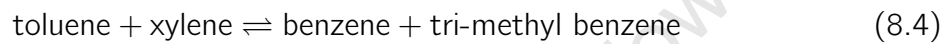
In the study by Stitt (2002), the author considers the toluene disproportionation reaction to benzene and the three xylene isomers



and ethyl benzene



with other side reactions resulting in heavier compounds



However, the study also states that in a conventional vapour phase reactor, the selectivity towards benzene and the xylene isomers is approximately 90%. The selectivity towards ethyl benzene is a further 4% and therefore Equations 8.2 and 8.3 will be used in the comparison.

The parameters used in the comparison study are given in Table 8.4 using a feed flow rate of 113mol/s. To reduce the possibility of flooding described in Section 8.1, the diameter of the column was chosen to allow for the high flow rates using the *fraction of flooding method*.

Using the method described in Section 6.2.2, the specification of 150,000 tons/year (roughly 48mol/s) of mixed xylenes was set as a constraint. This results in the following objective function

$$\max F(x) = \begin{cases} -TAC & \text{if } F_{Xylene} \geq 48 \text{ mol/s} \\ -(TAC_{max}) - \left(\frac{48 - F_{Xylene}}{48} \right) & \text{otherwise} \end{cases} \quad (8.6)$$

where F_{Xylene} is the flow rate of all three xylene isomers retrieved in the distillate of the column and TAC is the Total Annual Cost (in \$). The resulting optimal systems obtained are given in Tables 8.5 and 8.6, with graphical representations of these systems in Figure 8.5.

Table 8.4: Fixed side reactor system parameters used in the minimisation of Total Annual Costs using and equilibrium reactor and taking the ethylbenzene side reaction into account

Parameter	Value	Parameter	Value
Feed flow rate	113.0mol/s	Condenser type	Total
Feed composition:		Reboiler type	Partial
Benzene	0.0005	Height	20.0m
Toluene	0.9975	Diameter	3.0m
o-Xylene	0.0005	Packing type	50mm metal Pall rings
m-Xylene	0.0005	Feed quality	1.0
p-Xylene	0.0005		
Ethylbenzene	0.0005		

Table 8.5: Optimum systems to achieve minimum TAC using equilibrium reactors with ethylbenzene side reaction

	1 Reactor	2 Reactors	3 Reactors
Reflux Ratio	4.152	2.974	3.645
Boilup Ratio	4.837	4.435	4.392
Feed Height (m)	9.396	10.95	10.35
Sidestream ratio 1	0.582	0.490	0.213
Sidestream height 1 (m)	4.722	9.742	3.476
Return height 1 (m)	11.06	8.056	2.308
Sidestream ratio 2	-	0.840	0.555
Sidestream height 2 (m)	-	8.706	10.93
Return height 2 (m)	-	15.03	4.416
Sidestream ratio 3	-	-	0.547
Sidestream height 3 (m)	-	-	7.384
Return height 3 (m)	-	-	13.57
TAC (\$'000)	11,850	10,370	9,812

Table 8.6: External reactor details for the configurations to achieve minimum TAC using equilibrium reactors

	1 Reactor	2 Reactors	3 Reactors
Reactor 1 flow rate (mol/s)	469.1	238.8	65.36
Reactor 1 toluene conversion	0.345	0.373	0.169
Reactor 2 flow rate (mol/s)	-	206.8	195.2
Reactor 2 toluene conversion	-	0.318	0.391
Reactor 3 flow rate (mol/s)	-	-	144.7
Reactor 3 toluene conversion	-	-	0.368

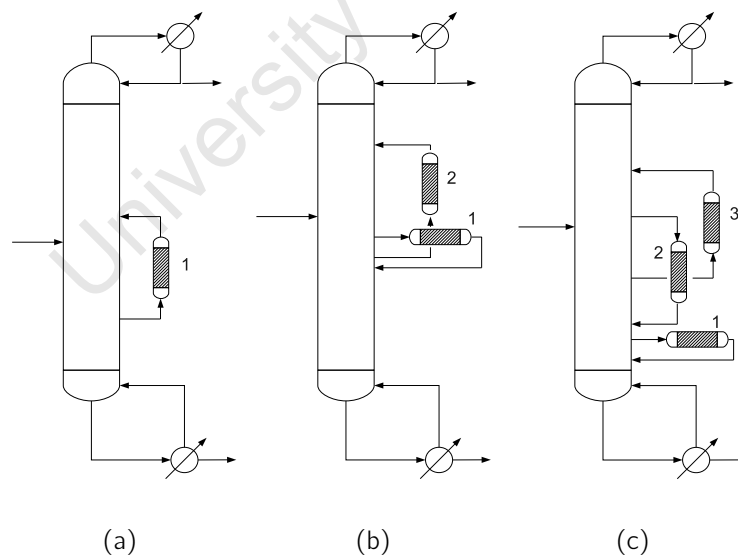


Figure 8.5: Optimal configurations for minimum TAC using (a) one external equilibrium side reactor, (b) two external equilibrium side reactors and (c) three external equilibrium side reactors

A few observations can be seen from these results. Firstly, the reflux and boilup ratios appear to be natural optimum values as the constraints of them lying between 0.1 and 5.0 are not enforced. Secondly, the optimal feed position seems to be roughly in the middle of the 20m column. This is most likely due to the components in the system and should allow for maximum separation and high toluene concentrations in the middle of the column.

One of the side reactors always has its feed drawn from below the feed and returns its products to a point above the feed (reactors 1, 2 and 3 for the systems consisting of one, two and three reactors respectively). A possible explanation for this is that the concentration of toluene is most likely to be highest just below the feed and by returning the products to above the feed, it allows for the large amounts of benzene to be removed in the vapour streams and out the top of the column. As for the other reactors, it appears that the best configuration is as *co-current* reactors. This would seem to reduce the flow through the reactors, but as mentioned before, these systems are highly integrated and so it is important to look at them as a whole.

From Table 8.6, it is clear that the conversion per pass is much greater in the equilibrium reactors in these systems, compared to those obtained in Table 8.3 for the optimisation of the overall conversion using kinetic reactors. Another observation is that all the reactors seem equally favoured in each system, compared to the obvious distinction seen in Table 8.3.

In the evaluation carried out by Stitt (2002), the cost of the reactors and catalyst were ignored due to insufficient information regarding the kinetics of the reactions and the cost of the catalysts required. Therefore, these were omitted in the following comparison between the capital and utility costs of the side reactor systems. Table 8.7 shows the capital and utility breakdown for the side reactor systems as well as the overall TAC used as the fitness function in the optimisation. Figures 8.6 and 8.7 provide a graphical representation of these results.

It is clear from these results that an increase in the number of reactors decreases the TAC. Both the capital and utility costs are reduced, thanks mainly to a reduction in the cost of the furnace and the fuel required to heat the furnace. This can be attributed to the decrease in the duty of the furnace and thus resulting in a decrease in the costs associated with it.

The results obtained by Stitt (2002) are given in Table 8.8 and include items such

Table 8.7: Capital and Utility cost breakdown for TAC optimum systems using equilibrium reactors and taking into account the ethylbenzene side reaction (\$'000)

	1 Reactor	2 Reactors	3 Reactors
Capital costs	4,452	4,216	3,984
Distillation column	953	953	953
Furnace	3,083	2,813	2,567
Heat exchangers	417	451	464
Utility costs (p.a.)	10,370	8,964	8,484
Process steam	4,735	4,124	4,333
Cooling water	413	360	332
Heating fuel	5,218	4,480	3,820
TAC	11,850	10,370	9,812

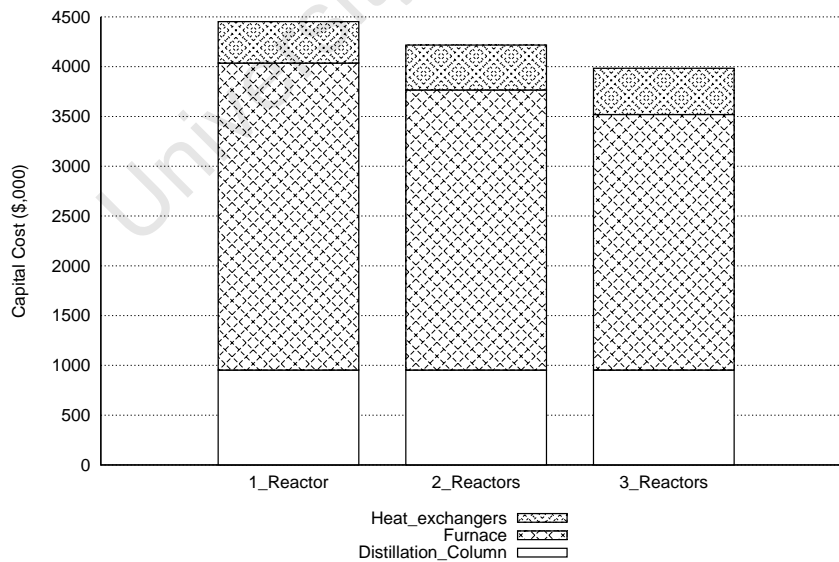


Figure 8.6: Capital cost breakdown for 1, 2 and 3 external equilibrium side reactor systems with ethyl benzene side reaction

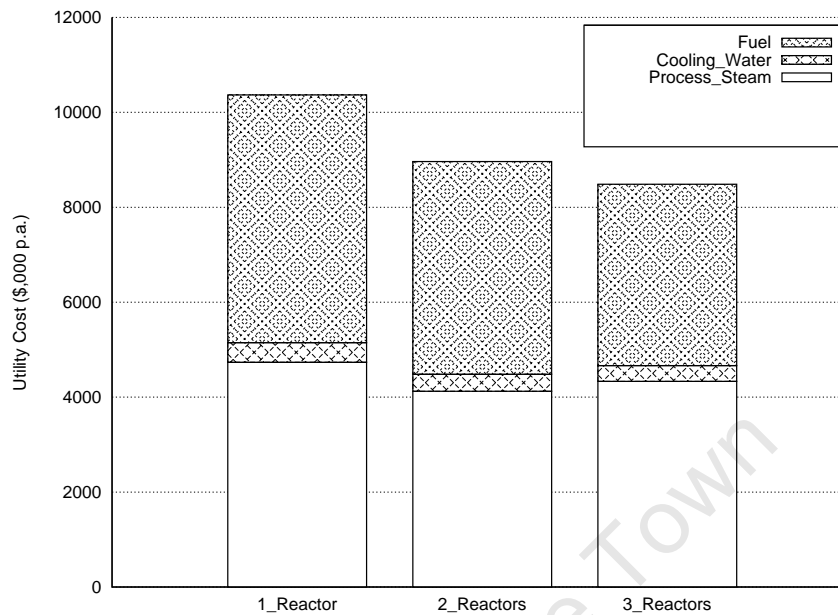


Figure 8.7: Utility cost breakdown for 1, 2 and 3 external equilibrium side reactor systems with ethyl benzene side reaction

Table 8.8: Capital costs obtained by Stitt (2002) - updated to 2008 values (\$'000)

	Reactive Distillation	Conventional Process
RD Column	13,794	-
Distillation columns	7,790	15,109
Furnace	7,522	11,867
Heat exchangers	5,896	7,808
Pumps & compressors	271	781
Reactors & vessels	92	1,250
Engineering & overheads	5,312	5,524
Total	40,679	42,339

as pumps and overheads. Unfortunately the systems evaluated by Stitt (2002) are more complex than those investigated in this study. They are shown in Figures 8.8 and 8.9. They have a much larger set of distillation columns for separating out the various components.

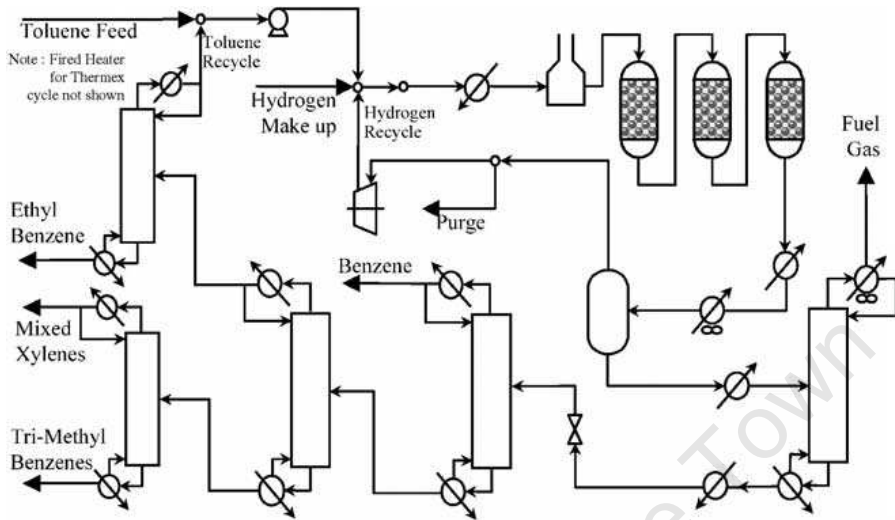


Figure 8.8: Conventional System used by Stitt (2002)

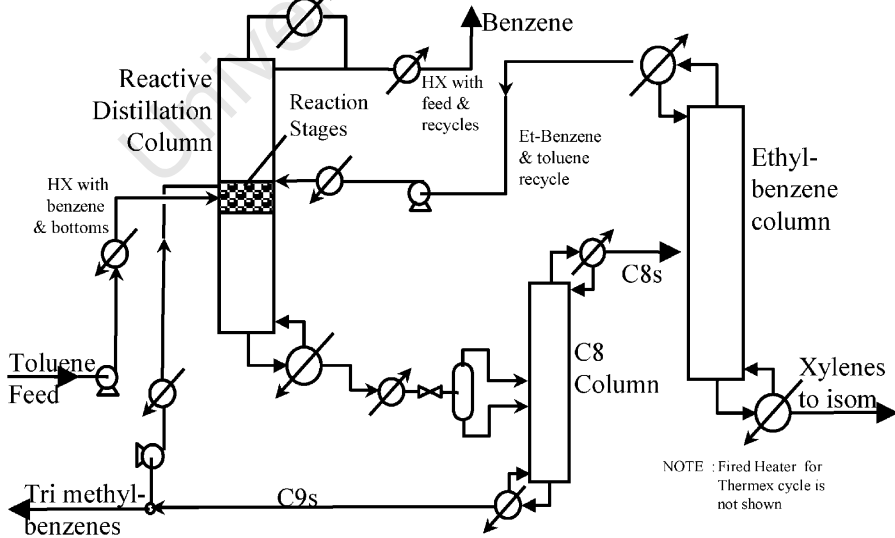


Figure 8.9: RD system used by Stitt (2002)

Table 8.9: Fixed side reactor system parameters used in the minimisation of Total Annual Costs

Parameter	Value	Parameter	Value
Feed flow rate	113.0mol/s	Condenser type	Total
Feed composition:		Reboiler type	Partial
Benzene	0.05	Height	20.0m
Toluene	0.98	Diameter	3.0m
o-Xylene	0.05	Feed quality	1.0
m-Xylene	0.05		
p-Xylene	0.05		

However, some conclusions can still be drawn from these results. If one compares the total capital cost for each of the three side reactor systems with the cost of the RD column in Stitt's work, then there is a significant decrease in the capital cost of that particular area of the system. This result shows that there is scope for using side reactor systems in circumstances where RD systems are unsuitable.

8.2.2 Comparison with Conventional Two Column System

Due to the difficulty in comparing the results obtained in this investigation with those obtained in literature, another comparison has been performed. Three side reactor systems were again compared, however in this study, the kinetics described in Section 6.4.1 were used (ignoring the ethyl benzene side reaction). The fixed parameters used in the optimisation studies are given in Table 8.9. The constraint of 150,000 tons/year of mixed xylenes was retained and the objective function is the same as Equation 8.6.

The conventional system consists of a single kinetic reactor followed by two distillation columns. The first column removes the benzene product in the distillate, while the second column separates the toluene (mostly recycled back to the reactor) and the mixed xylene product (see Figure 8.10). The optimum side reactor systems using the kinetic reactor and ignoring the ethyl benzene side reaction are given in Tables 8.10 and 8.11, and represented graphically by Figure 8.11.

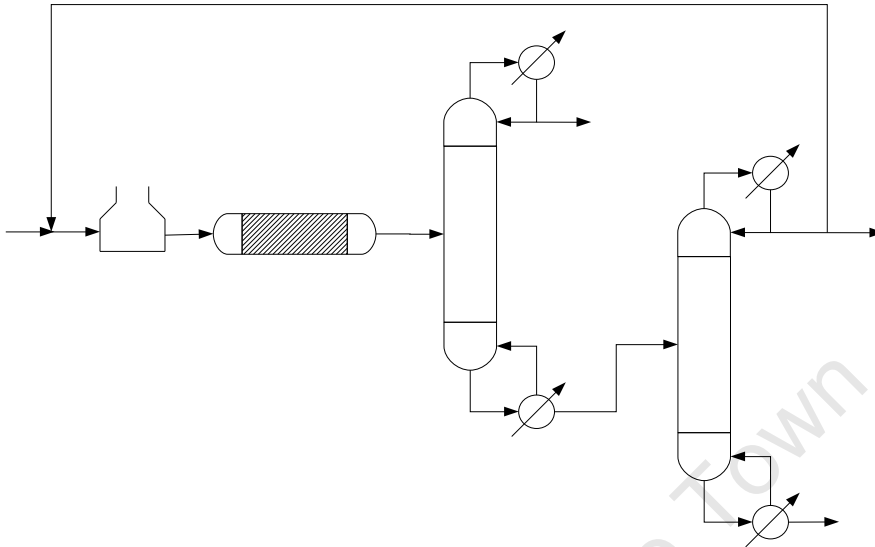


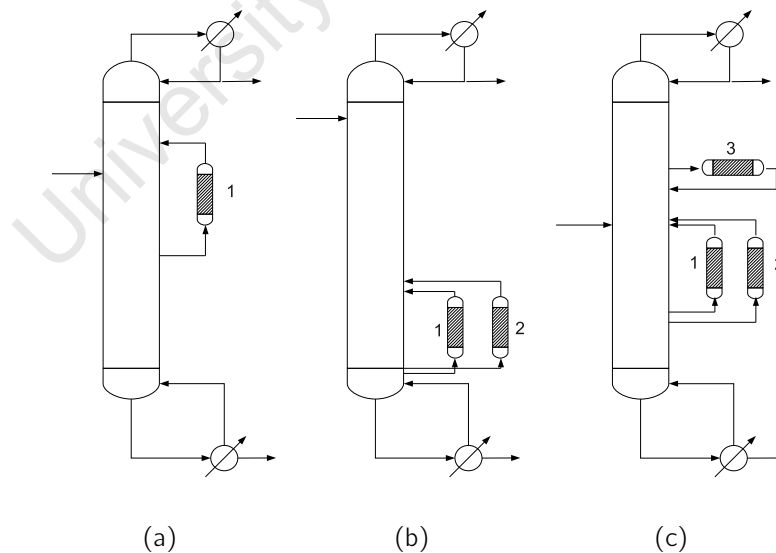
Figure 8.10: Two column conventional system used in optimisation comparison

Table 8.10: Optimum systems to achieve minimum TAC

	1 Reactor	2 Reactors	3 Reactors
Reflux Ratio	4.488	3.439	4.358
Boilup Ratio	4.976	4.100	4.229
Feed Height (m)	13.52	16.81	10.39
Sidestream ratio 1	0.845	0.668	0.807
Sidestream height 1 (m)	8.362	0.986	5.162
Return height 1 (m)	15.09	5.966	10.18
Sidestream ratio 2	-	0.492	0.164
Sidestream height 2 (m)	-	1.560	4.568
Return height 2 (m)	-	6.542	10.34
Sidestream ratio 3	-	-	0.918
Sidestream height 3 (m)	-	-	13.61
Return height 3 (m)	-	-	12.46
TAC (\$'000)	38,630	36,053	37,258

Table 8.11: External reactor details for the configurations to achieve minimum TAC using kinetic reactors

	1 Reactor	2 Reactors	3 Reactors
Reactor 1 flow rate (mol/s)	1945	601.1	1635
Reactor 1 toluene conversion	0.071	0.058	0.065
Reactor 2 flow rate (mol/s)	-	866.4	64.52
Reactor 2 toluene conversion	-	0.057	0.075
Reactor 3 flow rate (mol/s)	-	-	188.8
Reactor 3 toluene conversion	-	-	0.154

**Figure 8.11:** Optimal configurations for minimum TAC using (a) one external side reactor, (b) two external side reactors and (c) three external side reactors

From these results and those obtained using the equilibrium reactor, the different type of reactor is seen to have a major effect on the optimum configurations. A simple comparison of the graphical representations show marked differences in the locations and operation of the side reactors. For the equilibrium reactor systems, there is always a *counter-current* reactor bridging the feed position and then the other reactors are *co-current* reactors. Looking at the kinetic reactor systems, the bridging *counter-current* reactor appears to have been retained (it is absent in Figure 8.11(b)), but now the other reactors have become a mixture of *co-current* and *counter-current* reactors. The increase in the number of *counter-current* reactors suggests that the drop in conversion per pass in the external reactors (due to the use of kinetic rather than equilibrium reactors) has been accounted for by increasing the flow through the reactors. Table 8.11 reinforces this explanation as the flow rates through the reactors are much higher than those in the equilibrium reactor systems given in Table 8.6.

The other major consideration is that the cost of the catalyst and reactor are now taken into account. This would be a function of the flow rate through the reactor and would suggest that this would be minimised to keep the cost down. The other contributing factor is the lower conversions and therefore it would appear to be a compromise between cost of the reactor (a function of the flow rate) and the overall production of the xylene products.

Another interesting observation is the appearance of two reactors with nearly identical locations. This can be seen in Figures 8.11(b) and 8.11(c) and would seem to suggest that the conditions are in favour of these locations. However, the conversions in these reactors are still relatively low.

The two column conventional system's optimisation parameters were as follows:

- Reflux ratios of columns 1 and 2
- Boilup ratios of columns 1 and 2
- Feed heights for column 1 and 2
- Recycle ratio of recycle stream to purge stream.

The resulting optimum configuration for the two column conventional process is given by Table 8.12. The resulting comparable capital and utility costs are given in Table 8.13 and Figures 8.12 and 8.13.

Table 8.12: Optimum two column conventional system to achieve minimum TAC

Parameter	Value	Parameter	Value
Reflux Ratio 1	3.443	Reflux Ratio 2	1.887
Boilup Ratio 1	2.083	Boilup Ratio 2	3.740
Feed Height 1 (m)	5.776	Feed Height 2 (m)	10.43
Recycle ratio	0.945		

It is clear from these results that the conventional two column system is more cost effective than the integrated side reactor systems. The conventional system requires only approximately 30% and 60% of the capital and utility costs of the side reactor systems. This seems to contradict the previous results of the equilibrium reactor systems, but it must be noted that a high percentage of the capital costs are represented by the reactor (and associated catalyst) and the furnace. By adding these to the comparison, the real comparison shows that the side reactor systems are not economically attractive. This is mainly due to the large flows required to enter the reactor due to the dilution of the main reactant (toluene) in the distillation column. The conventional system has the advantage of obtaining much higher concentrations of toluene as a feed (due to the recycle stream).

A number of other interesting observations can be made and these include:

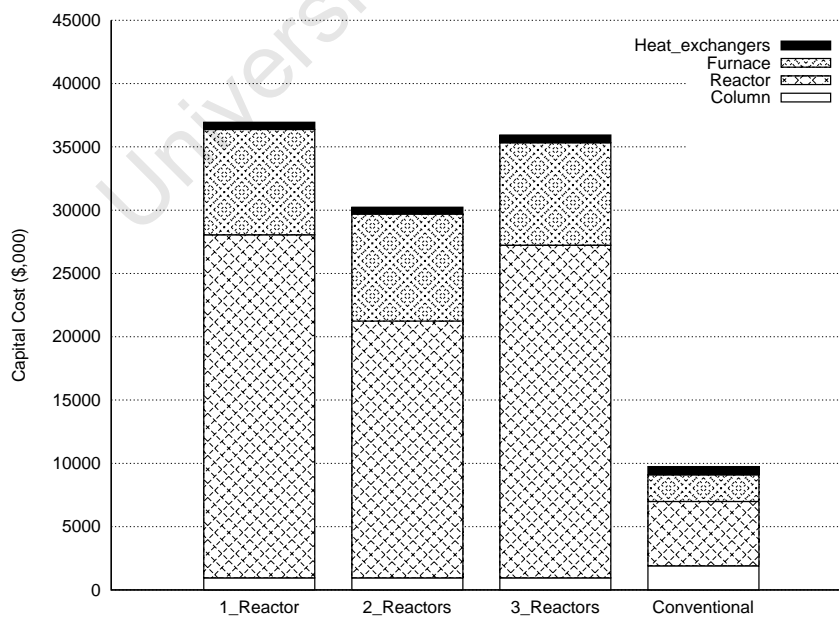
- The furnace fuel cost for the conventional system is much lower than the side reactor systems. This is as a result of the lower recycle flow rates and means that less material is heated to the reaction temperature.
- The process steam requirements for the conventional system is more than double the steam needed in the side reactor systems. This is mainly due to the increase in the number of the reboilers and the high flow rates of liquid in the distillation columns from the high recycle values.

Figure 8.14 shows the trends in capital, utility and total annual costs for side reactor systems consisting of between one and five reactors. It appears that there is a minimum in the costs when using two reactors, while adding additional reactors does not seem to be beneficial.

From the results obtained thus far, it is clear that the side reactor systems could

Table 8.13: Capital and Utility cost breakdown for TAC optimum systems (\$'000)

	1 Reactor	2 Reactors	3 Reactors	Conventional
Capital costs	36,950	30,230	35,940	9,738
Distillation column	953	953	953	1,906
Reactor	27,100	20,280	26,280	5,083
Catalyst	25,770	19,290	24,960	4,821
Furnace	8,321	8,463	8,092	2,106
Heat exchangers	573	533	610	643
Utility costs (p.a.)	26,310	25,980	25,280	14,962
Process steam	4,934	4,220	4,601	11,820
Cooling water	1,185	1,161	1,139	510
Heating fuel	20,190	20,600	19,540	2,624
TAC	38,630	36,060	37,260	18,200

**Figure 8.12:** Capital cost breakdown for 1, 2 and 3 external kinetic side reactor systems compared to the conventional system

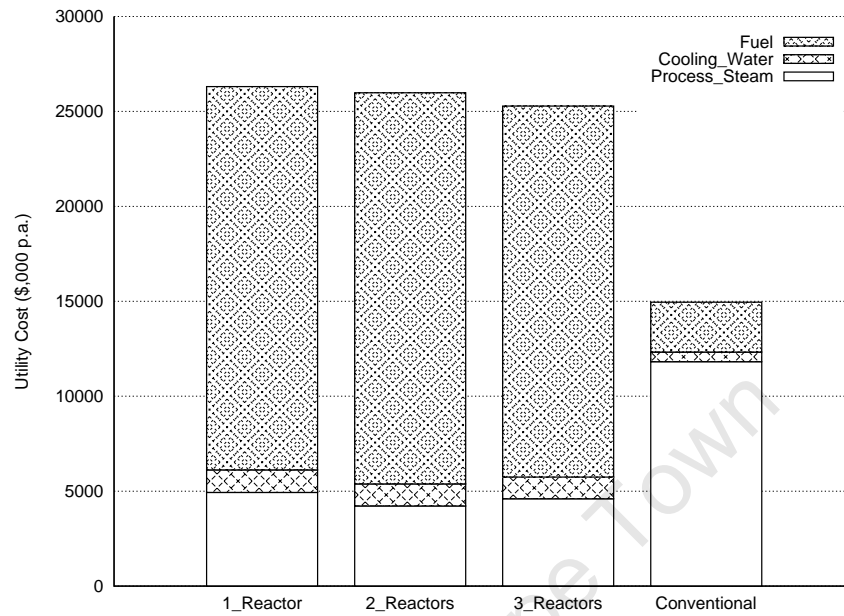


Figure 8.13: Utility cost breakdown for 1, 2 and 3 external kinetic side reactor systems compared to the conventional system

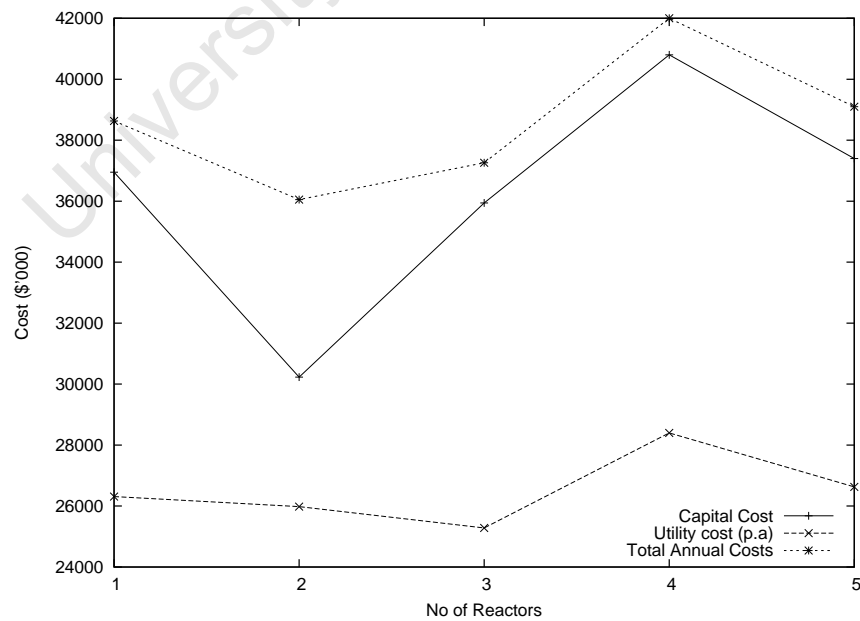


Figure 8.14: Cost trends using side reactor systems for toluene disproportionation

provide a potential improvement in capital and utility costs, but for a system producing mixed xylenes via toluene disproportionation it appears that the conventional system is still more cost effective, due mainly to keeping high concentrations of toluene in the reactor feed.

The process of obtaining these results has proved effective and shows that the use of nonequilibrium distillation models can be used in optimising complex distillation column models that have multiple side streams. The use of the orthogonal collocation method has provided useful in keeping the order of the model consistent and the computational times to a minimum.

University Of Cape Town

Chapter 9

Results: Methyl Acetate Synthesis

Only a few reaction systems have been investigated in literature when modelling side reactor systems. These include methyl acetate synthesis (Baur and Krishna (2004)) and the production of MTBE (Jakobsson et al. (2002)). These are likely candidates as they have both been successfully employed in industry using RD columns. Thus they both make for good systems when comparing RD with side reactor systems.

Therefore, the methyl acetate synthesis reaction was chosen as a case study to look at the effect of using a liquid phase reaction, instead of the gas phase reaction discussed in Chapter 8, and also allowed for comparisons to the results obtained by Baur and Krishna (2004). The reaction and kinetics are described in Section 6.4.2.

9.1 Overall Conversion

The study by Baur and Krishna (2004) looked at optimising side reactor systems. However, they only looked at using an equilibrium model to describe the column, and for the majority of the study, used an adiabatic equilibrium reactor model. Therefore, to add to this work, the same systems were investigated, with the additional complexity of using the *non-equilibrium collocation distillation model* described in Section 6.3.1.

9.1.1 Comparability

To ensure that the results were at least comparable, a simple equimolar feed of the four components (acetic acid, methanol, methyl acetate and water) was fed into a 43 equilibrium staged distillation model in *ChemSep*. The same feed was then used in the *nonequilibrium collocation model* and the height adjusted until comparable results were achieved. The *adiabatic equilibrium reactor model* was retained to attempt to produce comparable results.

9.1.2 Results

To optimise for the maximum overall conversion of acetic acid (the measure used by Baur and Krishna (2004) to determine system performance), the following objective function was used

$$\max f(x) = X_{overall}. \quad (9.1)$$

Using the results from Chapter 7, the decision was taken to only use the genetic algorithm method for this study. The same problems with discontinuous variables and objective functions remains and this rules out the other methods described earlier.

The results obtained by Baur and Krishna (2004) showed that a higher number of side reactors and a higher reactor throughput lead to higher overall acetic acid conversions. They stated that an economical trade off is required between higher throughputs (resulting in fewer reactors) and more side reactors (resulting in lower throughputs). These results are compared with similar side reactor systems with nonequilibrium distillation columns modelled and optimised using the techniques described in the rest of the thesis and can be seen in Figure 9.1.

Baur and Krishna (2004) used a different definition of a sidestream ratio called a pumparound ratio. This is defined as

$$R_{PA} = \frac{S_j}{L_j} \quad (9.2)$$

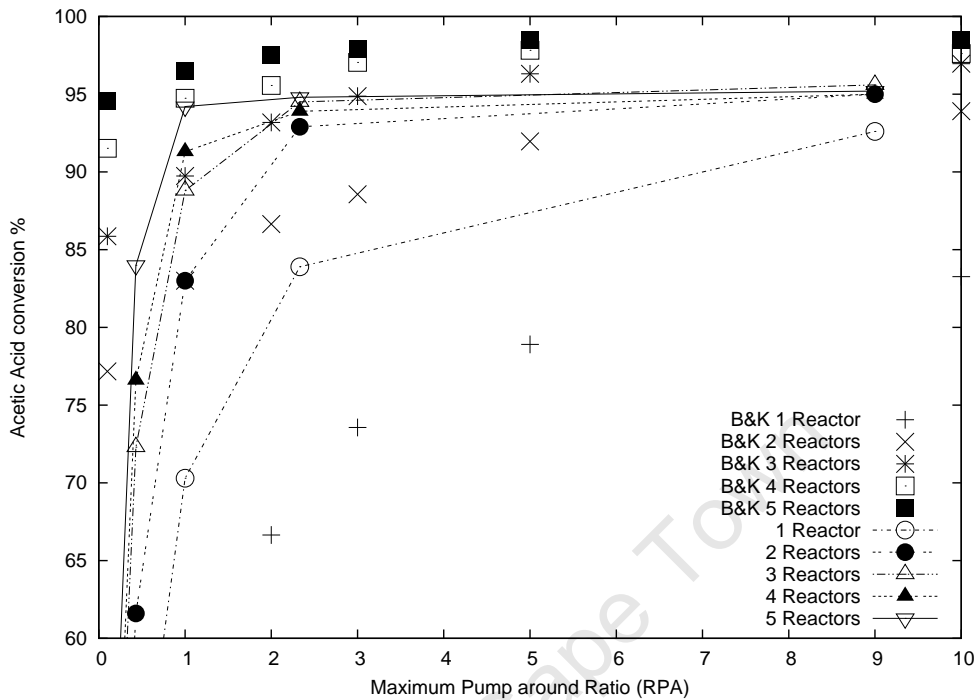


Figure 9.1: Comparison between Baur and Krishna (2004) and the collocation model for various optimum configurations

and so the following relationship between the two ratios is as follows:

$$R_S = \frac{R_{PA}}{1 + R_{PA}} \quad (9.3)$$

It is clear from Figure 9.1 that the results differ quite considerably and a possible explanation for the differences is the use of equilibrium and nonequilibrium models for modelling the distillation column. The nonequilibrium distillation model could result in lower separation in the column that could not be accounted for when using the equilibrium model.

Baur and Krishna's results generally show much higher conversions than the nonequilibrium collocation distillation model for very low pumparound ratios. This difference cannot be due to the reactor type (they are the same adiabatic equilibrium reactor) or the limits on the flows in the column (these should be similar due to the same specifications in the column). Using different types of distillation models should only make a shift in the conversion, not such a significant difference in the profile.

The results obtained by the collocation model developed in this work would appear to show a more realistic trend when looking at the effect of the pumparound ratio on

the overall acetic acid conversion. At very low pumparound ratios, very little material is drawn out of the column to go through the reactors. This would result in the low acetic acid conversion values obtained in this study and not the much higher values obtained in the work by Baur and Krishna (2004).

9.1.3 Multiple Steady States

The methyl acetate system has the potential to exhibit multiple steady states (Doherty and Malone (2001)). These were investigated by Baur and Krishna (2004) and in some cases, as many as seven steady states were observed. This is a concern when considering the optimisation of these side reactor systems. However, the use of GA's in the optimisation process would overcome these challenges as the optimum solution is often approached from multiple points and is modelled many times during the optimisation process and should identify true global optimums.

The study by Baur and Krishna (2004) showed that the operating regions used in both these studies do not contain multiple steady states. However, their distillation models were different and the possibility of these multiple steady states is still a concern. These should be looked at in future work, but does not form part of this work.

This study has shown that even with a single external reactor, more than 90% conversion of acetic acid can be achieved. However, it can be achieved without high pumparound ratios if more reactors are used. Therefore the tradeoff between the high throughputs and more reactors, as described by Baur and Krishna (2004), is still very much a factor in determining the best system. This aspect of these systems is investigated further in the following section.

9.2 Total Annual Cost

The previous results were obtained using an equilibrium reactor model and so the full implications of cost cannot be taken into account. Therefore, another study was performed using the kinetics described in Section 6.4.2 and the costs were compared with a more conventional process system as before in the toluene disproportionation case study.

This more conventional system can be seen in Figure 9.2, where a feed of *acetic acid* and *methanol* is fed to the reactor. The reactor products are then sent to the first

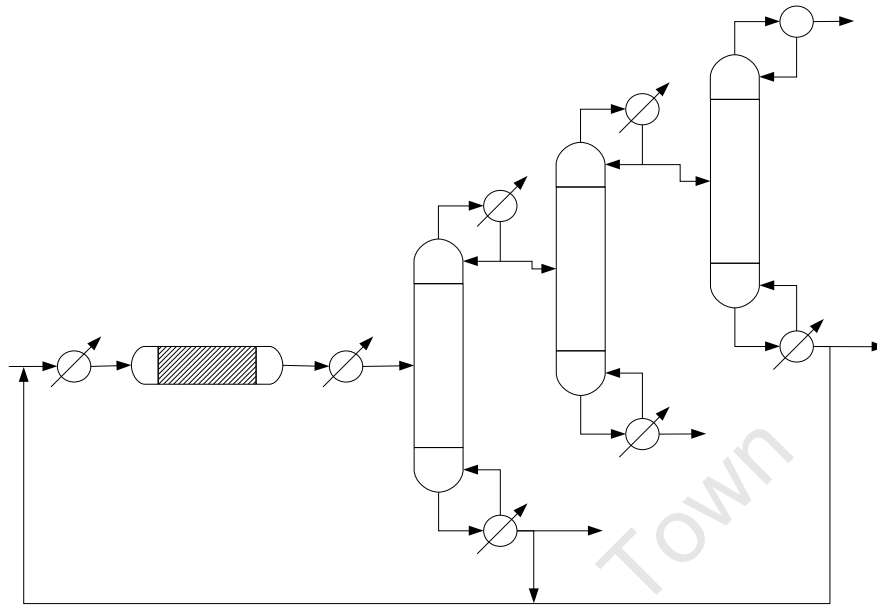


Figure 9.2: Three column system to produce Methyl Acetate from Acetic Acid and Methanol

column where acetic acid is drawn off in the bottoms and recycled, while the distillate is further separated in a second column, where *water* is removed in the bottoms. The distillate from the second column is finally separated into the *methyl acetate* product in the distillate, and the remaining *methanol* reactant is obtained in the bottoms and recycled back to the reactor.

To be able to produce comparable results, a minimum target production rate of 180 kmol/h (50 mol/s) of *methyl acetate* was used. This value is comparable to the production rates used in the work by Baur and Krishna (2004). To achieve this, the fixed parameters given in Table 9.1 were used for the side reactor systems, while those given in Table 9.2 were used in the conventional system. To keep the results comparable, 99 m³ of Amberlyst 15 ion-exchange resin was used in each study (Baur and Krishna (2004)). In the case of multiple side reactors, this amount was distributed equally between the reactors. The amount of packing was also kept constant and so each of the conventional system's three columns had 33% of the packing in the single column of the side reactor systems.

The ranges of the optimisation parameters are given in Table 9.3 with *Recycle Ratio 1* being the ratio of the bottoms stream of the first column being recycled, and *Recycle Ratio 2*, the ratio of the bottoms stream of the third column being recycled.

Table 9.1: Fixed system parameters used in the minimisation of Total Annual Costs for the side reactor system in the Methyl Acetate study

Parameter	Value	Parameter	Value
Feed flow rate	154.0mol/s	Condenser type	Total
Feed composition:		Reboiler type	Partial
Acetic Acid	0.5	Column Height	10.0m
Methanol	0.5	Column Diameter	1.0m
Methyl Acetate	0.0	Feed quality	1.0
Water	0.0		

Table 9.2: Fixed system parameters used in the minimisation of Total Annual Costs for the conventional system in the Methyl Acetate study

Parameter	Value	Parameter	Value
Feed flow rate	154.0mol/s	Condenser type	Total
Feed composition:		Reboiler type	Partial
Acetic Acid	0.5	Column Heights	3.33m
Methanol	0.5	Column Diameters	1.0m
Methyl Acetate	0.0	Feed quality	1.0
Water	0.0		

Using the constraint handling method described in Section 6.2.2, the resulting objective function is given by

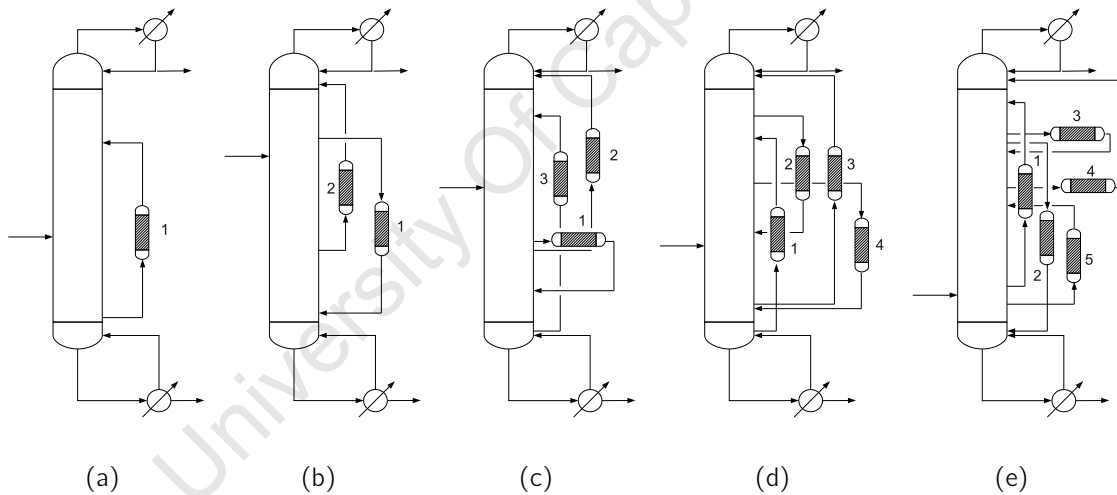
$$\max F(x) = \begin{cases} -TAC & \text{if } F_{MeOAc} \geq 50 \text{ mol/s} \\ -(TAC_{max}) - \left(\frac{50 - F_{MeOAc}}{50}\right) & \text{otherwise} \end{cases} \quad (9.4)$$

where F_{MeOAc} is the flow rate of the methyl acetate product retrieved in the distillate of the column in the case of the side reactor column, or the methyl acetate retrieved from the distillate of the third column in the case of the conventional system. The fitness is penalised if the target of 50mol/s is not achieved.

The resulting side reactor systems to achieve 50mol/s of methyl acetate with the

Table 9.3: Optimisation parameters used in the minimisation of Total Annual Costs for the Methyl Acetate study

Side reactor system		Three column system	
Parameter	Range	Parameter	Range
Reflux ratio	$0.1 \leq R \leq 5.0$	Recycle ratio 1	$0.001 \leq RR_1 \leq 0.99$
Boilup ratio	$0.1 \leq R_B \leq 5.0$	Recycle ratio 2	$0.001 \leq RR_2 \leq 0.99$
Feed height (m)	$0.1 \leq h_f \leq 9.9$	For each Column:	
For each Reactor:		Reflux ratio	$0.1 \leq R \leq 5.0$
Sidestream ratio	$0.001 \leq R_s \leq 0.99$	Boilup ratio	$0.1 \leq R_B \leq 5.0$
Sidestream height (m)	$0.1 \leq h_s \leq 9.9$	Feed height (m)	$0.1 \leq h_f \leq 3.33$
Return height (m)	$0.1 \leq h_r \leq 9.9$		

**Figure 9.3:** Optimal configurations for minimum TAC using the side reactor systems with (a) one, (b) two, (c) three, (d) four and (e) five external reactors

minimum TAC are given in Table 9.4 and the reactor details for each system in Table 9.5. These systems are represented graphically by Figure 9.3 with the height of the streams to scale with the height of the column. The problem with flooding seen in Chapter 8 is not as pronounced in this case. This can be seen in Figure 9.4 where most of the column has a fraction of flooding below 1.0, with only a small section flooding.

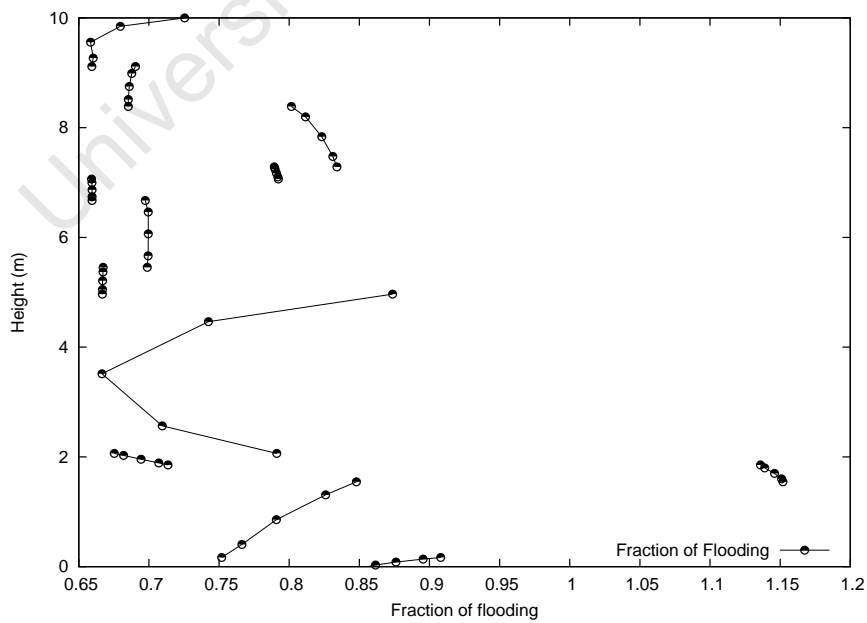
The resulting optimum system for the conventional system can be seen in Table 9.6.

Table 9.4: Optimum systems to achieve minimum TAC for methyl acetate synthesis

	1 Reactor	2 Reactors	3 Reactors	4 Reactors	5 Reactors
Reflux Ratio	0.220	0.617	0.301	0.119	0.234
Boilup Ratio	2.370	2.299	1.604	1.671	2.117
Feed Height (m)	3.788	6.509	5.426	3.443	1.853
Sidestream ratio 1	0.782	0.456	0.835	0.645	0.620
Sidestream height 1 (m)	1.039	7.151	3.625	0.129	2.064
Return height 1 (m)	6.930	1.288	1.901	7.128	8.386
Sidestream ratio 2	-	0.688	0.828	0.564	0.924
Sidestream height 2 (m)	-	3.424	3.319	7.917	7.064
Return height 2 (m)	-	8.980	9.268	3.941	0.167
Sidestream ratio 3	-	-	0.465	0.137	0.218
Sidestream height 3 (m)	-	-	0.550	1.537	7.285
Return height 3 (m)	-	-	7.974	9.651	6.672
Sidestream ratio 4	-	-	-	0.484	0.648
Sidestream height 4 (m)	-	-	-	5.618	5.455
Return height 4 (m)	-	-	-	1.365	9.114
Sidestream ratio 5	-	-	-	-	0.569
Sidestream height 5 (m)	-	-	-	-	1.547
Return height 5 (m)	-	-	-	-	4.966
TAC (\$'000)	5,682	5,575	5,508	5,425	5,369

Table 9.5: External reactor details for the configurations to achieve minimum TAC for the methyl acetate system

	1 Reactor	2 Reactors	3 Reactors	4 Reactors	5 Reactors
Reactor 1 flow rate (mol/s)	640.4	114.7	320.8	315.4	85.77
Reactor 1 acetic acid conversion	0.529	0.471	0.690	0.658	0.695
Reactor 2 flow rate (mol/s)	-	204.3	52.43	33.70	93.40
Reactor 2 acetic acid conversion	-	0.819	0.466	-0.277	-0.135
Reactor 3 flow rate (mol/s)	-	-	155.3	49.67	28.12
Reactor 3 acetic acid conversion	-	-	-0.283	0.807	-0.124
Reactor 4 flow rate (mol/s)	-	-	-	165.3	23.03
Reactor 4 acetic acid conversion	-	-	-	0.057	-0.139
Reactor 5 flow rate (mol/s)	-	-	-	-	120.4
Reactor 5 acetic acid conversion	-	-	-	-	0.922

**Figure 9.4:** Fraction of flooding with the column with 5 external reactors

The costs associated with these optimum systems can be seen in Figures 9.5, 9.6 and 9.7. These include the various equipment capital costs, the utility costs as well as the Total Annual Cost (the objective function minimised in each case).

Looking first at the side reactor systems, it is clear that the TAC decreases with an increase in the number of external reactors. This trend can be explained by looking at the breakdown of the costs in Figure 9.5. As the number of reactors is increased, the capital costs naturally increase, but the utility costs decrease. Now as the TAC is calculated as follows

$$TAC = C_{utility} + \frac{C_{capital}}{\text{Payback period}}, \quad (9.5)$$

and in this case the payback period is 3 years, the utility costs tend to dominate the TAC. This results in the TAC decreasing with the increase in the number of reactors (seen in Figure 9.5). The TAC given by Equation 9.5 is a simple first order estimate for costs used in chemical engineering (Pintaric and Kravanja (2006)), and is suitable for comparison purposes.

Despite the complicated layout of the side reactor streams in the systems shown in in Figure 9.3, it is still possible to observe some trends. As was the case in Chapter 8, there is always a *counter-current* reactor that bridges the feed location. This configuration has the potential to allow for higher flow rates through the reactor.

The other reactors are a mix of *co-* and *counter-current* reactors, but looking at the details in Tables 9.4 and 9.5, it is possible to see which of the reactors are preferred and which have the higher conversions per pass. Most of the sidestream ratios are relatively high, compared to the toluene systems, but the actual flow rates through the reactors are not as high as those in the toluene systems.

Table 9.5 shows that in some cases the reactor conversion of acetic acid per pass is negative. This is likely to happen when the concentrations of methyl acetate and water in the column are higher than the reactants. This effectively makes the reaction occur in reverse. However, as the objective was to minimise the TAC while producing 50mol/s of methyl acetate, the individual conversions are not as important as the overall performance of the system.

This holistic approach is very important and by modelling the system as a whole and using the GA to optimise it is an advantage. Therefore, a negative conversion may be beneficial to the overall performance of the system, as it could allow for higher reactant

concentrations in a more favourable position in the column. It could also allow for better separation due to differing concentration gradients caused by the side streams into the columns.

The optimum configuration of the conventional three column system is given in Table 9.6, where the reflux, boilup and recycle ratios are given, as well as the feed heights for each column. For the optimum system, the recycle flow rate is 69mol/s, resulting in a flow of 223mol/s of material entering the reactor. This is comparable to the flow rates given in Table 9.5, but comparing it to the side reactor system analogue of the single external reactor, the flow rate is nearly a third of the side reactor system. This low flow rate, coupled with higher acetic acid and methanol concentrations, allows for a much higher conversion of acetic acid in the reactor of 89%.

While the high conversion per pass obtained in the conventional system is positive, the cost comparisons shown in Figures 9.6 and 9.7 highlight the economic drawbacks of this system. The capital costs shown in Figure 9.6 are comparable over all the systems. The main cause for the increase in the capital costs with the increase in reactors for the side reactor systems is that each reactor requires additional heat exchangers to heat and cool the feeds and returning streams.

The major advantage the side reactor systems have over the conventional systems is the lower utility usage. Figure 9.7 shows that the conventional system has a much higher steam requirement, mainly due to the additional distillation columns. Each column adds to the amount of material that is required to be vapourised and cooled repeatedly. For the side reactor systems, the steam requirements actually decrease with the increase in the number of reactors.

Naturally the scenario can be altered, depending on the payback period chosen. This was chosen as three years, but should it be increased, then the capital costs have less of an impact on the TAC (this would further enhance the advantage of the side reactor systems). If the payback period were to be decreased, then the capital costs would become an increasing factor in the TAC and then it would favour the slightly lower capital cost requirements of the conventional system.

The results obtained in this study show that the side reactor systems do show potential when compared to more conventional systems. This is in contrast to the results from Chapter 8, where the gas phase reaction proved to have greater costs associated with it. These were mainly due to the heating of the sidestreams to vaporise the reactants and

Table 9.6: Optimum three column conventional system to achieve the minimum TAC of \$7.924 million for producing 50mol/s of methyl acetate

Parameter	Value	Parameter	Value	Parameter	Value
Reflux Ratio 1	0.268	Reflux Ratio 2	1.274	Reflux Ratio 3	0.766
Boilup Ratio 1	1.417	Boilup Ratio 2	3.764	Boilup Ratio 3	4.866
Feed Height 1 (m)	1.368	Feed Height 2 (m)	0.994	Feed Height 3 (m)	0.672
Recycle ratio 1	0.553			Recycle ratio 2	0.497

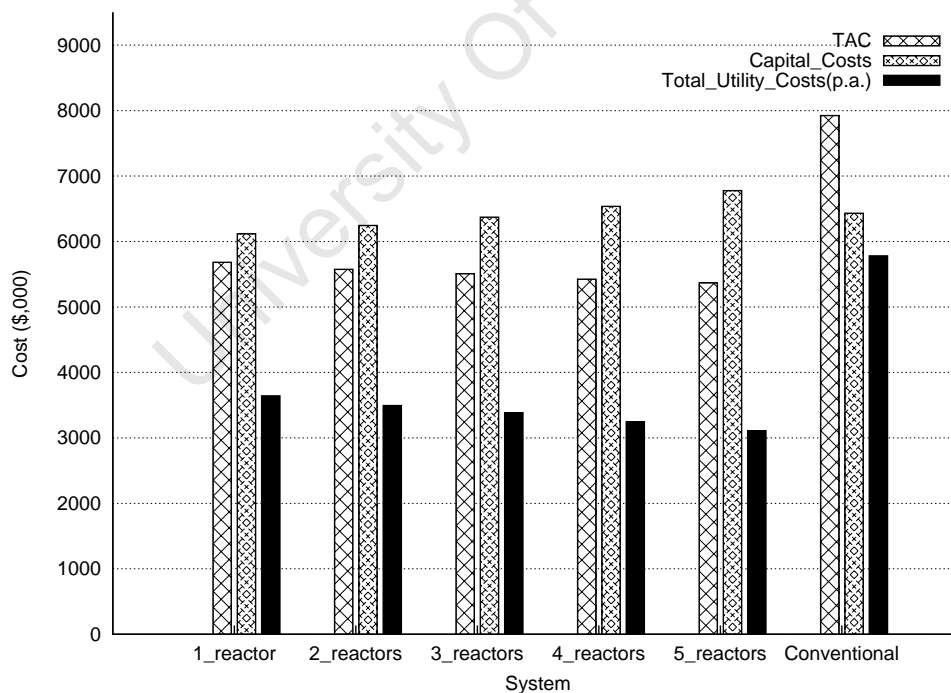


Figure 9.5: Cost trends using side reactor systems and the conventional system for methyl acetate production

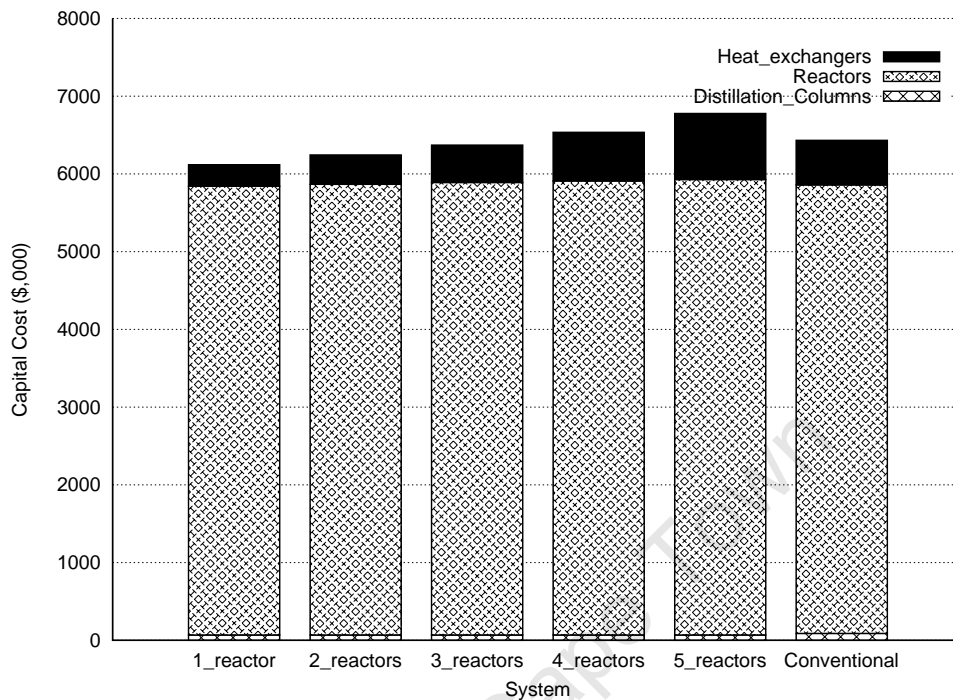


Figure 9.6: Comparison of capital costs for the side reactor systems and the conventional 3 column system for the production of methyl acetate

bring them to the high reaction temperature. The cooling of the reaction products also contributed to the high costs and so the side reactor system was unattractive in terms of costs in a side reactor system.

The lack of the high temperatures and associated heating and cooling means that the methyl acetate reaction is better suited to the side reactor systems. This would seem to suggest that side reactor systems should be considered as a possible process alternative when designing whole liquid phase reaction systems.

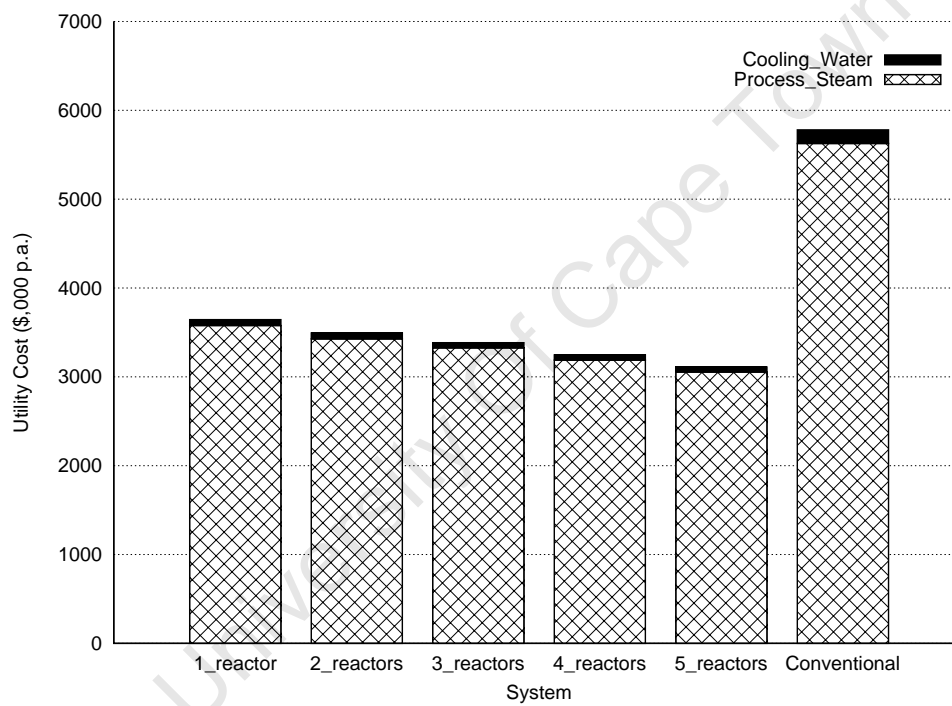


Figure 9.7: Comparison of utility costs for the side reactor systems and the conventional 3 column system for the production of methyl acetate

Chapter 10

Future Work

There are still a number of improvements to be made to the tool developed in this study to broaden its applicability. A number of areas of process optimisation and design could still be identified as candidates for the methods and techniques applied in this research.

10.1 Improvements to the program

The program works very well for the specific application investigated in this study. However for the program to be useful in a wider range of applications, the following improvements could be made.

1. Adding further VLE options
2. Increasing the component and mixture property methods
3. Develop a user interface, so that the tool may be more user friendly
4. Add a flooding calculation to determine the optimal diameter of the column, or
5. Use the flooding calculation as a constraint in the optimisation process to limit the flow rates within the distillation column
6. Investigate the effect of withdrawing vapour streams from the column instead of only liquid streams

10.2 Directions for future work and applications

The work covered in this research is focused on a specific type of process, namely integrated side reactor systems. The tools and techniques developed in this study can be applied to a much broader set of problems and processes.

As shown in Section 3.7, orthogonal collocation methods have been applied to many areas of process design. These applications can all be included in optimisation studies using collocation methods, with the benefit of reducing the calculation time.

The method of optimising complex distillation systems (in this case a single reactor with integrated side reactors) can be further applied to separation superstructures, where a large number of distillation sections can be linked in a number of interesting and non-conventional ways. Figure 10.1 shows just some of the possible configurations that need to be considered when separating just four components. As the number of components increase, so do the number of possibilities. The tool developed in this research could easily be configured to explore these quickly and find the optimum configuration.

Another area that this approach could be used is in reactive distillation. Although the model developed only looks at distillation columns linked to reactors, the nonequilibrium model for distillation can be extended to take into account reaction at each point along the column.

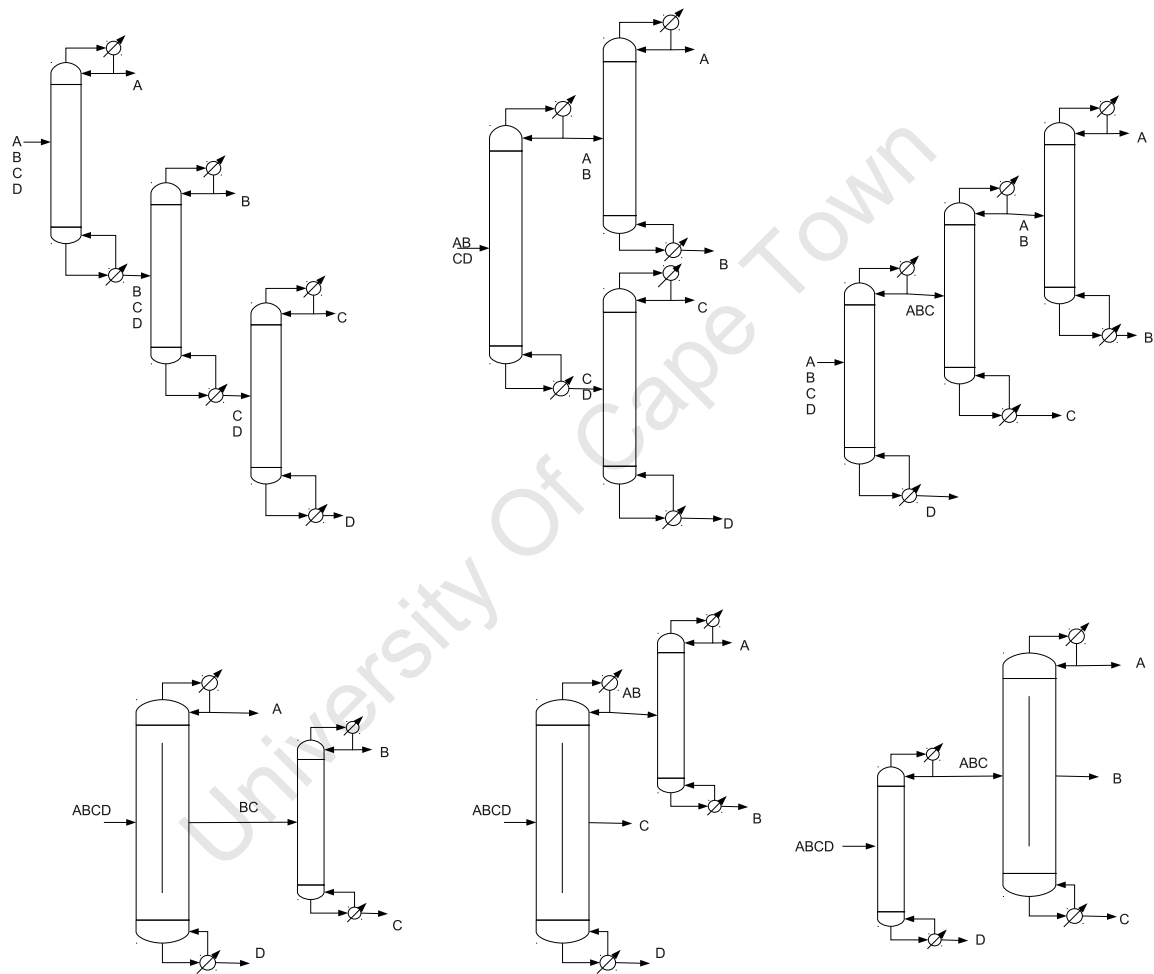


Figure 10.1: Various configurations of distillation columns to separate four components

University Of Cape Town

Chapter 11

Conclusions

The aim of this work was to develop a tool to optimise complex distillation columns (those with multiple side streams) using rigorous nonequilibrium distillation models. These models are usually avoided due to the high order of the problem resulting in long computational times. By using orthogonal collocation, these computational times were reduced and the models were successfully employed in optimisation studies.

These studies were particularly focused on packed distillation columns and by using orthogonal collocation on the differential form of the nonequilibrium model, it was not necessary for experimental studies to determine HETP values to apply a staged model to the packed column.

11.1 Toluene Disproportionation Case Study

The toluene disproportionation reaction using a side reactor system was used as a case study to iron out any potential problems along the way. Initially, two NLP techniques were used in the optimisation of a simple system consisting of a single external reactor. However, both of these techniques struggled due to the discontinuities inherent in the systems involving multiple sidestreams. This led to the decision to use a genetic algorithm due to the fact that it does not require gradients.

Once the optimisation technique was determined, the following conclusions could be drawn from the results

- An increase in the number of external kinetic side reactors results in a decrease in the overall toluene conversion
- An increase in the number of equilibrium external side reactors results in a decrease in the TAC of the system
- The capital cost of all the equilibrium side reactor systems are lower than an equivalent RD column
- The capital and utility costs (using kinetic reactor systems for more realistic costs) are higher than an equivalent conventional system. This is mainly due to the extra recycle flows to the furnace and reactors.
- The use of kinetic reactors when optimising these systems for minimum costs is very important, as the configurations obtained are significantly different.

Overall, the results have shown that the toluene disproportionation reaction is not suited to side reactor systems. This is due to the high cost of vaporising the reactor feeds and then condensing and cooling the products.

There is a possibility of extracting a vapour phase side stream and return the reactor products in the vapour phase. However, this is usually more difficult to implement and the side stream would still require compression and further heating to reach the reaction conditions.

11.2 Methyl Acetate Case Study

This reaction was chosen as a second case study to look at what difference a liquid phase reaction might have on the comparisons. It is also widely studied in RD comparisons and therefore, a large amount of information is available. The packed collocation side reactor system model was compared to an equilibrium staged model in literature. Both showed similar results, but there were some significant differences (particularly at low flow rates through the side reactors). The collocation model developed in this thesis showed much lower overall acetic acid conversions than those obtained using the equilibrium model in literature.

An economic evaluation was performed on side reactor systems with 1-5 external reactors. These results were compared to a more conventional three column system,

with the following observations:

- The TAC decreases with the increase in the number of external reactors. This is mainly due to the decrease in the utility costs, whereas the capital costs actually increase with the increase in reactors.
- *Counter-current* external reactors bridging the feed location are always present in the optimum configurations
- In some cases, the conversion per pass in each reactor is negative. However, the overall production of products is a function of many factors and a holistic approach is necessary when optimising these systems.
- The capital costs of the side reactor systems are comparable to those of the more conventional system.
- The utility costs of the conventional system are much higher than those of the side reactor systems. This is due to the high steam requirements for the reboilers needed for the three distillation columns.

11.3 Concluding Remarks

In this study, the optimisation of integrated side reactor systems were performed. These systems are relatively complex in that many parameters are involved and there is a large amount of interaction between process units and the streams connecting them. This means that it is important to view these systems as a single unit and optimise them accordingly.

From the results it was found that nonequilibrium distillation models can be used in these optimisation studies and that orthogonal collocation allows for a reduction in the order of the model, which translates into shorter computational times.

From the two case studies it is clear that the reaction and process conditions are important considerations when developing these integrated system. In the case of the gas phase toluene disproportionation reaction, the costs of vapourising and heating the sidestreams before entering the reactors, as well as the higher flow rates, proved prohibitive. This resulted in a more conventional system being preferred in terms of costs. However, for the liquid phase methyl acetate reaction, the findings were very different.

The integrated side reactor systems proved to be more efficient and cost effective than a more conventional system.

These contrasting results highlight the need for a tool, such as the one developed in this study, to be able to consider the possible options when designing a process. By using a nonequilibrium distillation model, with orthogonal collocation, a realistic representation of the process can be used as a basis for cost calculations.

Overall, this research has shown that integrated side reactor systems should be seriously considered as alternatives to RD systems when looking at liquid phase reactions. This is especially true when looking at making modifications to existing infrastructure. As these integrated side reactor systems make use of the same equipment as a conventional system (just a matter of piping changes), they should be considered when looking for the benefits of RD systems, but without investing in a whole new unit.

11.4 Summary of contributions

This research has contributed to the field of process design and optimisation by exploring the use of rigorous distillation models in optimisation studies. This is not normally done due to the high computational cost of the calculations, but with the combination described in this research, it is possible to provide quick and accurate results.

In summary, the work described in this thesis made the following contributions:

- **A program was developed to optimise complex distillation columns using rigorous models.** This model incorporated the orthogonal collocation method to reduce the time required to solve the system model, but retain accuracy.
- **Various optimisation techniques were evaluated.** The complexity of the system produced interesting difficulties in optimisation and as a result Genetic Algorithms are recommended when optimising complex distillation systems.
- **Integrated side reactor systems were investigated in terms of performance and cost.** These systems were compared to the more conventional systems of (i) reactors followed by a separation section and (ii) reactive distillation. The results showed that process conditions are important factors when choosing between these three technologies, with liquid phase reactions favoured.

Overall, these contributions extend the applicability of using the more accurate rate-based nonequilibrium distillation model in optimisation studies. They also provide insights into the integrated side reactor systems, showing that they have a place in the decision making, when choosing a reactor-separator technology.

University Of Cape Town

University Of Cape Town

Appendix A

Mass and Heat Transfer Derivations

A.1 Mass Transfer

A.1.1 Structured Packing

Bravo et al. (1985) developed correlations for predict mass transfer coefficients using the geometry shown in Figure A.1. The vapour phase Sherwood number is given by

$$Sh_V = 0.0338 Re_V^{0.8} Sc_V^{0.3333} \quad (A.1)$$

with the Sherwood number being defined as

$$Sh_V = \frac{k^V d_{eq}}{D^V} \quad (A.2)$$

where the vapour phase mass transfer coefficient (k^V) can be obtained.

The equivalent diameter (d_{eq}) is given by

$$d_{eq} = Bh \left[\frac{1}{B + 2S} + \frac{1}{2S} \right] \quad (A.3)$$

where B is the channel base, h is the height of the channel, and S is the channel side. The Reynolds number for the vapour phase is given by

$$Re_V = \frac{d_{eq} \rho_t^V (u_e^V + u_e^L)}{\eta^V} \quad (A.4)$$

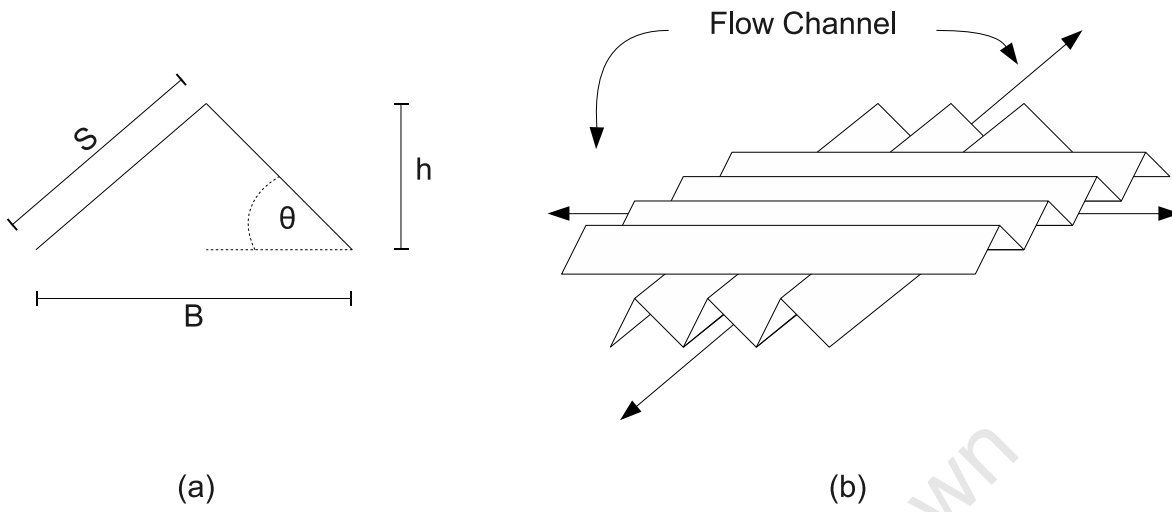


Figure A.1: Geometry of structured packing (a) Flow channel cross section (b) Flow channel arrangement

where the effective vapour (u_e^V) velocity is defined as

$$u_e^V = \frac{u^V}{\varepsilon \sin \theta} \quad (\text{A.5})$$

where u^V is the superficial velocity, ε is the void fraction, and θ is the channel angle (see Figure A.1). The effective liquid velocity is given by

$$u_e^L = \frac{3\Gamma}{2\rho_t^L} \left(\frac{(\rho_t^L)^2 g}{3\eta^L \Gamma} \right)^{0.3333} \quad (\text{A.6})$$

where Γ is the liquid flow rate per unit length of packing perimeter given by

$$\Gamma = \frac{\rho_t^L u^L}{PA_c} \quad (\text{A.7})$$

with A_c being the cross-sectional area of the column and P being packing perimeter defined by

$$P = \frac{4S + B}{Bh} \quad (\text{A.8})$$

To obtain the liquid phase mass transfer coefficients (k^L), a penetration model is used

$$k^L = 2 \left(\frac{D^L u_\epsilon^L}{\pi S} \right)^{0.5} \quad (\text{A.9})$$

A.1.2 Random Packing

Many methods for determining mass transfer coefficients in packed columns are available, however, only one method was used in this study. Onda et al. (1968) developed correlations for mass transfer coefficients in randomly packed columns where the vapour phase mass transfer coefficient is obtained from

$$\frac{k^V}{a_p D^V} = A Re_V^{0.7} Sc_V^{0.333} (a_p d_p)^{-2} \quad (\text{A.10})$$

where d_p is the nominal packing size, a_p is the specific surface area of the packing and A is a constant with the value of 2.0 when $d_p < 0.012\text{m}$ and 5.23 when $d_p \geq 0.012\text{m}$. With the vapour phase Reynolds number given by

$$Re_V = \frac{\rho_t^V u^V}{\eta^V a_p} \quad (\text{A.11})$$

and the Schmidt number in the vapour phase is

$$Sc_V = \frac{\eta^V}{\rho_t^V D^V} \quad (\text{A.12})$$

The liquid phase mass transfer coefficient is obtained from

$$k^L \left(\frac{\rho_t^L}{\eta^L g} \right)^{0.333} = 0.0051 (Re'_L)^{0.667} Sc_L^{-0.5} (a_p d_p)^{0.4} \quad (\text{A.13})$$

where the liquid phase Schmidt number is given by

$$Sc_L = \frac{\eta^L}{\rho_t^L D^L} \quad (\text{A.14})$$

and the liquid phase Reynolds number based on the interfacial area is given by

$$Re'_L = \frac{\rho_t^L u^L}{\eta^L a'} \quad (\text{A.15})$$

The value of interfacial area density is given by

$$a' = a_p \left\{ 1 - \exp \left[-1.45 \left(\frac{\sigma_c}{\sigma} \right)^{0.75} Re_L^{0.1} Fr_L^{-0.05} We_L^{0.2} \right] \right\} \quad (A.16)$$

where σ is the surface tension of the liquid, while σ_c is the critical surface tension of the packing. The Reynolds number based on the specific packing surface area is

$$Re_L = \frac{\rho_t^L u^L}{\eta^L a_p} \quad (A.17)$$

and the liquid phase Froude number is

$$Fr_L = \frac{a_p (u^L)^2}{g} \quad (A.18)$$

with the Weber number being

$$We_L = \frac{\rho_t^L (u^L)^2}{a_p \sigma} \quad (A.19)$$

A.1.3 Packing Characteristics

In the study, various structured and random packings were used in each model and their characteristics can be found in Table A.1. These values were used in the correlations described in the previous sections.

A.2 Heat Transfer

The vapour phase heat transfer coefficients were determined from the well known Chilton-Colburn analogy where

$$j_D = j_H = \frac{f}{2} \quad (A.20)$$

Table A.1: Random and Structured Packing Characteristics

	Random	Structured	
	Pall Rings	Sulzer BX	Koch Flexipac2
Material	Metal	Stainless Steel	Stainless Steel
Nominal packing size, d_p (m)	0.0508	-	-
Specific surface area, a_p (m^2/m^3)	112.6	492.0	223.0
Critical surface tension, σ_c (N/m)	0.075	-	-
Crimp height, h (m)	-	6.4×10^{-3}	1.24×10^{-2}
Channel base, B (m)	-	1.27×10^{-2}	2.59×10^{-2}
Channel side, S (m)	-	8.9×10^{-3}	1.8×10^{-2}
Void fraction, ε (m^3/m^3)	-	0.90	0.95
Channel flow angle, θ ($^\circ$)	-	60	45

where f is the Fanning friction factor and the j -factors for mass and heat transfer are defined as

$$j_D = St Sc_V^{\frac{2}{3}} \quad (\text{A.21})$$

and

$$j_H = St_H Pr_V^{\frac{2}{3}} \quad (\text{A.22})$$

These result in the following simplified equation for determining the vapour phase heat transfer coefficient

$$h^V = k^V \rho_t^V C_p^V \left(\frac{Sc_V}{Pr_V} \right)^{\frac{2}{3}} \quad (\text{A.23})$$

where the Schmidt and Prandtl numbers are given by

$$Sc_V = \frac{\eta^V}{\rho_t^V D^V} \quad (\text{A.24})$$

and

$$Pr_V = \frac{C_p^V \eta^V}{\lambda^V} \quad (\text{A.25})$$

where λ^V is the thermal conductivity of the vapour phase.

To calculate the liquid phase heat transfer coefficient, a penetration model was used, resulting in

$$h^L = k^L \rho_t^L C_p^L \left(\frac{Sc_L}{Pr_L} \right)^{0.5} \quad (\text{A.26})$$

with the Schmidt (Sc_L) and Prandtl (Pr_L) defined as in equations A.24 and A.25, respectively using the liquid phase properties.

University Of Cape Town

Appendix B

Physical Properties

B.1 Component Temperature Dependent Properties

Table B.1: Correlations used for Temperature Dependent properties

Property	Correlation
Liquid density	$\rho_i^L = \frac{A}{B(1+[1-\frac{T}{T_c}]^D)} MW_i$
Vapour density	$\rho_i^V = \left[\frac{P}{R \cdot T}\right] MW_i$
Liquid heat capacity	$C_{p,i}^L = A + \exp\left(\frac{B}{T} + C + DT + ET^2\right)$
Vapour heat capacity	$C_{p,i}^V = A + BT + CT^2 + DT^3$
Liquid viscosity	$\eta_i^L = \exp\left(A + \frac{B}{T} + C \ln T + DT^E\right)$
Vapour viscosity	$\eta_i^V = \frac{AT^B}{1+\frac{C}{T}+\frac{D}{T^2}}$
Vapour pressure	$P_i^{vap} = \exp\left(A + \frac{B}{T} + C \ln T + DT^E\right)$
Liquid thermal conductivity	$\lambda_i^L = A + \exp\left(\frac{B}{T} + C + DT + ET^2\right)$
Vapour thermal conductivity	$\lambda_i^V = \frac{AT^B}{1+\frac{C}{T}+\frac{D}{T^2}}$
Surface tension	$\sigma = A + \exp\left(\frac{B}{T} + C + DT + ET^2\right)$

University Of Cape Town

Appendix C

Cost Calculations

C.1 Capital Costs

The capital costs of all the process equipment were calculated using the method described by Turton et al. (2003) in which the cost of each unit is given by

$$C_{BM} = C_{BM,2001} \frac{CEPCI}{397} \quad (C.1)$$

where the value of the bare module cost in 2001 is defined as

$$C_{BM,2001} = C_P^{\circ} F_{BM} \quad (C.2)$$

For most units have a bare module factor defined as

$$F_{BM} = B_1 + B_2 F_M F_P \quad (C.3)$$

where B_1 and B_2 are specific to each unit, but other process units have predefined values of F_{BM} .

The values of the material factor (F_M) can be obtained from Table A.3 and Figure A.8 from Turton et al. (2003), while the pressure factors (F_P) can be obtained using the following equations

$$\log F_P = C_1 + C_2 \log P + C_3 (\log P)^2 \quad (C.4)$$

Table C.1: Utility cost coefficients

Utility	Cost Coefficients		Limits
	a	b	
Cooling Water ^a , \$/m ³	$7.0 \times 10^{-5} + 2.5 \times 10^{-5}q^{-1}$	0.003	$0.01 < q < 10\text{m}^3/\text{s}$
Process Steam ^b , \$/kg	$2.3 \times 10^{-5}m_s^{-0.9}$	$0.0034p^{0.05}$	$1 < p < 46\text{barg}$ $0.06 < m_s < 40\text{kg/s}$

^a q is the total water capacity, m³/s

^b p is the required pressure, and m_s is the boiler steam capacity

where C_1 , C_2 and C_3 are constants specific to each unit, and if the unit is a process vessel, then

$$F_P = \begin{cases} \frac{\frac{(P+1)D}{2[850-0.6(P+1)]} + 0.00315}{0.0063} & \text{if } t_{\text{vessel}} > 0.0063\text{m} \\ 1 & \text{otherwise} \end{cases} \quad (\text{C.5})$$

C.2 Utility Costs

The utility costs were estimated using the method described by Ulrich and Vasudevan (2006) where they link the cost of a utility to inflation and the cost of the fuel source. Their base equation is as follows

$$C_u = a(\text{CEPCI}) + b(C_f) \quad (\text{C.6})$$

where C_u and C_f are the costs of the utility and fuel respectively. The values of the coefficients for the various utilities can be found in Table C.1. The fuel used was No. 6 Fuel Oil at a cost of \$7.07/GJ.

Appendix D

Flooding calculations

The fraction of flooding is calculated by dividing the superficial gas velocity by the flooding superficial gas velocity:

$$f_F = \frac{u^V}{u_{flood}^V}. \quad (D.1)$$

The flooding superficial gas velocity is found by solving the pressure drop correlation by Leva (1992):

$$\frac{\Delta P}{\Delta z} = 22.3 F_{packing} (\eta^L)^{0.2} \phi V_a^2 \frac{10^{0.035 L_a \phi}}{g \rho^V} \quad (D.2)$$

where

$$\phi = \frac{\rho_{water}}{\rho^L} \quad (D.3)$$

and

$$V_a = \frac{VM^V}{A_t} \quad (D.4)$$

and

$$L_a = \frac{LM^L}{A_t}. \quad (D.5)$$

The pressure drop at flood is calculated from the correlation by Kister and Gill (1991):

$$\left. \frac{\Delta P}{\Delta z} \right]_{flood} = 93.9 F_{packing}^{0.7} \quad (D.6)$$

University Of Cape Town

Nomenclature

d	Driving force for mass diffusion [m^{-1}]
s	Direction vector
a'	Interfacial area [m^2]
a'	Packing interfacial area density [m^2/m^3]
A_c	Column cross-sectional area [m^2]
a_p	Packing specific surface area [m^2/m^3]
$A_{i,j}$	First derivative coefficient matrix
B	Packing channel base [m]
$B_{i,j}$	Second derivative coefficient matrix
c	Concentration [$mol.m^{-3}$]
c	Number of components
C_f	Fuel cost[\$]
C_u	Utility cost [\$]
C_{BM}	Bare module cost [\$]
$CEPCI$	<i>Chemical Engineering Plant Cost Index</i>
D	Diffusivity [$m^2.s^{-1}$]
d_p	Nominal packing size [m]
d_{eq}	Equivalent diameter [m]

E	Efficiency [-]
F	Feed molar flow rate [$mol.s^{-1}$]
f	Fanning friction factor [-]
f_F	Fraction of flooding [-]
F_M	Material factor [-]
F_P	Pressure factor [-]
$F_{packing}$	Packing factor [m^{-1}]
Fr	Froude number [-]
g	Gravitational constant [$m.s^{-2}$]
H	Height of packing [m]
H	Molar enthalpy [$J.mol^{-1}$]
h	Packing channel height [m]
$HETP$	Height Equivalent To Packing [m]
J	Molar diffusion flux [$mol.m^{-2}.s^{-1}$]
j_D	Chilton-Colburn j -factor for mass transfer [-]
j_H	Chilton-Colburn j -factor for heat transfer [-]
J_n	n -th order Jacobi polynomial
K	Equilibrium constant [-]
k	Mass transfer coefficient [$m.s^{-1}$]
K_D	TDP equilibrium constant [-]
k_D	TDP rate constant [$mol.g^{-1}.h^{-1}.atm^{-1}$]
K_T	Toluene adsorption constant [atm^{-1}]
K_X	Mixed xylene adsorption constant [atm^{-1}]
L	Liquid molar flow rate [$mol.s^{-1}$]

l_i	Lagrange interpolation polynomial
N	Mass transfer rate [$mol.s^{-1}$]
N	Molar flux [$mol.m^{-2}.s^{-1}$]
N_{eq}	Number of equivalent equilibrium stages
ORP	Order Reduction Parameter
P	Packing perimeter [m]
P_B	Benzene partial pressure [atm]
p_n	n -th order node polynomial
P_T	Toluene partial pressure [atm]
P_X	Mixed xylene partial pressure [atm]
Pr	Prandtl number [-]
q	Feed liquid fraction [-]
R	Gas constant [8.314 J/mol K]
R	Reaction rate [<i>Various</i>]
r	Sidestream ratio [-]
r_D	Toluene disproportionation reaction rate [$mol.g^{-1}.h^{-1}$]
Rc	Schmidt number [-]
Re	Reynolds number [-]
S	Packing channel side [m]
Sh	Sherwood number [-]
St	Stanton number [-]
St_H	Stanton number for heat transfer [-]
T	Temperature [K]
U	Liquid sidestream molar flow rate [$mol.s^{-1}$]

u	Superficial velocity [$m.s^{-1}$]
u_e	Effective velocity [$m.s^{-1}$]
V	Vapour molar flow rate [$mol.s^{-1}$]
W	Vapour sidestream molar flow rate [$mol.s^{-1}$]
w	Test or weighting function
We	Weber number [-]
x	Liquid mole fraction [-]
y	Vapour mole fraction [-]
z	Height [m]
z^F	Feed mole fraction [-]

Superscripts

e	Equilibrium
F	Feed
I	Interfacial
L	Liquid
MV	Murphree vapour
V	Vapour

Subscripts

$flood$	flooding
HK	Heavy key component
i	Component i
j	Stage j
LK	Light key component
n	Stage n

t Total

Greek Letters

ϵ Energy transfer rate [W]

η Viscosity [$Pa.s$]

Γ Liquid flow rate per unit length of packing perimeter [$kg.m^{-1}.s^{-1}$]

Γ Thermodynamic factor [-]

γ Activity coefficient [-]

λ Lagrangian equality multiplier vector

λ Thermal conductivity [$W.m^{-1}.K^{-1}$]

μ Chemical potential [$J.mol^{-1}$]

μ Lagrangian inequality multiplier vector

ν Stoichiometric coefficient

ϕ Trial function

σ Stepsize

σ Surface tension [$N.m^{-1}$]

σ_c Packing critical surface tension [$N.m^{-1}$]

θ Packing channel angle [rad]

ϵ Packing void fraction [-]

ϵ Reaction volume or liquid holdup [m^3]

University Of Cape Town

Bibliography

- Agreda, V. H. and Partin, L. R. (1984). Reactive distillation process for the production of methyl acetate. US Patent. 4435595.
- Aguirre, P., Corsano, G., and Barttfeld, M. (2001). Optimal synthesis of multicomponent distillation processes. *Latin American Applied Research*, 31:281–286.
- Algunsun, T., Proios, P., Michael, C., and Pistikopoulos, E. (2006). A framework for the synthesis of reactive absorption columns. *Chemical Engineering and Processing*, 45(4):276–290.
- Amundsen, N. R. and Pontinen, A. J. (1958). Multicomponent distillation calculations on a large digital computer. *Ind. Eng. Chem.*, 50:730–736.
- Androulakis, I. and Venkatasubramanian, V. (1991). A genetic algorithmic framework for process design and optimization. *Comput. Chem. Eng.*, 15:217–228.
- Backhaus, A. A. (1921). Continuous processes for the manufacture of esters. US Patent.
- Barttfeld, M., Aguirre, P. A., and Grossmann, I. E. (2003). Alternative representations and formulations for the economic optimization of multicomponent distillation columns. *Computers and Chemical Engineering*, 27:363–383.
- Bauer, M. H. and Stichlmair, J. (1998). Design and economic optimization of azeotropic distillation processes using mixed-integer nonlinear programming. *Computers & Chemical Engineering*, 22(9):1271–1286.
- Baur, R. and Krishna, R. (2004). Distillation column with reactive pump arounds: an alternative to reactive distillation. *Chemical Engineering and Processing*, 43(3):435–445.

- Bessling, B., Loning, J., Ohligschlager, A., Schembecker, G., and Sundmacher, K. (1998). Investigation on the synthesis of methyl acetate in heterogeneous reactive distillation process. *Chemical Engineering Technology*, 21(5):393.
- Bezzo, F., Bertucco, A., Forlin, A., and Barolo, M. (1999). Steady-state analysis of an industrial reactive distillation column. *Separation and Purification Technology*, 16:251–260.
- Bird, R., Stewart, W., and Lightfoot, E. (2002). *Transport Phenomena*. John Wiley & Sons, Inc, New York, 2nd edition.
- Bisowarno, B. H., Tian, Y.-C., and Tade, M. O. (2004). Application of side reactors on etbe reactive distillation. *Chemical Engineering Journal*, 99(1):35–43.
- Bravo, J., Rocha, J., and Fair, J. (1985). Mass transfer in gauze packings. *Hydrocarbon processing*, pages 91–95.
- Buehler, W. K. and Schoenmakers, H. G. (1982). Distillation column with external reactors - an alternative to the reaction column. *German Chemical Engineering*, 5:292–296.
- Carey, G. and Finlayson, B. A. (1975). Orthogonal collocation on finite elements. *Chemical Engineering Science*, 30(5-6):587–596.
- Carroll, D. (1996). Chemical laser modeling with genetic algorithms. *AIAA Journal*, 34:338–346.
- Chadda, N., Malone, M., and Doherty, M. (2001). Effect of chemical kinetics on feasible splits for reactive distillation. *AIChE Journal*, 47:590.
- Chiang, S.-F., Kuo, C.-L., Yu, C.-C., and Wong, D. (2002). Design alternatives for the amyl acetate process: Coupled reactor/column and reactive distillation. *Industrial & Engineering Chemistry Research*, 41(13):3233–3246.
- Cho, Y. S. and Joseph, B. (1983a). Reduced-order steady-state and dynamic models for separation processes. part i. development of the model reduction procedure. *AIChE Journal*, 29(2):261–269.
- Cho, Y. S. and Joseph, B. (1983b). Reduced-order steady-state and dynamic models for separation processes. part ii. application to nonlinear multicomponent systems. *AIChE Journal*, 29(2):270–276.

- Cho, Y. S. and Joseph, B. (1984). Reduced-order models for separation columns—iii : Application to columns with multiple feeds and sidestreams. *Computers & Chemical Engineering*, 8(2):81–90.
- Ciric, A. and Gu, D. (1994). Synthesis of nonequilibrium reactive distillation by minlp optimization. *AIChE Journal*, 40:1479–1487.
- Citro, F. and Lee, J. W. (2004). Widening the applicability of reactive distillation technology by using concurrent design. *Ind. Eng. Chem. Res.*, 43:375–383.
- Deb, K. (2000). An efficient constraint handling method for genetic algorithms. *Computer Methods in Applied Mechanics and Engineering*, 186(2-4):311–338.
- Doherty, M. and Malone, M. (2001). *Conceptual Design of Distillation Systems*. McGraw-Hill.
- Fick, A. (1855a). On liquid diffusion. *Phil. Mag.*, 10:35–39.
- Fick, A. (1855b). Uber diffusion. *Poggendorff's Ann*, 94:59–86.
- Finlayson, B. A. (1972). *The Method of Weighted Residuals and Variational Principles*. Academic Press.
- Forbes, R. J. (1970). *A Short History of the Art of Distillation from the Beginnings Up to the Death of Cellier Blumenthal*. Brill, 2nd edition.
- Galerkin, B. G. (1915). Series solution of some problems in elastic equilibrium of rods and plates. *Vestn. Inzh. Tech*, 19:897–908.
- Gangadwala, J. and Kienle, A. (2007). Minlp optimization of butyl acetate synthesis. *Chemical Engineering and Processing*, 46(2):107–118.
- Gardini, L., Servida, A., M., M., and Carra, S. (1985). Use of orthogonal collocation on finite elements with moving boundaries for fixed bed catalytic reactor simulation. *Computers and Chemical Engineering*, 9:1–17.
- Garrard, A. and Fraga, E. (1998). Mass exchange network synthesis using genetic algorithms. *Comput. Chem. Eng.*, 22:1837–1850.
- Gildert, G. (2001). Hydrogenation of benzene to cyclohexane. U.S. Patent 6,187,980.
- Goldberg, D. E. (1989). *Genetic algorithms in search, optimization and machine learning*. Addison-Wesley, Reading, MA.

- Goldberg, D. E. and Richardson, J. (1987). Genetic algorithms with sharing for multimodal function optimization. In *Genetic Algorithms and their Applications: Proceedings of the Second International Conference on Genetic Algorithms*.
- Gross, B. and Roosen, P. (1998). Total process optimization in chemical engineering with evolutionary algorithms. *Computers & Chemical Engineering*, 22(Supplement 1):S229–S236.
- Grossmann, I. E. and Kravanja, Z. (1995). Mixed-integer nonlinear programming techniques for process systems engineering. *Comput. Chem. Eng.*, 19:S189–S204. (Suppl).
- Harmsen, G. J. (2007). Reactive distillation: The front-runner of industrial process intensification: A full review of commercial applications, research, scale-up, design and operation. *Chemical Engineering and Processing*, 46(9):774–780.
- Holland, J. H. (1975). *Adaption in Natural and Artificial Systems*. University of Michigan Press.
- Huss, R. S., Chen, F., Malone, M., and Doherty, M. (2003). Reactive distillation for methyl acetate production. *Comput. Chem. Eng.*, 27:1855–1855.
- Huss, R. S. and Westerberg, A. W. (1996). Collocation methods for distillation design. 1. model description and testing. *Ind. Eng. Chem. Res.*, 35:1603–1610.
- Jakobsson, K., Pyhalahti, A., Pakkanen, S., Keskinen, K., and Aittamaa, J. (2002). Modelling of a side reactor configuration combining reaction and distillation. *Chemical Engineering Science*, 57(9):1521–1524.
- Kaczmarek, K., Mazzotti, M., Storti, G., and Morbidelli, M. (1995). Modelling fixed-bed absorption columns through orthogonal collocations on moving finite elements. *Computers and Chemical Engineering*, 21:641–660.
- Karacan, S., Cabbar, Y., Albaz, M., and Hapoglu, H. (1998). The steady-state and dynamic analysis of packed distillation column based on partial differential approach. *Chemical Engineering and Processing*, 37:379–388.
- Kaymak, D. and Luyben, W. (2004a). Design of distillation columns with external side reactors. *Industrial & Engineering Chemistry Research*, 43(25):8049–8056.
- Kaymak, D. and Luyben, W. (2004b). Effect of the chemical equilibrium constant on the design of reactive distillation columns. *Ind. Eng. Chem. Res.*, 43(14):3666–3671.

- Kaymak, D. and Luyben, W. (2004c). Quantitative comparison of reactive distillation with conventional multiunit reactor/column/recycle systems for different chemical equilibrium constants. *Ind. Eng. Chem. Res.*, 43(10):2493–2507.
- Kaymak, D., Luyben, W., and Smith, O. (2004). Effect of relative volatility on the quantitative comparison of reactive distillation and conventional multi-unit systems. *Ind. Eng. Chem. Res.*, 43(12):3151–3162.
- Keyes, D. (1932). Esterification processes and equipment. *Ind. Eng. Chem.*, 24:1096–1103.
- Kister, H. Z. and Gill, D. (1991). Predict flood point and pressure drop for modern random packings. *Chem. Eng. Progress*, 87:32.
- Kooijman, H. and Taylor, R. (2001). *The ChemSep Book*. Books on Demand.
- Krishnamurthy, R. and Taylor, R. (1985a). A nonequilibrium stage model of multicomponent separation processes. part i: Model description and method of solution. *AIChE Journal*, 31(3):449–456.
- Krishnamurthy, R. and Taylor, R. (1985b). A nonequilibrium stage model of multicomponent separation processes. part ii: Comparison with experiment. *AIChE Journal*, 31(3):456–465.
- Krishnamurthy, R. and Taylor, R. (1985c). A nonequilibrium stage model of multicomponent separation processes. part iii: The influence of unequal component-efficiencies in process design problems. *AIChE Journal*, 31(12):1973–1985.
- Lanczos, C. (1938). Trigonometric interpolation of empirical and analytical functions. *J. Math. Phys.*, 17:123–199.
- Leboreiro, J. and Acevedo, J. (2004). Processes synthesis and design of distillation sequences using modular simulators: a genetic algorithm framework. *Computers & Chemical Engineering*, 28(8):1223–1236.
- Lee, J. W. and Westerberg, A. W. (2001). Graphical design applied to mtbe and methyl acetate reactive distillation processes. *AIChE Journal*, 47:1333.
- Leva, M. (1992). Reconsider packed-tower pressure-drop correlations. *Chemical Engineering Progress*, page 65.

- Lewis, W. and Matheson, G. (1932). Studies in distillation-design of rectifying columns for natural and refinery gasoline. *Ind. Eng. Chem.*, 24:496–498.
- Leyes, C. and Othmer, D. (1945). Esterification of butanol and acetic acid. *Industrial & Engineering Chemistry*, 37:968–977.
- Maxwell, J. (1866). On the dynamical theory of gases. *Phil. Trans. Roy. Soc.*, 157:49–88.
- Maxwell, J. (1878). *Encyclopaedia Britannica*, volume 7, chapter Diffusion, pages 214–221.
- McCabe, W. L. and Thiele, E. W. (1925). Graphical design of fractionating columns. *Ind. Eng. Chem.*, 17(6):605–611.
- Murphree, E. V. (1925a). Graphical rectifying column calculations. *Ind. Eng. Chem.*, 17(9):960–964.
- Murphree, E. V. (1925b). Rectifying column calculations. *Ind. Eng. Chem.*, 17(7):747–750.
- Nava, J. A. O., Baur, R., and Krishna, R. (2004). Combining distillation and heterogeneous catalytic reactors. *Chemical Engineering Research and Design*, 82(A2):160–166.
- Nernst, W. (1904). Theory of reaction velocity in heterogeneous systems. *Z Physikal Chem*, 47:52–55.
- Novak, Z., Kravanja, Z., and Grossmann, I. E. (1996). Simultaneous synthesis of distillation sequences in overall process schemes using an improved minlp approach. *Comput. Chem. Eng.*, 20:1425.
- Onda, K., Takeuchi, H., and Okumoto, Y. (1968). Mass transfer coefficients between gas and liquid phases in packed columns. *J. Chem. Eng. Jpn.*, 1:56–62.
- Ouni, T., Jakobsson, K., Pyhalahti, A., and Aittama, J. (2004). Enhancing productivity of side reactor configuration through optimizing the reaction conditions. *Chemical Engineering Research and Design*, 82(A2):167–174.
- Paterson, W. R. and Cresswell, D. L. (1971). A simple method for the calculation of effectiveness factors. *Chemical Engineering Science*, 26(5):605–616.
- Petlyuk, F., Platanov, V., and Slavinskii, D. (1965). Thermodynamically optimal method for separating multicomponent mixtures. *International Journal of Chemical Engineering*, 5:555–561.

- Pintaric, Z. N. and Kravanja, Z. (2006). Selection of the economic objective function for the optimization of process flow sheets. *Industrial & Engineering Chemistry Research*, 45(12):4222–4232.
- Ponchon, M. (1921). Etude graphique de la distillation fractionne industrielle. *La technique modern*, 13:20–24,55–58.
- Popken, T., Steinigeweg, S., and Gmehling, J. (2001). Synthesis and hydrolysis of methyl acetate by reactive distillation using structured catalytic packings: Experiments and simulation. *Ind. Eng. Chem. Res.*, 40(6):1566–1574.
- Reklaitis, G., Ravindran, A., and Ragsdell, K. (1983). *Engineering optimisation: methods and applications*. Wiley.
- Rice, R. G. and Do, D. D. (1995). *Applied Mathematics and Modeling for Chemical Engineers*. John Wiley & Sons, Inc.
- Salcedo, R. (1992). Solving nonconvex nonlinear programming and mixed-integer nonlinear programming problems with adaptive random search. *Ind. Eng. Chem. Res.*, 31:262.
- Savarit, R. (1922). Eléments de distillation. *Arts et Métiers*, page 65.
- Seader, J. D. and Henley, E. J. (1998). *Separation Process Principles*. John Wiley & Sons, Inc.
- Seferlis, P. and Grievink, J. (2001). Optimal design and sensitivity analysis of reactive distillation units using collocation models. *Ind. Eng. Chem. Res.*, 40:1673–1685.
- Seferlis, P. and Hrymak, A. N. (1994). Optimization of distillation units using collocation models. *AIChE Journal*, 40(5):813–825.
- Shoemaker, J. and Jones, E. (1987). Cumene by catalytic distillation. *Hydrocarbon processing*, 66:57–58.
- Shor, N., Kiwiel, K., and Ruszcaynski (1985). *Minimization Methods for Non-Differentiable Functions*. Springer-Verlag.
- Siirola, J. (1996). Industrial applications of chemical process synthesis. In Anderson, J., editor, *Advances in Chemical Engineering, Process Synthesis*, volume 23. Academic Press.

- Slater, J. C. (1934). Electronic energy bands in metals. *Phys. Rev.*, 45(11):794–.
- Song, W., Venimadhavan, G., Manning, J. M., Malone, M., and Doherty, M. (1998). Measurement of residue curve maps and heterogeneous kinetics in methyl acetate synthesis. *Industrial Engineering and Chemical Research*, 37:1917.
- Sorel, E. (1893). *La rectification de l' alcool*. Gauthiers - Villais et fils, Paris.
- Spellucci, P. (1998). An sqp method for general nonlinear programs using only equality constrained subproblems. *Math. Prog.*, 82:413–448.
- Spes, H. (1966). Katalytische reaktionen in ionenaustauscherkolonnen unter verschiebung des chemische gleichgewichts. *Chemiker Atg/Chemische Apparatur*, 90:443–446.
- Srivastava, R. and Joseph, B. (1984). Simulation of packed-bed separation processes using orthogonal collocation. *Computers and Chemical Engineering*, 8:43–50.
- Srivastava, R. K. and Joseph, B. (1985). Reduced-order models for separation columns– v. selection of collocation points. *Computers & Chemical Engineering*, 9(6):601–613.
- Srivastava, R. K. and Joseph, B. (1987a). Reduced-order models for separation columns– iv. treatment of columns with multiple feeds and sidestreams via spline fitting. *Computers & Chemical Engineering*, 11(2):159–164.
- Srivastava, R. K. and Joseph, B. (1987b). Reduced-order models for staged separation columns - vi. columns with steep and flat composition profiles. *Comput. Chem. Eng.*, 11(2):165–176.
- Stefan, J. (1871). Uber das gleichgewicht und die bewegung, insbesondere die diffusion von gasmengen. *Sitzungsber. Akad. Wiss. Wien*, 63:63–124.
- Stewart, W. E., Levien, K., and Morari, M. (1985). Simulation of fractionation by orthogonal collocation. *Chemical Engineering Science*, 40(3):409–421.
- Stitt, E. H. (2002). Reactive distillation for toluene disproportionation: a technical and economic evaluation. *Chemical Engineering Science*, 57(9):1537–1543.
- Sundmacher, K. (1995). *Reaktivdestillation mit katalytischen fuellkoerperpackungen - ein neuer Process zur Herstellung der Kraftstoffkomponente MTBE*. PhD thesis, Universität Clausthal.
- Swartz, C. L. E. and Stewart, W. E. (1986). A collocation approach to distillation column design. *AIChE Journal*, 32(11):1832–1838.

- Tayal, M. C., Fu, Y., and Diwekar, U. M. (1999). Optimal design of heat exchangers: A genetic algorithm framework. *Industrial & Engineering Chemistry Research*, 38(2):456–467.
- Taylor, R. and Krishna, R. (1993). *Multicomponent Mass Transfer*. Wiley.
- Taylor, R. and Krishna, R. (2000). Modelling reactive distillation. *Chemical Engineering Science*, 55(22):5183–5229.
- Thiele, E. W. and Geddes, R. L. (1933). Computation of distillation apparatus for hydrocarbon mixtures. *Industrial & Engineering Chemistry*, 25(3):289–295.
- Torres, L., Martins, F., and Bogle, I. (2000). Comparison of a reduced order model for packed separation processes and a rigorous nonequilibrium stage model. *Brazilian Journal of Chemical Engineering*, 17:4–7.
- Towler, G. and Frey, S. (2000). Reactive distillation. In Kulprathipanja, S., editor, *Reactive separation processes*, chapter 2. Taylor and Francis, Philadelphia.
- Turton, R., Bailie, R. C., Whiting, W. B., and Shaeiwitz, J. A. (2003). *Analysis, synthesis, and design of chemical processes*. Prentice Hall, 2nd edition.
- Uguina, M. A., Sotelo, J. L., and Serrano, D. P. (1993). Kinetics of toluene disproportionation over unmodified and modified zsm-5 zeolites. *Ind. Eng. Chem. Res.*, 32:49–55.
- Ulrich, G. and Vasudevan, P. (2006). How to estimate utility costs. *Chemical Engineering*, 113(4):66–69.
- Venkataraman, S., Chan, W., and Boston, J. (1990). Reactive distillation using aspen plus. *Chemical Engineering Progress*, 86(8):45–54.
- Villadsen, J. and Michelsen, M. (1978). *Solution of Differential Equation Models by Polynomial Approximation*. Prentice Hall, Englewood Cliffs, New Jersey.
- Villadsen, J. V. and Stewart, W. E. (1967). Solution of boundary-value problems by orthogonal collocation. *Chemical Engineering Science*, 22(24):1483–1501.
- Viswanathan, J. and Grossmann, I. E. (1990). A combined penalty function and outer-approximation method for minlp optimization. *Computers & Chemical Engineering*, 14(7):769–782.

- Viswanathan, J. and Grossmann, I. E. (1993). An alternative minlp model for finding the number of trays required for a specified separation objective. *Comput. Chem. Eng.*, 17(9):949.
- Wajge, R. M., Wilson, J. M., Pekny, J. F., and Reklaitis, G. V. (1997). Investigation of numerical solution approaches to multicomponent batch distillation in packed beds. *Ind. Eng. Chem. Res.*, 36:1738–1746.
- Wang, J. and Henke, G. (1966). Tridiagonal matrix for distillation. *Hydrocarbon processing*, 45(8):155–163.
- Wang, K., Qian, Y., Yuan, Y., and Yao, P. (1998). Synthesis and optimization of heat integrated distillation systems using an improved genetic algorithm. *Computers & Chemical Engineering*, 23(1):125–136.
- Whitman, W. (1923). The two-film theory of gas adsorption. *Chemical and Meteorological Engineering*, 29 (4):146–148.
- Wong, K. and Luus, R. (1980). Model reduction of high-order multistage systems by the method of orthogonal collocation. *Canadian Journal of Chemical Engineering*, 58:382–388.
- Yeomans, H. and Grossmann, I. E. (2000). Disjunctive programming models for the optimal design of distillation columns and separation sequences. *Ind. Eng. Chem. Res.*, 39:1637–1648.

Index

- $A_{i,j}$, 28
 $B_{i,j}$, 28
- Bare Module Cost, 155
Bare Module Factor, 155
Batch distillation, 38
Binary Distillation, 6
Boundary conditions, 76
Boundary Value Problems, 19
- Chebyshev equation, 23
ChemSep, 11, 14, 83
Chilton-Colburn analogy, 150
Collocation method, 22
Constraint handling, 74
CSTR, 79
- Derivative matrices, 27
Discontinuities, 91, 96
DONLP2, 70, 89
- Efficiency Model, 11
Equilibrium Model, 9
- Fick's Law, 4
Finite difference method, 20
Froude number, 150
- Galerkin method, 22
Generalised Disjunctive Programming (GDP),
58
Genetic Algorithms, 60, 72, 96
- Constraints, 64
Crossover, 62
Initialisation, 62
Mutation, 63
Replacement, 63
Selection, 62
- Hahn polynomials, 25
HETP, 16
- Integrated Side Reactor Systems, 47
- Jacobi polynomials, 24
JCOBI, 25
- Lagrange polynomials, 27
- Material Factor, 155
Maxwell-Stefan Relations, 5
McCabe-Thiele Diagram, 6
Pseudo McCabe-Thiele Diagrams, 9
Method of weighted residuals, 20
Methyl acetate, 80, 123
MINLP, 56
Model structure, 69
Multicomponent Distillation, 9
Murphree Efficiency, 6
- NLP, 70
OCFE, 29, 34
Optimisation, 55

Order Reduction Parameter (ORP), 33

Packed columns, 15

PFR, 78

Prandtl number, 151

Pressure Factor, 155

Process Intensification, 41

Program structure, 67

Rate-based Model, 12

Reactive Distillation, 37, 41

Reactor model, 78

Reynolds number, 147

Schmidt number, 149

Sherwood number, 147

Shooting Method, 19

Shor's r -algorithm, 71

SolvOpt, 71, 95

Toluene Disproportionation, 79

Toluene Distillation, 101

Total Annual Cost, 107, 126

Two-film theory, 12

Variable transformations, 35

Weber number, 150